

STRENGTHENING OF SHEAR DEFICIENT RC T-BEAMS WITH EXTERNALLY BONDED FRP SHEETS

ARCHANA KUMARI PANIGRAHI



**Department of Civil Engineering
National Institute of Technology, Rourkela
Rourkela-769 008, Odisha, India**

STRENGTHENING OF SHEAR DEFICIENT RC T-BEAMS WITH EXTERNALLY BONDED FRP SHEETS

A THESIS SUBMITTED IN PARTIAL FULFILMENT
OF THE REQUIREMENTS FOR THE DEGREE OF

Master of Technology (Research)

in

Structural Engineering

by

ARCHANA KUMARI PANIGRAHI

(Roll No. 609CE309)



**DEPARTMENT OF CIVIL ENGINEERING
NATIONAL INSTITUTE OF TECHNOLOGY, ROURKELA
ROURKELA – 769 008, ODISHA, INDIA
January 2013**

STRENGTHENING OF SHEAR DEFICIENT RC T-BEAMS WITH EXTERNALLY BONDED FRP SHEETS

A THESIS SUBMITTED IN PARTIAL FULFILMENT
OF THE REQUIREMENTS FOR THE DEGREE OF

Master of Technology (Research)

in

Structural Engineering

by

ARCHANA KUMARI PANIGRAHI

Under the guidance of

Prof. K. C. BISWAL

&

Prof. M. R. BARIK



**DEPARTMENT OF CIVIL ENGINEERING
NATIONAL INSTITUTE OF TECHNOLOGY, ROURKELA
ROURKELA – 769 008, ODISHA, INDIA
January 2013**

Albert Einstein:

If we knew what it was we were doing,

It would not be called research.

Would it?

Dedicated To my beloved husband



**Department of Civil Engineering
National Institute of Technology, Rourkela
Rourkela – 769 008, Odisha, India**

CERTIFICATE

*This is to certify that the thesis entitled, “**STRENGTHENING OF SHEAR DEFICIENT RC T-BEAMS WITH EXTERNALLY BONDED FRP SHEETS**” submitted by **ARCHANA KUMARI PANIGRAHI** bearing Roll No. **609CE309** in partial fulfillment of the requirements for the award of **Master of Technology (Research) Degree in Civil Engineering** with specialization in “**Structural Engineering**” during 2010-12 session at National Institute of Technology, Rourkela is an authentic work carried out by her under our supervision and guidance.*

To the best of our knowledge, the matter embodied in the thesis has not been submitted to any other University/Institute for the award of any Degree or Diploma.

Prof. K. C. Biswal

Prof. M. R. Barik

Date:

Place: Rourkela

ABSTRACT

The rehabilitation of existing reinforced concrete (RC) bridges and building becomes necessary due to ageing, corrosion of steel reinforcement, defects in construction/design, demand in the increased service loads, and damage in case of seismic events and improvement in the design guidelines. Fiber-reinforced polymers (FRP) have emerged as promising material for rehabilitation of existing reinforced concrete structures. The rehabilitation of structures can be in the form of strengthening, repairing or retrofitting for seismic deficiencies. RC T-section is the most common shape of beams and girders in buildings and bridges. Shear failure of RC T-beams is identified as the most disastrous failure mode as it does not give any advance warning before failure. The shear strengthening of RC T-beams using externally bonded (EB) FRP composites has become a popular structural strengthening technique, due to the well-known advantages of FRP composites such as their high strength-to-weight ratio and excellent corrosion resistance.

A few studies on shear strengthening of RC T-beams using externally bonded FRP sheets have been carried out but still the shear performance of FRP strengthened beams has not been fully understood. The present study therefore explores the prospect of strengthening structurally deficient T-beams by using an externally bonded fiber reinforced polymer (FRP).

This study assimilates the experimental works of glass fiber reinforced polymer (GFRP) retrofitted RC T-beams under symmetrical four-point static loading system. The thirteen number of beams were of the following configurations, (i) one number of beam was considered as the control beam, (ii) seven number of the beams were strengthened with different configurations and orientations of GFRP sheets, (iii) three number of the beams strengthened by GFRP with steel bolt-plate, and (iv) two number of beams with web openings strengthened by U-wrap in the shear zone of the beams.

The first beam, designated as control beam failed in shear. The failures of strengthened beams are initiated with the debonding failure of FRP sheets followed by brittle shear failure. However, the shear capacity of these beams has increased as compared to the control beam which can be further improved if the debonding failure is prevented. An innovative method of anchorage technique has been used to prevent these premature failures, which as a result ensure full utilization of the strength of FRP. A theoretical study has also been carried out to support few of the experimental findings.

ACKNOWLEDGMENT

“The will of God will never take you where Grace of God will not protect you...”

Thank you God for showing me the path...

I owe my deep gratitude to the individuals who have prominently contributed in completion of this thesis.

Foremost, I would like to express my heartfelt gratitude to my esteemed supervisor, Prof. Kishore Chandra Biswal for providing me a platform to work on challenging regions of Structural Engineering. His profound intuitions and consistent devotion towards microscopic details have been enormous inspirations contributed power plus to my research work.

Also, I am highly grateful to my esteemed co-supervisor, Prof. Manoranjan Barik who has afforded me continuous encouragement and support to carry out research. His enthusiasm and consistent notation in my works has motivated me to work for excellence.

I express my honest thankfulness to honorable Prof. Sunil Kumar Sarangi, Director, NIT Rourkela, Prof. N. Roy, Professor and HOD, Dept. of Civil Engineering, NIT, Rourkela for stimulating me for the best with essential facilities in the department.

I will be guilty if I will forget the altruistic cooperation of the most respected Sj. Sarat Chandra Choudhary. So, I happily thank Choudhary Sir for all his help & cooperation with stimulated me to move forward with a lot of enthusiasm and patience.

Many special thanks to my dearest friends Miss Sreelatha, Mr. Haran, Mr. Venkateswara Rao & Mr. Jukti for their generous contribution towards enriching the quality of the work and in elevating the shape of this thesis.

I would also express my obligations to Mr. S.K. Sethi, Mr. R. Lugun & Mr. Sushil, Laboratory team members of Department of Civil Engineering, NIT, Rourkela and academic staffs of this department for their extended cooperation.

I would like to appreciate all my friends, juniors and seniors for their inspiration and support. Their help can never be composed with literatures.

This acknowledgement would not be ever completed without expressing my heartfelt gratitude & abundant regards to my husband Er. Jitesh Kumar Panda and my in-laws. Definitely their consistent love, patience, encouragement, guidance, support & understanding are the source of my motivation and inspiration throughout my work which was the principal reinforcement to my achievement.

Eventually, I would like to dedicate my work and this thesis to my beloved family.

Archana Kumari Panigrahi

TABLE OF CONTENT

	Page
ABSTRACT	i
ACKNOWLEDGMENTS	ii
LIST OF FIGURES	vi
LIST OF TABLES	x
NOTATIONS	xi
ACRONYMS AND ABBREVIATIONS	xii
<u>CHAPTER 1</u>	
INTRODUCTION	
1.1 Preamble	1
1.2 Objective	5
1.3 Thesis Organization	5
<u>CHAPTER 2</u>	
REVIEW OF LITERATURE	
2.1 Brief Review	6
2.2 Strengthening of Reinforced Concrete (RC) Rectangular Beams	6
2.3 Strengthening of Reinforced Concrete (RC) T-Beams	19
2.4 Strengthening of RC Rectangular and T-Beams with web opening ..	24
2.5 Critical Observations	26
2.6 Scope of the Present Investigation	27
<u>CHAPTER 3</u>	
EXPERIMENTAL PROGRAM	
3.1 Casting of the Specimens	28
3.2 Material Properties	29
3.2.1 Concrete	29
3.2.2 Cement	30
3.2.3 Fine Aggregate	30
3.2.4 Coarse Aggregate	31
3.2.5 Water	32
3.2.6 Reinforcing Steel	32
3.2.7 Detailing of Reinforcement in RC T-Beams	33

3.2.8 Fiber Reinforced Polymer (FRP)	34
3.2.9 Epoxy Resin	34
3.2.10 Fabrication of GFRP Plate for Tensile Strength	35
3.2.11 Determination of Ultimate Stress, Ultimate Load & Young's Modulus of FRP	37
3.2.12 Form Work	39
3.2.13 Mixing of Concrete	40
3.2.14 Compaction	40
3.2.15 Curing of Concrete	40
3.2.16 Strengthening of Beams with FRP sheets	41
3.3 Experimental Setup	43
3.4 Description of Specimens	46
3.4.1 Beam-1 (Control Beam (CB))	46
3.4.2 Beam-2 (Strengthened Beam 1 (SB1))	46
3.4.3 Beam-3 (Strengthened Beam 2 (SB2))	47
3.4.4 Beam-4 (Strengthened Beam 3 (SB3))	48
3.4.5 Beam-5 (Strengthened Beam 4 (SB4))	48
3.4.6 Beam-6 (Strengthened Beam 5 (SB5))	49
3.4.7 Beam-7 (Strengthened Beam 6 (SB6))	50
3.4.8 Beam-8 (Strengthened Beam 7 (SB7))	50
3.4.9 Beam-9 (Strengthened Beam 8 (SB8))	51
3.4.10 Beam-10 (Strengthened Beam 9 (SB9))	52
3.4.11 Beam-11 (Strengthened Beam 10 (SB10))	52
3.4.12 Beam-12 (Strengthened Beam 11 (SB11))	53
3.4.13 Beam-13 (Strengthened Beam 12 (SB12))	54
3.5 Summary	54

CHAPTER 4

TEST RESULTS & DISCUSSIONS

4.1 Introduction	58
4.1.1 Crack Behaviour and Failure Modes	59
4.1.1.1 Control Beam (CB)	59
4.1.1.2 Strengthened Beam (SB)	62
4.1.1.2.1 Strengthened Beam 1 (SB1)	62
4.1.1.2.2 Strengthened Beam 2 (SB2)	64

4.1.1.2.3 Strengthened Beam 3 (SB3)	66
4.1.1.2.4 Strengthened Beam 4 (SB4)	68
4.1.1.2.5 Strengthened Beam 5 (SB5)	70
4.1.1.2.6 Strengthened Beam 6 (SB6)	72
4.1.1.2.7 Strengthened Beam 7 (SB7)	73
4.1.1.2.8 Strengthened Beam 8 (SB8)	75
4.1.1.2.9 Strengthened Beam 9 (SB9)	77
4.1.1.2.10 Strengthened Beam 10 (SB10)	79
4.1.1.2.11 Strengthened Beam 11 (SB11)	81
4.1.1.2.12 Strengthened Beam 12 (SB12)	83
4.1.2 Load-deflection History	86
4.2 Load at Initial Crack	99
4.3 Ultimate Load Carrying Capacity	100
<u>CHAPTER 5</u> THEORETICAL STUDY	
5.1 General	107
5.2 Factors affecting the shear contribution of FRP	107
5.3 Shear strength of RC beams strengthened with FRP reinforcement	
using ACI code guidelines	107
5.3.1 Design of Material Properties	107
5.3.2 Nominal shear strength	109
5.3.3 Design shear strength	109
5.3.4 FRP system contribution of shear strength	110
5.3.5 Effective strain in FRP laminates	111
5.3.6 Reduction coefficient based on Rupture failure mode	112
5.3.7 Reduction coefficient based on Debonding failure mode	112
5.4 Theoretical Calculations	114
5.5 Comparison of Experimental Results with ACI prediction	117
<u>CHAPTER 6</u> CONCLUSIONS & RECOMMENDATIONS	
6.1 Conclusions	120
6.2 Recommendations for Future work	121
<u>CHAPTER 7</u> BIBLIOGRAPHY	122

LIST OF FIGURES

Figure	Page
Chapter 1	
1-1. Fiber directions in composite materials	4
Chapter 3	
3-1. Detailing of Reinforcement	33
3-2. Reinforcement Detailing of T-Beam	34
3-3. Specimens for tensile testing of woven Glass/Epoxy composite	36
3-4. Experimental setup of INSTRON universal testing Machine (SATEC) of 600 kN capacity	37
3-5. Specimen during testing	37
3-6. Steel frame used for casting of RC T-Beam	40
3-7. Application of epoxy and hardener on the beam	42
3-8. Fixing of GFRP sheets on the beam	42
3-9. Roller used for the removal of air bubble	43
3-10. Details of the Test setup with location of dial gauges	44
3-11. Experimental setup for testing of beams	45
3-12. Shear force and bending moment diagram for four point static loading	45
3-13. Model of T-beam without GFRP – CB	46
3-14. Model of T-beam with GFRP – SB1	47
3-15. Model of T-beam with GFRP – SB2	47
3-16. Model of T-beam with GFRP – SB3	48
3-17. Model of T-beam with GFRP – SB4	49
3-18. Model of T-beam with GFRP – SB5	49
3-19. Model of T-beam with GFRP – SB6	50
3-20. Model of T-beam with GFRP – SB7	51
3-21. Model of T-beam with GFRP – SB8	51
3-22. Model of T-beam with GFRP – SB9	52
3-23. Model of T-beam with GFRP – SB10	53
3-24. Model of T-beam with GFRP – SB11	53
3-25. Model of T-beam with GFRP – SB12	54

Chapter 4

4-1.	(a) Experimental setup of the CB under four-point loading	60
	(b) Hair line crack started at 70kN in shear region	60
	(c) Crack pattern at L/3 distance (Near Left Support)	61
	(d) Crack pattern at ultimate failure of specimen CB	61
4-2.	(a) Experimental Setup of beam SB1	62
	(b) Initiation of debonding of GFRP sheet	63
	(c) Complete debonding followed by shear failure	63
4-3.	(a) Experimental Setup of beam SB2	64
	(b) Initiation of debonding of GFRP sheet	65
	(c) Shear failure of beam-Debonding of GFRP sheet	65
4-4.	(a) Experimental Setup of beam SB3	66
	(b) Hair Line Crack Started at load of 100 kN on concrete surface	67
	(c) Completely tearing & debonding of GFRP sheet followed by shear failure	67
4-5.	(a) Experimental Setup of beam SB4	68
	(b) Hair Line Crack Started at load of 90 kN on concrete surface	69
	(c) Debonding of GFRP sheet followed by shear failure	69
4-6.	(a) Experimental Setup of beam SB5	70
	(b) Initiation of tearing of GFRP sheet started at load of 80kN	71
	(c) Tearing of GFRP sheet followed by shear failure	71
4-7.	(a) Experimental Setup of beam SB6	72
	(b) Debonding of GFRP sheet followed by shear failure	73
4-8.	(a) Experimental Setup of beam SB7	74
	(b) Debonding of GFRP sheet followed by shear failure	74
4-9.	(a) Experimental Setup of beam SB8	75
	(b) Magnified view of Tearing of GFRP	76
	(c) Failure pattern of SB8	76
4-10.	(a) Experimental Setup of beam SB9	77
	(b) Prevention of debonding of GFRP sheet due to Anchorage System	78
	(c) Magnified view of Tearing of GFRP followed by shear failure	78
4-11.	(a) Experimental Setup of beam SB10	79
	(b) Crack shifted to the un-strengthened part of the shear span	80
	(c) Crushing of concrete near the support and the loading point	80

	(d) Failure pattern of SB10	81
4-12.	(a) Experimental Setup of beam SB11	82
	(b) Debonding of GFRP sheet	82
	(c) Failure Pattern of SB11 (Beam-type shear failure)	83
4-13.	(a) Experimental Setup of beam SB12	84
	(b) Tearing of GFRP sheet followed by Beam-type shear failure	84
	(c) Crack Pattern of SB12	85
4-14.	Load vs. Deflection Curve for CB	86
4-15.	Load vs. Deflection Curve for SB1	87
4-16.	Load vs. Deflection Curve for SB2	87
4-17.	Load vs. Deflection Curve for SB3	88
4-18.	Load vs. Deflection Curve for SB4	88
4-19.	Load vs. Deflection Curve for SB5	89
4-20.	Load vs. Deflection Curve for SB6	89
4-21.	Load vs. Deflection Curve for SB7	90
4-22.	Load vs. Deflection Curve for SB8	90
4-23.	Load vs. Deflection Curve for SB9	91
4-24.	Load vs. Deflection Curve for SB10	91
4-25.	Load vs. Deflection Curve for SB11	92
4-26.	Load vs. Deflection Curve for SB12	92
4-27.	Loads vs. Deflection Curve for CB vs. SB1 and SB3	93
4-28.	Load vs. Deflection Curve for CB vs. SB2 and SB4	94
4-29.	Load vs. Deflection Curve for CB vs. SB5, SB6 and SB7	95
4-30.	Load vs. Deflection Curve for CB vs. SB8 and SB9	96
4-31.	Load vs. Deflection Curve for SB9 vs. SB10	97
4-32.	Load vs. Deflection Curve for SB11 vs. SB12	98
4-33.	Load at initial crack of Beams CB, SB3, SB4, SB5, SB6, and SB7	99
4-34.	Ultimate load carrying capacity of beams CB, SB1 and SB3	100
4-35.	Ultimate load carrying capacity of beams CB, SB2 and SB4	101
4-36.	Ultimate load carrying capacity of beams CB, SB5, SB6 and SB7	102
4-37.	Ultimate load carrying capacity of beams CB, SB8 and SB9	103
4-38.	Ultimate load carrying capacity of beams SB9 and SB10	104
4-39.	Ultimate load carrying capacity of beams SB11 and SB12	105

Chapter 5

5-1. Illustration of the dimensional variables used in shear-strengthening calculations for repair, retrofit, or strengthening using FRP laminates.	
(a) Cross-section	
(b) Vertical FRP strips	
(c) Inclined FRP strips	110

LIST OF TABLES

Table	Page
3.1 Nominal Mix Proportions of Concrete	28
3.2 Test Results of Cubes after 28 days	29
3.3 Sieve Analysis of Fine Aggregate	31
3.4 Sieve Analysis of Coarse Aggregate	31
3.5 Tensile Strength of reinforcing steel bars	32
3.6 Size of the Specimens for tensile test	38
3.7 Result of the Specimens	39
3.8 Beam test parameters and material properties	55
4.1 Ultimate load and nature of failure for various beams	106
5.1 Comparisons of experimental and ACI predicted shear strength results	118
5.2 Comparisons of shear contribution of GFRP sheet from experimental and ACI Guidelines	119

NOTATIONS

A_{st}	Area of steel
a	shear span
b_f	width of the flange
b_w	width of the web
d_f	depth of the flange
d_w	depth of the web
d	effective depth
d'	effective cover
D	Overall depth of the beam
ρ	reinforcing ratio
ρ_{max}	maximum reinforcing ratio
ϕ	diameter of the reinforcement
f_y	yield stress of the reinforcement bar
L	span length of the beam
P_u	ultimate load
λ	load enhancement ratio

ACRONYMS AND ABBREVIATIONS

ACI	American Concrete Institute
CB	Control Beam
CFRP	Carbon Fiber Reinforced Polymer
EB	Externally Bonded
FRP	Fiber Reinforced Polymer
FGPB	Fiber Glass Plate Bonding
GFRP	Glass Fiber Reinforced Polymer
HYSD	High-Yield Strength Deformed
IS	Indian Standard
NSM	Near Surface Mounted
PSC	Portland Slag Cement
RC	Reinforced Concrete
SB	Strengthened Beam

CHAPTER - 1

INTRODUCTION



CHAPTER - 1

INTRODUCTION

1.1 PREAMBLE

The deterioration of civil engineering infrastructures such as buildings, bridge decks, girders, offshore structures, parking structures are mainly due to ageing, poor maintenance, corrosion, exposure to harmful environments. These deteriorated structures cannot take the load for which they are designed. A large number of structures constructed in the past using the older design codes in different parts of the globe are structurally unsafe according to the new design codes and hence need upgradation.

Many natural disasters, earthquake being the most affecting of all, have produced a need to increase the present safety levels in buildings. The knowledge of understanding of the earthquakes is increasing day by day and therefore the seismic demands imposed on the structures need to be revised. The design methodologies are also changing with the growing research in the area of seismic engineering. So the existing structures may not qualify to the current requirements. As the complete replacement of such deficient structures leads to incurring a huge amount of public money and time, retrofitting has become the acceptable way of improving their load carrying capacity and extending their service lives.

The conventional retrofitting techniques available are concrete-jacketing and steel-jacketing. The concrete-jacketing makes the existing section large and thus improves the load carrying capacity of the structure. But these techniques have several demerits such as construction of new formworks, additional weight due to enlargement of section, high installation cost etc. The steel-jacketing has proven to be an effective technique to enhance the performance of structures, but this method requires difficult welding work in the field and have potential problem of corrosion which increases the cost of maintenance.

With increase in research and introduction of new materials and technology there are new ways of retrofitting the structure with many added advantages. Introduction of Fiber Reinforced Polymer (FRP) Composite is one of them.

FRP composites comprise fibers of high tensile strength embedded within a thermosetting matrix such as epoxy, polymer or vinyl ester. The most widely used matrix is epoxy. FRP

was originally developed for aircraft, helicopters, space-craft, satellites, ships, submarines, high speed trains because of its light weight. The application of FRP in the civil engineering structures has started in 1980s. Then, the use of FRP for strengthening of existing or new reinforced concrete (RC) structures against normal and seismic loads increases at a rapid pace because of numerous advantages enlisted as follows:

1. FRP materials are not vulnerable to the swift electrochemical corrosion that occurs with steel
2. They can be easily rolled which makes transportation easy
3. High fatigue resistance
4. High strength to weight ratio
5. Fiber composite materials are available in very long lengths while steel plate is generally limited to 6m. The availability of long length and the flexibility of the material simplify the installation process
6. Time required for installation is very less
7. Fiber composite strengthening materials have higher ultimate strength and lower density as compared to those of steel
8. Low energy consumption during fabrication of raw material and structure, and has the potential for real time monitoring
9. Tailorability and ease of application
10. Excellent durability

However, FRP composites are sensitive to hygrothermal environment which is a disadvantage.

FRP are available in many forms and are used as a structural reinforcement for the concrete structures. Some of these forms are bars, plates and sheets. The FRP sheets are more commonly used to strengthen the existing structures because of greater flexibility compared to other forms.

The first application of FRP strengthening was made to reinforce the concrete beams. The beams are load bearing structural elements that are designed to carry both vertical gravity loads and horizontal loads due to seismic or wind. The structurally deficient beams fail during such events. There are mainly two types of failure of beams i.e, flexural and shear.

Hence, the strengthening of such beams is needed in flexure or shear or both zones and the use of external FRP strengthening to beams may be classified as:

- Flexural strengthening
- Shear strengthening

Flexural strengthening

Beams are strengthened in flexure through the use of FRP composites bonded to their tension zone using epoxy. The direction of fibers is parallel to that of high tensile stresses. Both prefabricated FRP strips, as well as sheets are applied. Several studies have been conducted to examine the flexural strengthening of RC members with FRP composite; however, few researchers have addressed shear strengthening.

Shear strengthening

The shear failure of an RC beam is distinctly different from the flexural failure. The flexural failure of a beam is ductile in nature, whereas shear failure is brittle and catastrophic. When the RC beam is deficient in shear, or when its shear capacity is less than the flexural capacity after flexural strengthening, shear strengthening must be considered. It is critically important to examine the shear capacity of RC beams which are intended to be strengthened in flexure.

Both FRP composite plates and sheets can be used in shear zone to enhance the capacity of beam, but the latter are more popular because of their flexible nature and ease of handling and applications. There are various FRP bonding schemes which can be applied to increase the shear resistance of RC beams. These include (1) bonding FRP to the sides of the beam only, (2) bonding FRP U jackets covering both the sides and the tension face, and (3) wrapping FRP around the whole cross section of the beam. As the reinforced concrete T-section is the most common shape of beams and girders in building and bridges, complete wrap is not a feasible alternative.

FRPs are strong only in the directions of fibers. The fiber directions in FRP composites may be unidirectional, bi-directional or multi-directional as shown in figure 1. The use of fibers in two directions can be beneficial with respect to shear resistance even if strengthening for reversed loading is not required, except for unlikely case in which one of the fiber directions is exactly parallel to the shear cracks.

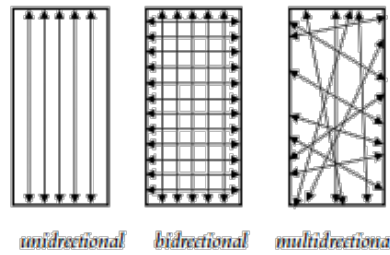


Figure 1-1. Fiber directions in composite materials

Modes of failure of FRP strengthened beams are:

A. Fiber failure in the FRP

It occurs when the tensile stress in the fibers exceeds the tensile strength. It is characterized by a rapid progressive fiber failure in the composite, particularly for sheets, but the failure is brittle in most of the cases. The orientation of the fibers with respect to the principal strain in concrete affects the ductility of the composite.

B. Bond failure

Bond failure is governed by the properties of the weaker materials in contact, i.e. concrete and adhesive. When the shear strength of one of these exceeds the force then transfer cannot be ensured anymore and a “slip” is produced. The debonding can take place in the concrete, between the concrete and the adhesive, in the adhesive, between the adhesive and the fibers. The most common debonding failure observed is at the surface of the concrete, which is an understandable phenomenon since the concrete is the weakest element in this “interaction chain”. The bond failure is considered as more dangerous than tensile failure because it can neither be foreseen nor be controlled.

Although fully wrapping the beam cross-section with FRP has been demonstrated to provide the most effective strengthening solution for shear and torsion applications, it is seldom achieved in practice due to the presence of physical obstructions such as beam flanges. The use of side-bonded FRP sheets enhance the shear capacity of the flange beam, but strength of FRP sheets in fullest extent may not be utilized due to the bond failure between the FRP and the concrete. U-jacketing is currently the most popular shear strengthening solution due to its high practicality, but it is limited by end peeling of the U-jacket legs. These drawbacks have opened up a new area of research on development of anchorage system.

1.2 OBJECTIVE

The main objectives of the present work are:

- To study the structural behaviour of reinforced concrete (RC) T-beams under static loading condition.
- To study the contribution of externally bonded (EB) Fiber Reinforced Polymer (FRP) sheets on the shear behaviour of RC T-beams.
- To examine the effect of different fiber orientations, number of layers etc. on the response of beam in terms of failure modes, enhancement of load carrying capacity and load deflection behaviour.
- To investigate the effect of a new anchorage scheme on the shear capacity of the beam.

1.3 THESIS ORGANIZATION

The present thesis is divided into seven chapters.

The general introduction to retrofitting of reinforced concrete (RC) beams and its importance in different engineering fields along with the objective of the present work are outlined in chapter 1.

A review comprising of literature on strengthening of different types of beams under different load, support conditions and different orientation of fiber are presented in chapter 2. The critical observations on earlier published works are highlighted and the scope of the present research work is outlined.

Chapter 3 deals with the description of the experimental program. The constituent materials, the beam specimens, and FRP installation procedure are presented. A brief description of test set up and procedure is given.

Chapter 4 contains the test results and discussion. The observed crack behaviours and modes of failure are reported. In addition, comparisons among test results are given.

Chapter 5 deals with the design approach for computing the shear capacity of the strengthened beams.

The important conclusions and the scope for further extension of the present work are outlined in chapter 6.

A list of important references cited in the present thesis is presented at the end.

CHAPTER - 2

REVIEW OF LITERATURE



CHAPTER - 2

REVIEW OF LITERATURE

2.1 BRIEF REVIEW

The state of deterioration of the existing civil engineering concrete structures is one of the greatest concerns to the structural engineers worldwide. The renewal strategies applied to existing structures comprise of rehabilitation and complete replacement. The latter involves a huge expenditure and time; hence the rehabilitation is the only option available. Fiber reinforced polymers (FRP) are the promising materials in rehabilitation of the existing structures and strengthening of the new civil engineering structures.

This chapter presents a brief review of the existing literature in the area of reinforced concrete (RC) beams strengthened with epoxy-bonded FRP. The major achievements and results reported in the literature are highlighted. The review of the literature is presented in the following three groups:

- a) Strengthening of Reinforced Concrete (RC) Rectangular Beams
- b) Strengthening of Reinforced Concrete (RC) T-Beams
- c) Strengthening of RC Rectangular and T- Beams with web opening

2.2 Strengthening of Reinforced Concrete (RC) Rectangular Beams:

When the RC beam is deficient in shear, or when its shear capacity is less than the flexural capacity after flexural strengthening, shear strengthening must be considered. It is critically important to examine the shear capacity of RC beams which are intended to be strengthened in flexure.

Many existing RC members are found to be deficient in shear strength and need to be repaired. Shear failure of RC beams are catastrophic which could occur without any forewarning. Shear deficiencies in reinforced concrete beams may crop up due to factors such as inadequate shear reinforcement, reduction in steel area due to corrosion, use of outdated design codes, increased service load, poor workmanship and design faults. The application of Glass Fiber Reinforced Polymer (GFRP) composite material, as an

external reinforcement is a viable technology recently found to be worth for improving the structural performance of reinforced concrete structures.

Ghazi et al. (1994) studied the shear repair of reinforced concrete (RC) beams strengthened with fiber glass plate bonding (FGPB) for structural and non-structural cracking behaviour due to a variety of reasons. Results from a study on strengthening of RC beams having deficient shear strength and showing major diagonal tension cracks have been presented. The beams with deficient shear strength were damaged to a predetermined level (the appearance of the first shear crack) and then repaired by fiber glass plate bonding (FGPB) techniques. Different shear repair schemes using FGPB to upgrade the beams shear capacity were used, i.e., FGPB repair by shear strips, by shear wings, and by U-jackets in the shear span of the beams. The study results also show that the increase in shear capacity by FGPB was almost identical for both strip and wing shear repairs. However, this increase was not adequate to cause beams repaired by these two schemes to fail in flexure.

Experimental and analytical studies were conducted by Norris et al. (1997) to examine the behaviour of damaged or under strength concrete beams retrofitted with thin carbon fiber reinforced plastic (CFRP) sheets, epoxy bonded to the tension face and web of the concrete beams to enhance their flexural and shear strengths. The effect of CFRP sheets on strength and stiffness of the beams is considered for various orientations of the fibers with respect to the axis of the beam. The beams were fabricated, loaded beyond concrete cracking strength, and retrofitted with different CFRP systems. The beams were subsequently loaded to failure. Finally, they concluded that there is increase in strength and stiffness of the existing concrete structures after providing CFRP sheets in the tension face and web of the concrete beam depending upon the different orientation of fiber.

Varastehpour and Hamelin (1997) examined the application of composite materials in civil engineering by strengthening of a reinforced concrete beam in situ by externally-bonded fiber reinforced polymer (FRP). The study of the mechanical properties of the interface and the rheological behaviour of composite materials are very important to design. For the experimental determination of the mechanical properties of the concrete/glue/plate interface, a new test was suggested. An iterative analytical model capable of simulating the bond slip and the material non-linearity, based on the compatibility of deformation and the equilibrium of forces was developed in order to predict the ultimate forces and deflections. Finally, a series of large-scale beams strengthened with fiber reinforced plastic was tested up to failure.

Load deflection curves were measured and compared with the predicted values to study the efficiency of the externally bonded plate and to verify the test results.

Chaallal et al. (1998) investigated a comprehensive design approach for reinforced concrete flexural beams and unidirectional slabs strengthened with externally bonded fiber reinforced plastic (FRP) plates. The approach complied with the Canadian Concrete Standard. This was divided into two parts, namely flexural strengthening and shear strengthening. In the first part, analytical models were presented for two families of failure modes: classical modes such as crushing of concrete in compression and tensile failure of the laminate, and premature modes such as debonding of the plate and ripping off of the concrete cover. These models were based on the common principles of compatibility of deformations and equilibrium of forces. They can be used to predict the ultimate strength in flexure which can be achieved by such elements, given the FRP cross-sectional area, or conversely, the required FRP cross-sectional area to achieve a targeted resisting moment for rehabilitated flexural elements. In the second part, design equations were derived to enable calculation of the required cross-sectional area of shear lateral FRP plates or strips for four number of plating patterns: vertical strips, inclined strips, wings, and U-sheet jackets.

Khalifa et al. (2000) studied the shear performance and the modes of failure of reinforced concrete (RC) beams strengthened with externally bonded carbon fiber reinforced polymer (CFRP) wraps experimentally. The experimental program consisted of testing twenty-seven, full-scale, RC beams. The variables investigated in this research study included steel stirrups (i.e., beams with and without steel stirrups), shear span-to depth ratio (i.e., a/d ratio 3 versus 4), CFRP amount and distribution (i.e., Continuous wrap versus strips), bonded surface (i.e., lateral sides versus U-wrap), fiber orientation (i.e., $90^\circ/0^\circ$ fiber combination versus 90° direction), and end anchor (i.e., U-wrap with and without end anchor). As part of the research program, they examined the effectiveness of CFRP reinforcement in enhancing the shear capacity of RC beams in negative and positive moment regions, and for beams with rectangular and T-cross section. The experimental results indicated that the contribution of externally bonded CFRP to the shear capacity is significant and dependent upon the variable investigated. For all beams, results show that an increase in shear strength of 22 to 145% was achieved.

Kachlakev and McCurry (2000) studied the behaviour of full-scale reinforced concrete (RC) beams retrofitted for shear and flexure with fiber reinforced polymer (FRP) laminates. Of the

four number of beams, one served as a control beam and the remaining three were implemented with varying configurations of carbon FRP (CFRP) and glass FRP (GFRP) composites to simulate the retrofit of the existing structure. CFRP unidirectional sheets were placed to increase flexural capacity and GFRP unidirectional sheets were utilized to mitigate shear failure. Here, four-point bending test were conducted. Load, deflection and strain data were collected. Fiber optic gauges were utilized in high flexure and shear regions and conventional resistive gauges were placed in eighteen locations to provide behavioural understanding of the composite material strengthening. Results from this study show that the use of FRP composites for structural strengthening provides significant static capacity increase to about 150% compared to unstrengthened sections. Load at first crack and post cracking stiffness of all beams were increased primarily due to flexural CFRP. The test results suggest the static demand of 658 kN-m sustaining up to 868kN-m applied moment. This allowed ultimate deflections to be 200% higher than the pre-existing shear deficient beam.

Duthinh and Starnes (2001) tested seven concrete beams reinforced internally with steel and externally with carbon FRP laminate applied after the concrete had cracked under four-point loading. Results showed that FRP was very effective for flexural strengthening. As the amount of steel increases, additional strength provided by the carbon decreases. Compared to a beam reinforced heavily with steel only, the beams reinforced with both steel and carbon have adequate deformation capacity in spite of their brittle mode of failure. Clamping or wrapping of the ends of the FRP laminate combined with adhesive bonding was effective in anchoring the laminate.

Alex et al. (2001) studied experimentally the effect of shear strengthening of RC beams on the stress distribution, initial cracks, crack propagation, and ultimate strength. Five types of beams with different strengthening carbon-fiber-reinforced plastic sheets are often strengthened in flexure. The experimental results show that it is not necessary to strengthen the entire concrete beam surface. The general and regional behaviors of concrete beams with bonded carbon-fiber-reinforced plastic sheets are studied with the help of strain gauges. The appearance of the first cracks and the crack propagation in the structure up to the failure is monitored and discussed for five different strengthened beams. In particular, for one of the strengthened RC beams, the failure mode and the failure mechanism are fully analyzed.

Khalifa and Antonio (2002) examined experimentally the shear performance and modes of failure of the rectangular simply supported reinforced concrete (RC) beams designed with shear deficiencies. These members were strengthened with externally bonded carbon fiber reinforced polymer (CFRP) sheets and evaluated in the laboratory. The experimental program consisted of twelve full-scale RC beams tested to fail in shear. The variables investigated within this program included steel stirrups, and the shear span-to-effective depth ratio as well as amount and distribution of CFRP. The experimental results indicated that the contribution of externally bonded CFRP to the shear capacity was significant. They concluded that, the beams tested in this program, increases in shear strength upto 40 to 138%. The contribution of externally CFRP reinforcement to the shear capacity is influenced by the a/d ratio. The test results indicated that contribution of CFRP benefits the shear capacity at a greater degree for beams without shear reinforcement than for beams with adequate shear reinforcement.

Sheikh et al. (2002) studied the damage sustained by foundation walls and large beams in a building simulated in full-size to near-full-scale model specimens in the laboratory. The damaged specimens were repaired with carbon and glass fiber-reinforced polymer (CFRP and GFRP) sheets and wraps, and tested to failure. Test results showed that fiber-reinforced polymers (FRP) were effective in strengthening for flexure as well as shear. Available analytical procedures and building code provisions were found to simulate the behaviour of specimens retrofitted with FRP reasonably well. The experimental program included testing of three wall-slab specimens and two beams. The wall-slab specimens were 250 mm thick, 1200 mm wide, and 1.2 m long, and the beams were 550 mm wide, 1000 mm deep, and 4.8 m long. Various analytical techniques were used to simulate experimental behaviour of the specimens. Both carbon and glass composites provided significant enhancement (more than 148%) in flexural strength to the extent that the failure of the wall-slab specimens shifted to shear mode which, in some cases, may not be acceptable. The wrapping of the beam of section size 550 x 1000 mm with one layer of CFRP resulted in changing the brittle mode of shear failure at 1700 kN to a very ductile flexure failure at 2528 kN. The deflection at failure increased from 14 mm in the control specimen, to 143 mm in the retrofitted specimen. The theoretical failure load for the retrofitted beam based on its shear capacity was approximately 5000 kN.

Sheikh (2002) studied on retrofitting with fiber reinforced polymers (FRP) to strengthen and repair damaged structures, which was a relatively new technique. In an extensive research programme at the University of Toronto, application of FRP in concrete structures was being

investigated for its effectiveness in enhancing structural performance both in terms of strength and ductility. The structural components tested so far include slabs, beams, columns and bridge culverts. Research on columns had particularly focused on improving their seismic resistance by confining them with FRP. All the specimens tested were considered as full-scale to two-third scale models of the structural components generally used in practice. Results indicated that retrofitting with FRP offers an attractive alternative to the traditional techniques.

Hadi (2003) examined the strength and load carrying capacity enhancement of reinforced concrete (RC) beams, those had been tested and failed in shear. A total of sixteen sheared beam specimens with a length of 1.2m and cross-sectional area of 100 x 150 mm were retrofitted by using various types of fiber reinforced polymer (FRP) and then retested. The retrofitted beam specimens wrapped with different amounts and types of FRP were subjected to four-point static loading. Load, deflection and strain data were collected during testing the beam specimens to failure. Results of the experimental program indicate that there were several parameters that affect the strength of the beams. The results also show that the use of FRP composites for shear strengthening provides significant static capacity increase.

Chen and Teng (2003) carried out an investigation on the shear capacity of FRP-strengthened RC beams. These studies have established clearly that such strengthened beams fail in shear mainly in one of the two modes, i.e., FRP rupture and FRP debonding, and have led to preliminary design proposals. This study was concerned with the development of a simple, accurate and rational design proposal for the shear capacity of FRP-strengthened beams which fail by FRP debonding. Existing strength proposals were reviewed and their deficiencies highlighted. Based on a rational bond strength model between FRP and concrete, a new shear strength model was then developed for debonding failures in FRP shear strengthened RC beams. This new model explicitly recognises the non-uniform stress distribution in the FRP along a shear crack as determined by the bond strength between the FRP strips and the concrete.

Rabinovitch and Frostig (2003) studied strengthening, upgrading, and rehabilitation of existing reinforced concrete structures using externally bonded composite materials. Five numbers of strengthened, retrofitted, or rehabilitated reinforced concrete beams were experimentally and analytically investigated. Emphasis was placed on the stress concentration that arises near the edge of the fiber reinforced plastic strips, the failure modes

triggered by these edge effects, and the means for the prevention of such modes of failure. Three beams were tested with various edge configurations that include wrapping the edge region with vertical composite straps and special forms of the adhesive layer at its edge. The last two beams were preloaded up to failure before strengthening and the ability to rehabilitate members that endured progressive or even total damage was examined. The results revealed a significant improvement in the serviceability and strength of the tested beams and demonstrated that the method was suitable for the rehabilitation of severely damaged structural members.

Taljsten (2003) studied the method of strengthening concrete structures with CFRP composite sheets. First traditional strengthening methods are studied briefly, then the use of CFRP composites for shear strengthening. Tests on beams strengthened in shear with CFRP sheets and how to design for shear strengthening with CFRP is given. Furthermore, a field application of a parking slab strengthened for shear with CFRP unidirectional fabric is investigated. The laboratory tests show the importance of considering the principal directions of the shear crack in relation to the unidirectional fiber and the field application shows that it is easy to strengthen existing structures for shear with CFRP fabrics.

Chen and Teng (2003) carried out an investigation on the shear capacity of Fiber-Reinforced Polymer-strengthened RC beams. These studies have established clearly that such strengthened beams fail in shear mainly in one of the two modes, i.e., FRP rupture and FRP debonding, and have led to preliminary design proposals. This study was concerned with the development of a simple, accurate and rational design proposal for the shear capacity of FRP-strengthened beams which fail by FRP rupture. Existing strength proposals were reviewed and their deficiencies highlighted. Based on a rational bond strength model between FRP and concrete, a new shear strength model was then developed for rupture failures in FRP shear strengthened RC beams. This new model explicitly recognises the non-uniform stress distribution in the FRP along a shear crack as determined by the bond strength between the FRP strips and the concrete.

Santhakumar et al. (2004) investigated the numerical study to simulate the behaviour of retrofitted reinforced concrete (RC) shear beams. The study was carried out on the unretrofitted RC beam designated as control beam and RC beams retrofitted using carbon fiber reinforced plastic (CFRP) composites with $\pm 45^\circ$ and 90° fiber orientations. The effect of retrofitting on uncracked and precracked beams was studied too. In this study the finite

elements are adopted by using ANSYS. A quarter of the beam was used for modelling by taking advantage of the symmetry of the beam and loadings. The load deflection plots obtained from numerical study show good agreement with the experimental plots reported by Norris et al. (1997). At ultimate stage there is a difference in behaviour between the uncracked and precracked retrofitted beams though not significant. The crack patterns in the beams are also presented. The numerical results show good agreement with the experimental values reported by Norris et al. This numerical modelling helps to track the crack formation and propagation especially in case of retrofitted beams in which the crack patterns cannot be seen by the experimental study due to wrapping of CFRP composites.

Teng et al. (2004) have studied the shear strengthening of reinforced concrete (RC) beams with FRP composites. A recent technique for the shear strengthening of RC beams is to provide additional FRP web reinforcement, commonly in the form of bonded external FRP strips/sheets. Over the last few years, a large amount of research has been conducted on this new strengthening technique, which has established its effectiveness and has led to a good understanding of the behaviour and strength of such shear-strengthened beams. Here, the methods of strengthening were described first, followed by a summary of experimental observations of failure processes and modes. The accuracy of existing design provisions was examined next through comparisons with test results. Limitations of existing experimental and theoretical studies were also highlighted.

Islam et al. (2005) investigated shear strengthening of RC deep beams using externally bonded FRP systems. In this study, six identical beams were fabricated and tested to failure for this purpose. One of these beams was tested in its virgin condition to serve as reference, while the remaining five beams were tested after being strengthened using carbon fiber wrap, strip or grids. The test results have shown that the use of a bonded FRP system leads to a much slower growth of the critical diagonal cracks and enhances the load-carrying capacity of the beam to a level quite sufficient to meet most of the practical upgrading requirements. Although FRP grids placed in normal orientation demonstrated to be the most effective system as far as the amount of material used in strengthening is concerned, other systems were found to be almost equally effective. An enhancement of shear strength in the order of about 40%, was achieved in this study.

Cao et al. (2005) studied the shear strengthening of reinforced concrete (RC) beams with bonded fiber reinforced polymer strips. The beams may be strengthened in various ways:

complete FRP wraps covering the whole cross section i.e., complete wrapping, FRP U jackets covering the two sides and the tension face i.e., U jacketing, and FRP strips bonded to the sides only i.e., side bonding. Shear failure of such strengthened beams is generally in one of two modes: FRP rupture and debonding. The former mode governs in almost all beams with complete FRP wraps and some beams with U jackets, while the latter mode governs in all beams with side strips and U jackets. In RC beams strengthened with complete wraps, referred to as FRP wrapped beams, the shear failure process usually starts with the debonding of FRP from the sides of the beam near the critical shear crack, but ultimate failure is by rupture of the FRP. Most previous research has been concerned with the ultimate failure of FRP wrapped beams when FRP ruptures. However, debonding of FRP from the sides is at least a serviceability limit state and may also be taken as the ultimate limit state. This study presents experimentally on this debonding failure state in which a total of 18 number beams were tested. The study focuses on the distribution of strains in the FRP strips intersected by the critical shear crack, and the shear capacity at debonding. A simple model is proposed to predict the contribution of FRP to the shear capacity of the beam at the complete debonding of the critical FRP strip.

Saafan (2006) studied the shear strengthening of reinforced concrete (RC) beams using GFRP wraps. The objective of the experimental work was to investigate the efficiency of GFRP composites in strengthening simply supported reinforced concrete beams designed with insufficient shear capacity. Using the hand lay-up technique, successive layers of a woven fiber glass fabric were bonded along the shear span to increase the shear capacity and to avoid catastrophic premature failure modes. The strengthened beams were fabricated with no web reinforcement to explore the efficiency of the proposed strengthening technique using the results of control beams with closed stirrups as web reinforcement. The test results of 18 number of beams were reported, addressing the influence of different shear strengthening schemes and variable longitudinal reinforcement ratios on the structural behaviour. The results indicated that significant increase in the shear strength and improvements in the overall structural behaviour of beams with insufficient shear capacity could be achieved by proper application of GFRP wraps. It was observed that the layers can easily slip down under self weight.

Al-Amery and Al-Mahaidi (2006) experimentally investigated the coupling of shear-flexural strengthening of RC beams. The presence of shear straps to enhance shear strength has the dual benefit of delaying de-bonding of CFRP sheets used for flexural strengthening. Six

number of RC beams were tested; having various combinations of CFRP sheets and straps in addition to a strengthened beam as control test. The instrumentation used in these tests cover the strain measurements in different CFRP layers and located along the span, in addition to the slip occurring between the concrete and CFRP sheets. Test results and observations showed that a significant improvement in the beam strength was gained due to the coupling of CFRP straps and sheets. Further, a more ductile behaviour was obtained as the debonding failure prevented.

Esfahani et al. (2007) studied the flexural behaviour of reinforced concrete (RC) beams strengthened using carbon fiber reinforced polymer (CFRP) sheets. The effect of reinforcing bar ratio (ρ) on the flexural strength of the strengthened beams was examined. Twelve number of concrete beam specimens with dimensions of 150 mm width, 200 mm depth, and 2000 mm length were manufactured and tested. Beam sections with three different reinforcing ratios, ρ , were used as longitudinal tensile reinforcement in specimens. Nine number of specimens were strengthened in flexure by CFRP sheets. The other three specimens were considered as control specimens. The width, length and number of layers of CFRP sheets varied in different specimens. The flexural strength and stiffness of the strengthened beams increased compared to the control specimens. From the results of this study, it was concluded that the design guidelines of ACI 440.2R-02 and ISIS Canada overestimate the effect of CFRP sheets in increasing the flexural strength of beams with small ρ values compared to the maximum value (ρ_{\max}) specified in these two guidelines. With the increase in the ρ value in the beams, the ratios of test load to the load calculated using ACI 440 and ISIS Canada increased. Therefore, the equations proposed by the two design guidelines are more appropriate for beams with large ρ values. In the strengthened specimens with the large reinforcing bar ratio, close to the maximum code value of ρ_{\max} , failure occurred with adequate ductility.

Mosallam and Banerjee (2007) studied experimentally on shear strength enhancement of reinforced concrete beams externally reinforced with fiber-reinforced polymer (FRP) composites. A total of nine full-scale beam specimens of three different classes, as-built (unstrengthened), repaired and retrofitted were tested. Three composite systems namely carbon/epoxy wet layup, E-glass/epoxy wet layup and carbon/epoxy procured strips were used for retrofit and repair evaluation. Experimental results indicated that the composite systems provided substantial increase in ultimate strength of repaired and strengthened beams as compared to the pre-cracked and as-built beam specimens. A comparative study of the

experimental results with published analytical models, including the ACI 440 model, was also conducted in order to evaluate the different analytical models and identify the influencing factors on the shear behaviour of FRP strengthened reinforced concrete beams. Comparison indicates that the shear span-to-depth ratio (a/d) is an important factor that actively controls the shear failure mode of beam and consequently influences on the shear strength enhancement.

Kim et al. (2008) studied the shear strength of RC beams strengthened by fiber material. It consists of a plasticity model for web crushing, a truss model for diagonal tension, and a simple flexural theory based on the ultimate strength method. To analyze the shear strengthening effect of the fiber, the model considers the interfacial shear-bonding stress between base concrete and the fiber. This reflects that the primary cause of shear failure in strengthened RC beams is rapid loss of load capacity due to separation of the strengthening fibers from the base material. The predictive model can estimate load capacities of each failure mode, and is compared to tested specimen data including extreme load failure. The analysis matches well with the experiments concerning load capacity and failure mode. Also, the experimental results of other published data are compared to the predictive model to evaluate its application. The results show that the predictive model has good adaptability and high accuracy.

Balamuralikrishnan (2009) has studied the flexural behaviour of RC beams strengthened with carbon fiber reinforced polymer (CFRP) fabrics. For flexural strengthening of RC beams, total ten number of beams were cast and tested over an effective span of 3000 mm up to failure under monotonic and cyclic loads. The beams were designed as under-reinforced concrete beams. Eight number of beams were strengthened with bonded CFRP fabric in single layer and two layers which are parallel to beam axis at the bottom under virgin condition and tested until failure; the remaining two beams were used as control specimens. Static and cyclic responses of all the beams were evaluated in terms of strength, stiffness, ductility ratio, energy absorption capacity factor, compositeness between CFRP fabric and concrete, and the associated failure modes. The theoretical moment-curvature relationship and the load-displacement response of the strengthened beams and control beams were predicted by using software ANSYS. Comparison has been made between the numerical (ANSYS) and the experimental results. The results show that the strengthened beams exhibit increased flexural strength, enhanced flexural stiffness, and composite action until failure.

Siddiqui (2009) has studied the experimental investigation of RC beams strengthened with externally bonded fiber reinforced polymer (FRP) composites. Use of externally bonded FRP sheets/strips/plates is a modern and convenient way for strengthening of RC beams. Although in the past substantial research has been conducted on FRP strengthened RC beams, but the behaviour of FRP strengthened beams under different schemes of strengthening is not well established. In this study, practical FRP schemes for flexure and shear strengthening of RC beams has been studied. For this purpose, 6 RC beams were cast in two groups, each group containing 3 beams. The specimens of first group were designed to be weak in flexure and strong in shear, whereas specimens of second group were designed just in an opposite manner i.e. they were made weak in shear and strong in flexure. In each group, out of the three beams, one beam was taken as a control specimen and the remaining two beams were strengthened using two different carbon fiber reinforced polymer (CFRP) strengthening schemes. All the beams of two groups were tested under similar loading. The response of control and strengthened beams were compared and efficiency and effectiveness of different schemes were evaluated. It was observed that tension side bonding of CFRP sheets with U-shaped end anchorages is very efficient in flexural strengthening; whereas bonding the inclined CFRP strips to the side faces of RC beams are very effective in improving the shear capacity of beams. He concluded that for shear strengthening, externally bonded inclined CFRP-strips show a far better performance than vertical CFRP-strips as specimen strengthened using inclined strips gives higher shear and deformation capacity than specimen strengthened using vertical strips. Also the inclined CFRP-strips arrest the propagating cracks more effectively than the vertical CFRP-strips.

Sundarraja and Rajamohan (2009) studied on strengthening of reinforced concrete (RC) beams which are deficient in shear using glass fiber reinforced polymer(GFRP) inclined strips experimentally. Included in the study are effectiveness in terms of width and spacing of inclined GFRP strips, spacing of internal steel stirrups, and longitudinal steel rebar section on shear capacity of the RC beam. The study also aims to understand the shear contribution of concrete, shear strength due to steel bars and steel stirrups and the additional shear capacity due to GFRP strips in a RC beam. And also the failure modes, shear strengthening effect on ultimate force and load deflection behaviour of RC beams bonded externally with GFRP inclined strips on the shear region of the beam. The use of GFRP strips had effect in delaying the growth of crack formation, which is, evident from the load causing the initial cracks. When both the wrapping schemes were considered, it was found that the retrofitted beams

with inclined U-wrap GFRP strips had a better load-deflection behaviour compared to the side strips, which is very important for shear strengthening of the RC beams. Finally, the use of inclined GFRP strips was able to avoid the brittle failure of the beams.

Pannirselvam et al. (2009) have studied the strength behaviour of fiber reinforced polymer (FRP) of strengthened beam, the objective of this work was to evaluate the structural behaviour of reinforced concrete (RC) beams with externally bonded FRP reinforcement. Beams bonded with four different types of glass fiber reinforced polymer (GFRP) having 3.50 mm thickness were used. Totally five rectangular beams of 3 m length were cast. One beam was used as reference beam and the remaining beams were provided with GFRP laminates on their soffit. The variable considered for the study was the type of GFRP laminate. The study parameters of this investigation included first crack load, yield load, ultimate load, first crack deflection, yield deflection, ultimate deflection, crack width, deflection ductility, energy ductility, deflection ductility ratios and energy ductility ratios of the test beams. The performance of FRP plated beams was compared with that of unplated beam. The test results showed that the beams strengthened with GFRP laminates exhibited better performance.

Bukhari et al. (2010) investigated on the shear strengthening of reinforced concrete (RC) beams with carbon fiber reinforced polymer (CFRP). The paper reviews existing design guidelines for strengthening beams in shear with CFRP sheets and proposes a modification to Concrete Society Technical Report TR55. It goes on to present the results of an experimental programme which evaluated the contribution of CFRP sheets towards the shear strength of continuous reinforced concrete (RC) beams. A total of seven, two-span concrete continuous beams with rectangular cross-sections were tested. The control beam was not strengthened, and the remaining six were strengthened with different arrangements of CFRP sheets. The experimental results showed that the shear strength of the beams was significantly increased by the CFRP sheet and that it was beneficial to orient the FRP at 45° to the axis of the beam. The shear strength of FRP strengthened beams is usually calculated by adding the shear resistance of individual components from the concrete, steel stirrups and FRP.

Martinola et al. (2010) examined the use of a jacket made of fiber reinforced concrete (FRP) with tensile hardening behaviour for strengthening RC beams by means of full-scale tests on 4.55 m long beams. A 40 mm jacket of this material was directly applied to the beam surface. Both the strengthening and the repair of RC beams were studied. In particular, in the latter

case the beam was initially damaged and eventually repaired. A numerical analysis was also performed in order to better understand the reinforcement behaviour. The experimental and numerical results show the effectiveness of the proposed technique both at ultimate and serviceability limit states.

Ceroni (2010) experimentally studied on RC beams externally strengthened with carbon fiber reinforced plastic (FRP) laminates and Near Surface Mounted (NSM) bars under monotonic and cyclic loads, the latter ones characterized by a low number of cycles in the elastic and post-elastic range. Comparisons between experimental and theoretical failure loads were discussed in detail.

More recently, Obaidat et al. (2011) investigated experimentally, the behaviour of the structurally damaged full-scale reinforced concrete beams retrofitted with CFRP laminates in shear or in flexure. The main variables considered were the internal reinforcement ratio, position of retrofitting and the length of CFRP. The experimental results, generally, indicate that beams retrofitted in shear and flexure by using CFRP laminates are structurally efficient and are restored to stiffness and strength values nearly equal to or greater than those of the control beams. Employing externally bonded CFRP plates resulted in an increase in maximum load. The increase in maximum load of the retrofitted specimens reached values of about 23% for retrofitting in shear and between 7% and 33% for retrofitting in flexure. Moreover, retrofitting shifts the mode of failure to be brittle. It was found that the efficiency of the strengthening technique by CFRP in flexure varied depending on the length. The main failure mode in the experimental work was plate debonding which reduces the efficiency of retrofitting. Based on the conclusion deeper studies should be performed to investigate the behaviour of the interface layer between the CFRP and concrete. Also numerical work should be done to predict the behaviour of retrofitted beams and to evaluate the influence of different parameters on the overall behaviour of the beams.

2.3 Strengthening of Reinforced Concrete (RC) T-Beams:

Saadatmanesh and Ehsani (1992) examined the static strength of five RC rectangular beams and one T-beam strengthened by gluing glass fiber reinforced polymer (GFRP) plates to their tension flanges experimentally. Here, the beams were tested to failure under four-point loading. The measured load versus strain in GFRP plate, steel rebar, extreme compression

fiber of concrete, and the load versus deflection for the section at mid span of the beams were plotted and compared to the predicted values. The results generally indicate that the flexural strength of strengthened beams was significantly increased by gluing GFRP plates to the tension face. In addition, the epoxy bonded plates improved the cracking behaviour of the beams by delaying the formation of visible cracks and reducing crack widths at higher load levels. The gain in the ultimate flexural strength was more significant in beams with lower steel reinforcement ratios.

Chajes et al. (1995) worked on shear strengthening of reinforced concrete beams using externally composite fabrics. Here, a series of 12 under-reinforced concrete T-beams was tested to study the effectiveness of beams using externally applied composite fabrics as a method of increasing beam shear capacity. Oven composite fabrics made of aramid, E-glass, and graphite fibers were bonded to the web of the T-beams using a two-component epoxy. The three different fabrics were chosen to allow various fabric stiffness's and strengths to be studied. The beams were tested in flexure, and the performance of eight beams with external shear reinforcement was compared to results of four control beams with no external reinforcement. All the beams failed in shear and those with composite reinforcement displayed excellent bond characteristics. For the beams with external reinforcement, 60 to 150 % of increase in ultimate strength was achieved.

Khalifa et al. (2000) studied the shear performance and the modes of failure of simply supported RC T-beams externally strengthened in shear with FRP composites. Here, two different FRP-based strengthening systems were investigated, namely, externally bonded FRP sheets and Near Surface Mounted (NSM) FRP rods. The latter is a novel technique on which no literature is available to date. The experimental program consisted of testing eleven full-scale, RC T beams. The beams were grouped into three series i.e., the first series was tested to investigate the influence on the shear capacity of the concrete surface roughness and axial rigidity of the carbon FRP sheets. The second series focused on the capability of externally bonded CFRP reinforcement to enhance the ultimate capacity of beams that already have adequate internal steel reinforcement. In addition, a beam with internal glass FRP stirrups was tested in this series. In the third series, the novel shear strengthening system of NSM CFRP rods was evaluated. Then, the test results confirm that externally bonded CFRP sheets and NSM CFRP rods can be used to increase significantly the shear capacity,

with efficiency that varies depending on the tested variables. Moreover, the test results indicate that the contribution of CFRP sheets to the shear capacity increases as CFRP axial rigidity increases. The experimental verification of NSM FRP rods as strengthening technique showed their effectiveness in increasing the shear capacity.

Khalifa and Nanni (2000) studied the improving shear capacity of existing reinforced concrete (RC) T-section beams using carbon FRP (CFRP) composites. Different configurations of externally bonded CFRP sheets were used to strengthen the specimens in shear. The experimental program consisted of six full-scale, simply supported beams. One beam was used as a bench mark and five beams were strengthened using different configurations of CFRP. The parameters investigated in this study included wrapping schemes, CFRP amount, 90°/0° ply combination, and CFRP end anchorage. The experimental results showed that externally bonded CFRP can increase the shear capacity of the beam significantly. In addition, the results indicated that the most effective configuration was the U-wrap with end anchorage. Design algorithms in ACI code format as well as Euro code format are proposed to predict the capacity of referred members. Results showed that the proposed design approach is conservative and acceptable. Here, the beams tested in the experimental program were achieved 35 – 145% of increase in shear strength.

Bousselham and Chaallal (2006) analyzed the behaviour of reinforced concrete (RC) T-beams strengthened in shear with externally bonded carbon fiber reinforced polymer (CFRP) experimentally. In total, 22 numbers of tests were performed on 4520 mm-long T-beams. The parameters investigated were as follows: (i) the CFRP ratio (that is, the number of CFRP layers); (ii) the internal shear steel reinforcement ratio (that is, spacing); and (iii) the shear length to the beams depth ratio, a/d (that is, deep beam effect). The main objective of the study was to analyze the behaviour of RC T-beams strengthened in shear with externally applied CFRP by varying the aforementioned parameters. The results showed that the contribution of the CFRP to the shear resistance is not in proportion to the CFRP thickness (that is, the stiffness) provided, and depends on whether the strengthened beam is reinforced in shear with internal transverse steel reinforcement. Results also confirmed the influence of the ratio a/d on the behaviour of RC beams retrofitted in shear with external fiber-reinforced polymer (FRP). Finally, comparison of the shear resistance values predicted by ACI 440.2R-02 guidelines, with the test results clearly indicated that the guidelines fail to capture important aspects, such as the presence of the transverse steel and the ratio a/d on the one

hand, and overestimates the shear resistance for high FRP thickness (and hence high FRP stiffness), on the other.

Ozgur (2008) performed another research work based on the strengthening of RC T-section beams with low strength concrete using carbon fiber reinforced polymer (CFRP) composites subjected to the cyclic load. He studied the various methods developed for strengthening of RC beams against shear. Nowadays, external bonding of different composite materials to RC beams was very popular and successful technique. This study presents test results on strengthening of shear deficient RC beams by external bonding of CFRP straps. Six RC beams with a T-section were tested under cyclic loading. Width of the CFRP straps, arrangements of straps along the shear span, and anchorage techniques that were applied at the ends of straps were the main parameters that were investigated during experimental study. Shear deficient beams with low strength concrete were strengthened by using CFRP straps for obtaining ductile flexural behaviour. The test results confirmed that all CFRP arrangements improved the strength, stiffness and energy dissipation capacity of the specimens significantly. The failure mode and ductility of specimens were proved to differ according to the CFRP strap width and arrangement along the beam.

Tanarslan and Altin (2009) have studied an experimental investigation on reinforced concrete (RC) beams having T-section strengthened with externally bonded carbon fiber reinforced polymer (CFRP) strips. Specimens, one of which was the control specimen and the remaining six were the shear deficient test specimens, were tested under cyclic load to investigate the effect of CFRP strips on behaviour and strength. Five number of shear deficient specimens were strengthened with side bonded and U-jacketed CFRP strips, remaining one tested with its virgin condition without strengthening. According to the test results, premature debonding was the dominant failure modes of externally strengthened RC beams so the effect of anchorage usage on behaviour and strength was also investigated.

Dias and Barros (2010) have studied experimentally the effectiveness of the Near Surface Mounted (NSM) technique with carbon fiber polymer (CFRP) laminates for the shear strengthening of T-cross section reinforced concrete (RC) beams. Three inclinations (45° , 60° and 90°) of the laminates were tested and, for each one, three percentages of CFRP were adopted. The RC beams with NSM laminates had a percentage of steel stirrups of 0.10%. The highest percentage of laminates was designed to provide a maximum load similar to that of a

reference RC beam with a steel stirrup reinforcement ratio of 0.28%. The results showed, that the inclined laminates were more effective than vertical laminates, an increase in the percentage of laminates produced an increase in the shear capacity of the beams, the contribution of the laminates for the shear resistance of the beam was limited by the concrete tensile strength; the failure modes of the beams were influenced by the percentage of the laminates. For each percentage of laminates, a homologous RC beam strengthened with U-shaped CFRP wet layup sheets (discrete strips) applied according to the Externally Bonded Reinforcement (EBR) technique was also tested, with the purpose of comparing the effectiveness of these two CFRP strengthening techniques. NSM was the most effective, not only in terms of increasing beam shear resistance but also in assuring better utilization of the tensile strength of the CFRP material. Except for the beams with the highest percentage of CFRP, the NSM technique was more effective than the EBR technique in terms of deformation capacity at beam failure. The ACI and fib (Federation International du Beton) analytical formulations have predicted a larger contribution of the EBR shear strengthening systems than the values recorded experimentally. The formulation provided by Nanni et al. (2004) for the NSM technique predicted a CFRP contribution around 61% of the experimentally registered values.

Deifalla and Ghobarah (2010) have studied several cases of loading, geometrical configurations, flexure beams and girders, RC T-beams strengthened using fiber reinforced polymer (FRP) fabrics subjected to combined shear and torsion. Failure of a structural element under combined shear and torsion is brittle in nature. Externally bonded FRP fabrics are currently being studied and used for the rehabilitation, repair, and retrofit of concrete structure. Six half-scale beams, two control specimen and four strengthened beams were constructed and tested using a specially designed test setup that subjects the beam to combined shear and torsion with different ratios. Four strengthening techniques using carbon FRPs were used. An innovative strengthening technique namely the extended U-jacket showed promising results in terms of strength and ductility while being quite feasible for strengthening. The shear and torsion carrying capacities were increased up to 71% more than the control specimen, as well as increasing the stiffness of the beams after cracking as compared to that of the control beam. Strengthening increased the deformability of the beam and preserved its integrity up to failure.

Lee et al. (2011) have investigated the behaviour and performance of reinforced concrete (RC) deep beams having T-section strengthened in shear with CFRP sheets. Key variables evaluated in this study were strengthening length, fiber direction combination of CFRP sheets, and an anchorage using U-wrapped CFRP sheets. A total of 14 RC T-section deep beams were designed to be deficient in shear with a shear span-to-effective depth ratio (a/d) of 1.22. Crack patterns and behaviour of the tested deep beams were observed during four-point loading tests. Except the CS-FL-HP (CS exhibits the deep beams full strengthening in shear with CFRP sheets on both sides - FL denote full strengthening length of the shear span from the supports – HP signify $0^\circ/0^\circ$ fiber direction combinations) specimen, almost all strengthened deep beams showed a shear-compression due to partial delamination of the CFRP sheets. From the load-displacement ($p-u$) curves, the effects of key variables on the shear performance of the strengthened deep beams were addressed. It was concluded from the test results that the key variables of strengthening length, fiber direction combination, and anchorage have significant influence on the shear performance of strengthened deep beams.

2.4 Strengthening of RC Rectangular and T- Beams with web opening:

Generally, in the construction of modern buildings, a network of pipes and ducts are necessary to accommodate essential services like water supply, sewage, ventilating, air-conditioning, electricity, telephone, and computer network. Openings in concrete beams enable the installation of these services.

Shanmugamt and Swaddiwudhipongt (1988) have studied the strength of fiber reinforced concrete deep beams with openings. In this study, nine beams were tested to failure, all the beams were of the same dimensions having a length of 1550 mm, overall depth of 650 mm and width of 80 mm. Steel fiber content in all the beams was kept the same equal to 1% by volume. Two rectangular openings, one in each shear span, were placed symmetrically about the vertical axis in each of the beams. The beams were simply supported on a clear span of 1300 mm, and are tested under two point loading. The experimental results presented here confirm previous findings, i.e., the effect of opening on the behaviour and ultimate shear strength of deep beams depends primarily on the extent to which it intercepts the natural load path and the location at which this interception occurs.

Mansur (1998) has studied effect of openings on the behaviour and strength of reinforced concrete (RC) beams in shear. In this study, the behaviour and design of a beam containing a transverse opening and subjected to a predominant shear are briefly reviewed. Based on the observed structural response of the beam, suitable guidelines are proposed for classifying an opening as small or large. For small openings, a design method compatible with the current design philosophy for shear is proposed and illustrated by a numerical design example. In the method proposed, the maximum shear allowed in the section to avoid diagonal compression failure has been assumed to be the same as that for solid beam except for considering the net section through the opening.

Mansur (2006) has studied the design of reinforced concrete beams with web openings. To investigate the problem of openings in beams, the author initiated a research program in the early 1980s. Since then extensive research has been carried out giving a comprehensive coverage on both circular and large rectangular openings under various combinations of bending, shear and torsion. In this study, major findings relevant to the analysis and design of such beams under the most commonly encountered loading case of bending and shear are extracted and summarized. An attempt has been made to answer the frequently asked questions related to creating an opening in an already constructed beam and how to deal with multiple openings. It has been shown that the design method for beams with large openings can be further simplified without sacrificing rationality and having unreasonable additional cost.

Maaddawy and Sherif (2009) have studied the results of a research work aimed at examining the potential use of upgrade reinforced concrete (RC) deep beams with openings. A total of 13 deep beams with openings were constructed and tested under four-point bending. Test specimen had a cross-section of 80 x 500 mm and a total length of 1200mm. Two square openings, one in each shear span, were placed symmetrically about the mid-point of the beam. Test parameters included the opening size, location, and the presence of the CFRP sheets. The structural response of RC deep beams with openings was primarily dependent on the degree of the interruption of the natural load path. Externally bonded CFRP shear strengthening around the openings was found very effective in upgrading the shear strength of RC deep beams. The strength gain caused by the CFRP sheets was in the range of 35 - 73%. Based on the test results concluded that, the CFRP shear-strengthened RC deep beams with openings failed suddenly due to a formation of diagonal shear cracks in the top and bottom chords of the opening. In all strengthened beams, the concrete was pulled out from

the U-shaped CFRP jacket wrapped around the top chord of the opening. The shear strength gain caused by CFRP sheets was in the range of 66 - 71% when the opening was located at the mid-point of the shear span. The shear strength gain was maximum (72%) when the opening was located at the top of the beam where most of the shear force was carried by the bottom chord that was fully wrapped with CFRP. Only a strength gain of 35% was recorded for the beam with bottom openings because most of the shear force was carried by the top chord that had a U-shaped CFRP sheet.

2.5 Critical Observations

The following critical observations are made from the review of existing literature in the area of reinforced concrete (RC) beams strengthened with epoxy-bonded FRP.

- Most of the research efforts have been made to study the flexural and shear behaviour of RC rectangular beams strengthened with fiber reinforced polymer (FRP) composites.
- Despite the growing number of field applications, there is limited number of reports on shear behaviour of strengthened RC T-beams using externally bonded FRP composites.
- A limited works have been reported on strengthening of RC T-beams with web openings.
- There is a gain in shear capacity of RC beams when strengthened with FRP composites, peeling of FRP sheets from main concrete has been reported due to improper anchorage.
- The study on anchorage system used for the prevention of debonding of FRP and concrete on shear behaviour of RC beams is limited.
- Many researchers are of the opinion that the previous design provisions do not have comprehensive understanding of the shear behaviour.

2.6 Scope of the present Investigation

Based on the critical review of the existing literature and to fulfil the objective outlined earlier, the scope of the present work is defined as follows:

- To study the shear behaviour of RC T-Beams under static loading condition.
- To study the behaviour of shear deficient RC T-beams with transverse openings in web portion.
- To study the contribution of GFRP composites on ultimate load carrying capacity and failure pattern of reinforced concrete beams.
- To study the effect of anchorage system used for prevention of debonding of FRP and concrete on the shear capacity of RC T-beams.
- To compute theoretically the shear strength of the RC T-beams.

CHAPTER - 3

EXPERIMENTAL PROGRAM



CHAPTER - 3

EXPERIMENTAL PROGRAM

The objective of the experimental program is to study the effect of externally bonded (EB) fiber reinforced plastic (FRP) sheets on the shear capacity of reinforced concrete T-beam under static loading condition. Thirteen number of reinforced concrete T-beams are cast and tested up to failure by applying symmetrical four-point static loading system. Out of thirteen number of beams, one beam was not strengthened by FRP and was considered as a control beam, whereas all other twelve beams were strengthened with externally bonded GFRP sheets in shear zone of the beam. The variables investigated in this research study included GFRP amount and distribution (i.e., continuous wrap versus strips), bonded surface (i.e., lateral sides versus U-wrap), GFRP ratio (i.e., no. of layers), and end anchor (i.e., U-wrap with and without end anchor).

3.1 CASTING OF THE SPECIMENS

For conducting experiment, the proportions in the concrete mix are tabulated in Table 3.1 as per IS: 456-2000. The water cement ratio is fixed at 0.6. The mixing is done by using concrete mixture. The beams are cured for 28 days. For each beam six concrete cube specimens were made at the time of casting and were kept for curing, to determine the compressive strength of concrete at the age of 7 days & 28 days. The uniaxial compressive tests on the specimens (150 × 150 × 150 mm concrete cube) were performed and the average concrete compressive strength at 7 days & 28 days for each beam are shown in Table 3.2.

Table 3.1 Nominal Mix Proportions of Concrete

Description	Cement	Sand (Fine Aggregate)	Coarse Aggregate	Water
Mix Proportion (by weight)	1	1.67	3.33	0.6
Quantities of materials for one specimen beam (kg)	29	48.02	47.91	18

3.2 MATERIAL PROPERTIES

3.2.1 Concrete

Concrete is a material composed of cement and water combined with sand, gravel, crushed stone, or other inert material such as expanded slag or vermiculite. A strong stone-like mass is formed from chemical reaction of the cement and water. The concrete paste can be easily molded into any form or trowelled to produce a smooth surface. Hardening starts immediately after mixing, but precautions are taken, usually by covering, to avoid rapid loss of moisture since the presence of water is necessary to continue the chemical reaction and increase the strength. Too much of water, however, produces a concrete that is more porous and weaker. The quality of the paste formed by the cement and water largely determines the character of the concrete.

The compression tests on control and strengthened specimen of cubes are performed at 7 days and 28 days. The test results of cubes are presented in Table 3.2.

Table 3.2 Test Result of Cubes after 28 days

Specimen Name	Specimen ID	Size of Cube Specimen (mm ³)	Average Cube Compressive Strength (MPa)
Control Beam	CB	150x150x150	22.21
Strengthened Beam 1	SB1	150x150x150	24.88
Strengthened Beam 2	SB2	150x150x150	24.00
Strengthened Beam 3	SB3	150x150x150	23.32
Strengthened Beam 4	SB4	150x150x150	23.13
Strengthened Beam 5	SB5	150x150x150	24.12
Strengthened Beam 6	SB6	150x150x150	23.68
Strengthened Beam 7	SB7	150x150x150	24.10

Strengthened Beam 8	SB8	150x150x150	24.06
Strengthened Beam 9	SB9	150x150x150	23.08
Strengthened Beam 10	SB10	150x150x150	23.47
Strengthened Beam 11	SB11	150x150x150	23.68
Strengthened Beam 12	SB12	150x150x150	23.92

3.2.2 Cement

Cement is a material, generally in powdered form, which can be made into a paste usually by the addition of water and, when molded or poured, will set into a solid mass. Numerous organic compounds used for an adhering, or fastening materials, are called cements, but these are classified as adhesives, and the term cement alone means a construction material. The most widely used of the construction cements is Portland cement. It is bluish-gray powdered obtained by finely grinding the clinker made by strongly heating an intimate mixture of calcareous and argillaceous minerals. Portland Slag Cement (PSC) Konark Brand was used for this investigation. It is having a specific gravity of 2.96.

3.2.3 Fine Aggregate

Fine aggregate/sand is an accumulation of grains of mineral matter derived from disintegration of rocks. It is distinguished from gravel only by the size of the grains or particles, but is distinct from clays which contain organic material. Sand is used for making mortar and concrete and for polishing and sandblasting. Sands containing a little clay are used for making molds in foundries. Clear sands are employed for filtering water. Here, the fine aggregate/sand is passing through 4.75 mm sieve and having a specific gravity of 2.64. The grading zone of fine aggregate is zone III as per Indian Standard specifications IS: 383-1970.

Table 3.3 Sieve Analysis of Fine Aggregate

Description of Sample	Specific Gravity	GRADING			Remarks
		Sieve Designation in mm	% PASSING		
			Obtained	Required	
Sand	2.64	10.0	100	100	Sand comes under Grading zone III as per IS: 383-1970 specifications.
		4.75	99	90-100	
		2.36	97	85-100	
		1.18	96	75-100	
		0.600	67	60-79	
		0.300	16	12-40	
		0.150	4	0-10	

3.2.4 Coarse Aggregate

Coarse aggregates are the crushed stone is used for making concrete. The commercial stone is quarried, crushed, and graded. Much of the crushed stone used is granite, limestone, and trap rock. The coarse aggregates of two grades are used one retained on 10 mm size sieve and another grade contained aggregates retained on 20 mm size sieve. The maximum size of coarse aggregate was 20 mm and is having specific gravity of 2.88 grading confirming to IS: 383-1970.

Table 3.4 Sieve Analysis of Coarse Aggregate

Description of Sample	Specific Gravity	GRADING			Remarks
		Sieve Designation in mm	% PASSING		
			Obtained	Required	
Coarse Aggregate (20mm :: 10mm : 60 : 40 by weight)	2.88	40	100	100	Confirms to 20mm full graded Coarse aggregate as per IS: 383-1970 specifications.
		20	95	95-100	
		10	32	25-55	
		4.75	0	0-10	

3.2.5 Water

Water fit for drinking is generally considered good for making the concrete. Water should be free from acids, alkalis, oils, vegetables or other organic impurities. Soft water produces weaker concrete. Water has two functions in a concrete mix. Firstly, it reacts chemically with the cement to form a cement paste in which the inert aggregates are held in suspension until the cement paste has hardened. Secondly, it serves as a vehicle or lubricant in the mixture of fine aggregates and cement. Ordinary clean portable tap water is used for concrete mixing in all the mix.

3.2.6 Reinforcing Steel

High-Yield Strength Deformed (HYSD) bars conforming to IS 1786:1985. The reinforcements used were 20 mm and 10 mm diameter are used for the longitudinal reinforcement and the stirrups are 8 mm diameter. The yield strength of steel reinforcements used in this experimental program is determined by performing the standard tensile test on the three specimens of each bar. The proof stress or yield strength of the specimens are averaged and shown in Table 3.5. The modulus of elasticity of steel bars was 2×10^5 MPa.

Table 3.5 Tensile Strength of reinforcing steel bars

Sl. no. of sample	Diameter of bar (mm)	0.2% Proof stress (N/mm ²)	Avg. Proof Stress (N/mm ²)
1	20	475	470
2	20	472	
3	20	463	
4	10	530	529
5	10	535	
6	10	521	
7	8	520	523
8	8	527	
9	8	521	

3.2.7 Detailing of Reinforcement in RC T-Beams

For all the thirteen reinforced concrete T-beams, the same arrangement for shear reinforcement is made. The tension reinforcement consists of 2 numbers of 20 mm ϕ and 1 number of 10 mm ϕ HYSD bars. Three bars of 8 mm ϕ steel bars are also provided as hang up bars.

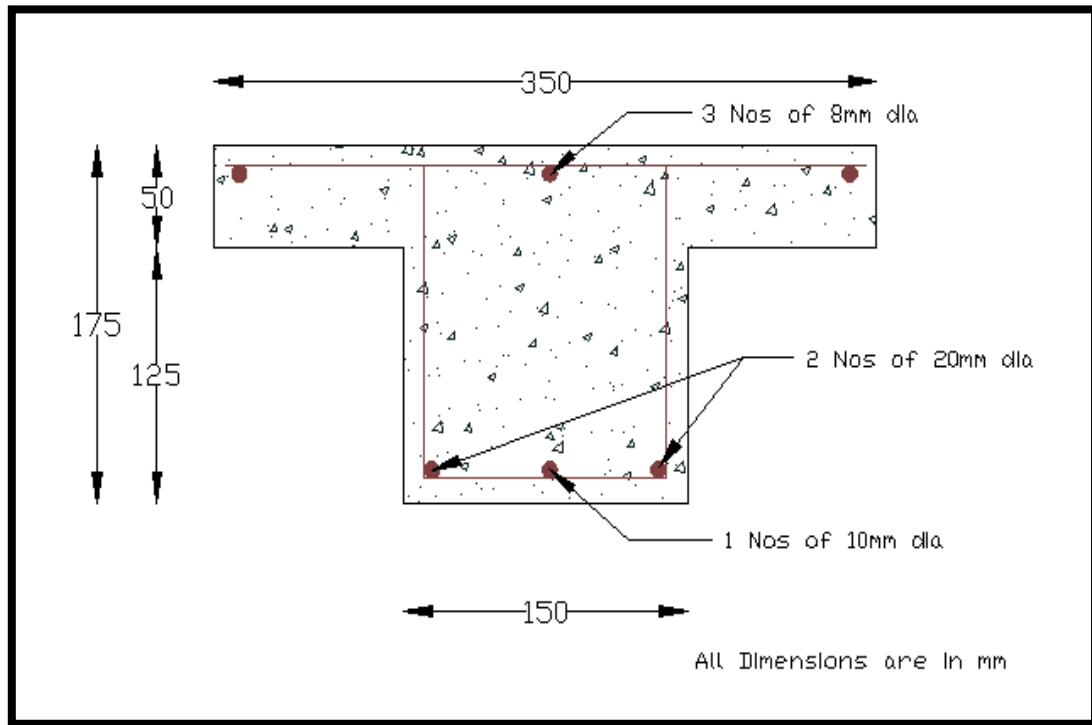


Figure 3-1. Detailing of Reinforcement



Figure 3-2. Reinforcement Detailing of T- Beam

3.2.8 Fiber Reinforced Polymer (FRP)

Continuous fiber reinforced materials with polymeric matrix (FRP) can be considered as composite, heterogeneous, and anisotropic materials with a prevalent linear elastic behaviour up to failure. Normally, Glass and Carbon fibers are used as reinforcing material for FRP. Epoxy is used as the binding material between fiber layers.

For this study, one type of FRP sheet was used during the tests i.e., a bidirectional FRP with the fiber oriented in both longitudinal and transverse directions, due to the flexible nature and ease of handling and application, the FRP sheets are used for shear strengthening. Throughout this study, E-glass was used manufactured by Owens Corning.

3.2.9 Epoxy Resin

The success of the strengthening technique primarily depends on the performance of the epoxy resin used for bonding of FRP to concrete surface. Numerous types of epoxy resins with a wide range of mechanical properties are commercially available in the market. These

epoxy resins are generally available in two parts, a resin and a hardener. The resin and hardener used in this study are Araldite LY 556 and hardener HY 951 respectively.

3.2.10 Fabrication of GFRP Plate for tensile strength

There are two basic processes for moulding, that is, hand lay-up and spray-up. The hand lay-up process is the oldest, simplest, and most labour intense fabrication method. This process is the most common in FRP marine construction. In hand lay-up method liquid resin is placed along with reinforcement (woven glass fiber) against finished surface of an open mould. Chemical reactions in the resin harden the material to a strong, light weight product. The resin serves as the matrix for the reinforcing glass fibers, much as concrete acts as the matrix for steel reinforcing rods. The percentage of fiber and matrix was 50:50 in weight.

The following constituent materials are used for fabricating the GFRP plate:

- i. Glass FRP (GFRP)
- ii. Epoxy as resin
- iii. Hardener as diamine (catalyst)
- iv. Polyvinyl alcohol as a releasing agent

Contact moulding in an open mould by hand lay-up was used to combine plies of woven roving in the prescribed sequence. A flat plywood rigid platform was selected. A plastic sheet was kept on the plywood platform and a thin film of polyvinyl alcohol was applied as a releasing agent by use of spray gun. Laminating starts with the application of a gel coat (epoxy and hardener) deposited on the mould by brush, whose main purpose was to provide a smooth external surface and to protect the fibers from direct exposure to the environment. Ply was cut from roll of woven roving. Layers of reinforcement were placed on the mould at top of the gel coat and gel coat was applied again by brush. Any air bubble which may be entrapped was removed using serrated steel rollers. The process of hand lay-up was the continuation of the above process before the gel coat had fully hardened. Again, a plastic sheet was covered the top of the plate by applying polyvinyl alcohol inside the sheet as releasing agent. Then, a heavy flat metal rigid platform was kept top of the plate for compressing purpose. The plates were left for a minimum of 48 hours before being transported and cut to exact shape for testing.

Plates of 2 layers, 4 layers, 6 layers and 8 layers were casted and three specimens from each thickness were tested.



Figure 3-3. Specimens for tensile testing of woven Glass/Epoxy composite

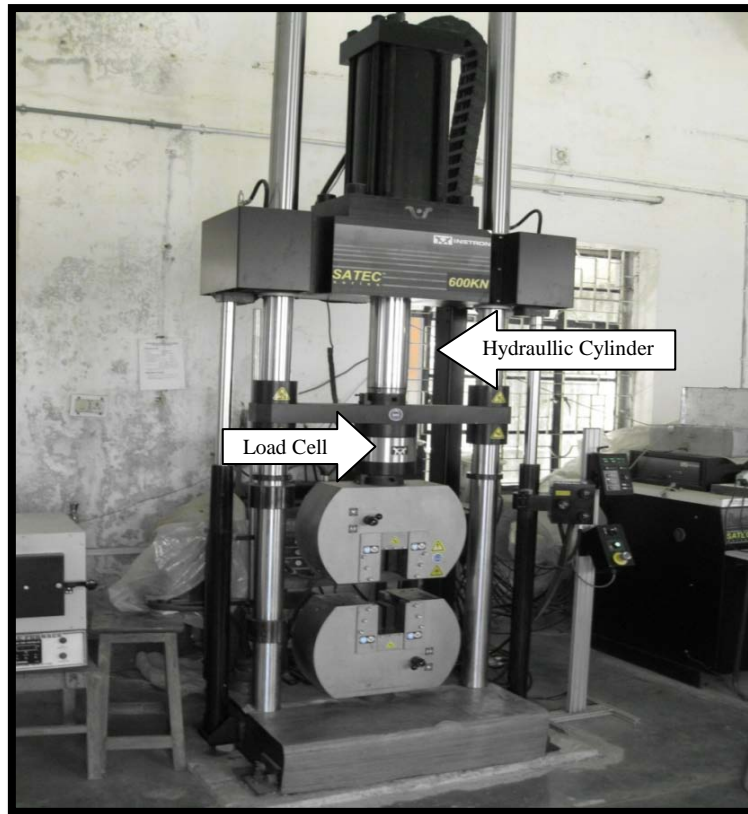


Figure 3-4. Experimental setup of INSTRON universal testing Machine (SATEC) of 600 kN capacities



Figure 3-5. Specimen during testing

3.2.11 Determination of Ultimate Stress, Ultimate Load & Young's Modulus of FRP

The ultimate stress, ultimate load and young's modulus was determined experimentally by performing unidirectional tensile tests on specimens cut in longitudinal

and transverse directions. The specimens were cut from the plates by diamond cutter or by hex saw. After cutting by hex saw, it was polished with the help of polishing machine. At least three replicate sample specimens were tested and mean values adopted. The dimensions of the specimens are shown in below table 3.6.

Table 3.6 Size of the Specimens for tensile test

No. of Layers	Length of sample (cm)	Width of sample (cm)	Thickness of sample (cm)
2	15	2.3	0.1
4	15	2.3	0.25
6	15	2.3	0.3
8	15	2.3	0.45

For measuring the tensile strength and young's modulus, the specimen is loaded in INSTRON 600 kN in Production Engineering Lab, NIT, Rourkela. Specimens were gripped in the fixed upper jaw first and then gripped in the movable lower jaw. Gripping of the specimen should be proper to prevent the slippage. Here, it is taken as 50 mm from the each side. Initially, the strain is kept zero. The load, as well as the extension, was recorded digitally with the help of a load cell and an extensometer respectively. From these data, stress versus strain graph was plotted, the initial slope of which gives the young's modulus. The ultimate stress and ultimate load were obtained at the failure of the specimen. The average value of each layer of the specimens is given in the below Table 3.7.

Table 3.7 Result of the Specimens

GFRP plate of	Ultimate Stress (MPa)	Ultimate Load (N)	Young's Modulus (MPa)
2 layers	172.79	6200	6829.9
4 layers	209.09	9200	7788.5
6 layers	236.23	12900	7207.4
8 layers	253.14	26200	7333.14

3.2.12 Form Work

Fresh concrete being plastic in nature requires good form work to mould it to the required shape and size. So the form work should be rigid and strong to hold the weight of wet concrete without bulging anywhere. The joints of the form work are sealed to avoid leakage of cement slurry. Mobil oil was then applied to the inner faces of form work. The bottom rest over thick polythene sheet lead over the rigid floor. The reinforcement cage was then lowered, placed in position inside the side work carefully with a cover of 20mm on sides and bottom by placing concrete cover blocks.



Figure 3-6. Steel Frame Used For Casting of RC T-Beam

3.1.1 Mixing of Concrete

Mixing of concrete is done thoroughly with the help of standard concrete mixer machine, to ensure that a uniform quality of concrete is obtained. First coarse and fine aggregates are fed alternately, followed by cement. Then required quantity of water is slowly added into the mixer to make the concrete workable until a uniform colour is obtained. The mixing is done for two minutes after all ingredients are fed inside the mixer as per IS: 456-2000.

3.1.2 Compaction

All specimens were compacted by using 30mm size needle vibrator for good compaction of concrete, and sufficient care was taken to avoid displacement of the reinforcement cage inside the form work. Finally, the surface of concrete was leveled and smoothed by metal trowel and wooden float. After seven hours, the specimen detail and date of concreting was written on top surface to identify it properly.

3.1.3 Curing of Concrete

Curing is done to prevent the loss of water which is essential for the process of hydration and hence for hardening. Usually, curing starts as soon as the concrete is sufficiently hard. Here,

curing is done by spraying water on the jute bags or by spending wet hessians cloth over the surface for a period of 28 days.

3.1.4 Strengthening of Beams with FRP sheets

All the loose particles of concrete surface at the bottom sides of the beam were chiseled out by using a chisel. Then the required region of concrete surface was made rough using a coarse sand paper texture and cleaned with an air blower to remove all dirt and debris particles. Once the surface was prepared to the required standard, the epoxy resin was mixed in accordance with manufacturer's instructions. The mixing is carried out in a plastic container (100 parts by weight of Araldite LY 556 to 10 parts by weight of Hardener HY 951) and was continued until the mixture was in uniform. After their uniform mixing, the fabrics are cut according to the size then the epoxy resin is applied to the concrete surface. After their uniform mixing, the fabrics are cut according to the size then the epoxy resin is applied to the concrete surface. Then the GFRP sheet is placed on top of epoxy resin coating and the resin is squeezed through the roving of the fabric with the roller .Air bubbles entrapped at the epoxy/concrete or epoxy/fabric interface are eliminated. Then the second layer of the epoxy resin was applied and GFRP sheet was then placed on top of epoxy resin coating and the resin was squeezed through the roving of the fabric with the roller and the above process was repeated. The composite laminate was attached starting at one end and applying enough pressure to press out any excess epoxy from the sides of the laminate. During hardening of the epoxy, a constant uniform pressure is applied on the composite fabric surface in order to extrude the excess epoxy resin and to ensure good contact between the epoxy, the concrete and the fabric. This operation is carried out at room temperature. Concrete beams strengthened with glass fiber fabric are cured for minimum of one week at room temperature before testing.



Figure 3-7. Application of epoxy and hardener on the beam



Figure 3-8. Fixing of GFRP sheets on the beam



Figure 3-9. Roller used for the removal of air bubble

3.2 EXPERIMENTAL SETUP

All the specimens are tested as simple RC T-beams using four-point static loading frame with shear span to effective depth ratio (a/d) equal to 2.38. The tests were carried out at the ‘Structural Engineering’ Laboratory of Civil Engineering Department, NIT Rourkela. The testing procedure for the entire specimen is same. After the curing period of 28 days are over, then the beam surface is cleaned with the help of sand paper for clear visibility of cracks. Figure 3-10 shows the details of the test setup.

A load cell with a capacity of 500 kN and attached to a hydraulic jack was used to measure the load during testing.

Four-point loading is conveniently provided by the arrangement shown in Figure 3-10. The load is transmitted through a load cell and spherical seating on to a spreader beam. This spreader beam is installed on rollers seated on steel plates bedded on the test member with cement in order to provide a smooth leveled surface. The test member is supported on roller bearings acting on similar spreader plates. The loading frame must be capable of carrying the expected test loads without significant distortion. Ease of access to the middle third for crack observations, deflection readings and possibly strain measurements is an important

consideration, as is safety when failure occurs. The specimen is placed over the two steel rollers bearing leaving 150mm from the ends of the beam. The remaining 1000mm is divided into three equal parts of 333mm as shown in the figure 3-10. Load is applied by hydraulic jack of capacity 500kN. Lines are marked on the beam to be tested at $L/3$, $L/2$, & $2L/3$ locations from the left support ($L=1300\text{mm}$), three dial gauges are used for recording the deflection of the beams. One dial gauge is placed just below the centre of the beam, i.e. at $L/2$ distance and the remaining two dial gauges are placed just below the point loads, i.e. at $L/3$ and $2L/3$ to measure the deflections.

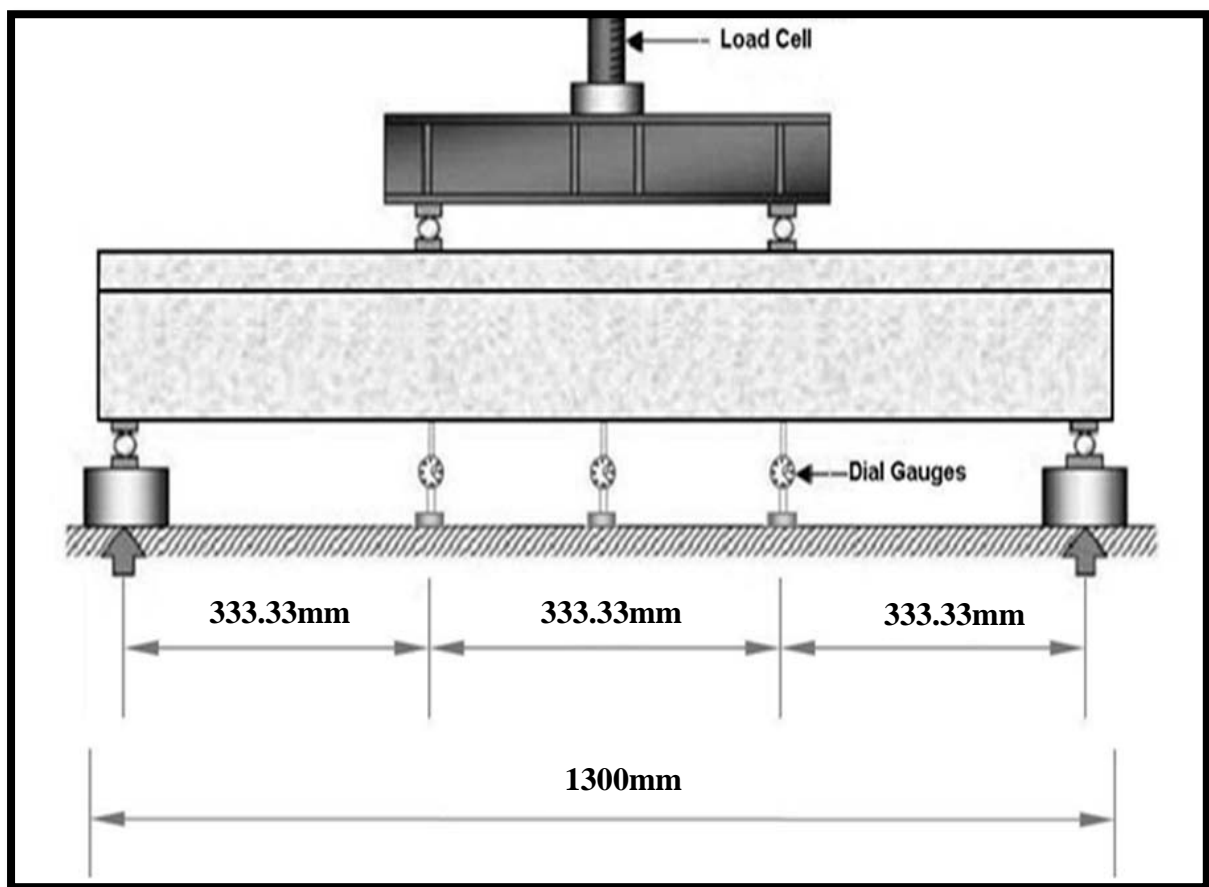


Figure 3-10. Details of the Test setup with location of dial gauges

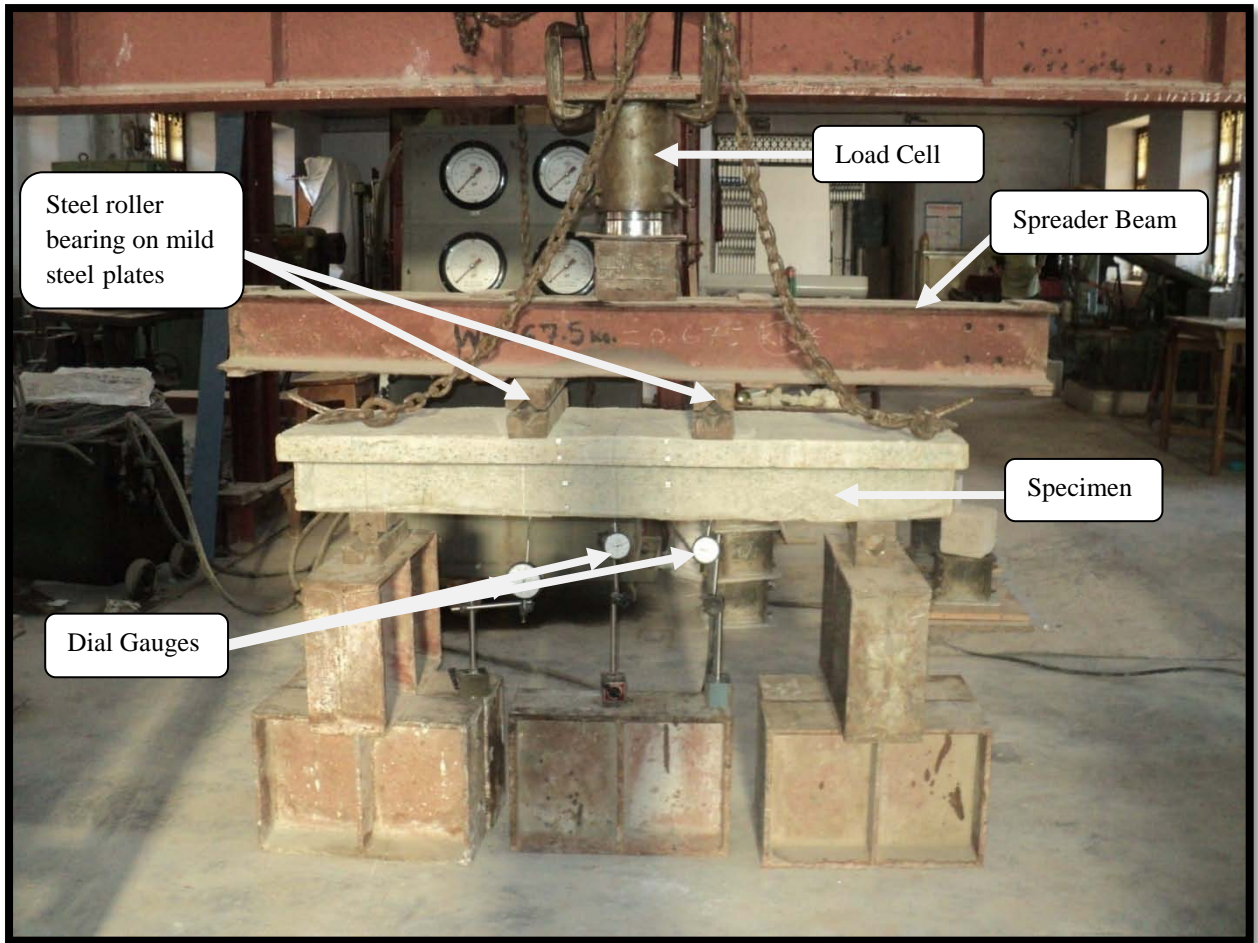


Figure 3-11. Experimental Setup for testing of beams

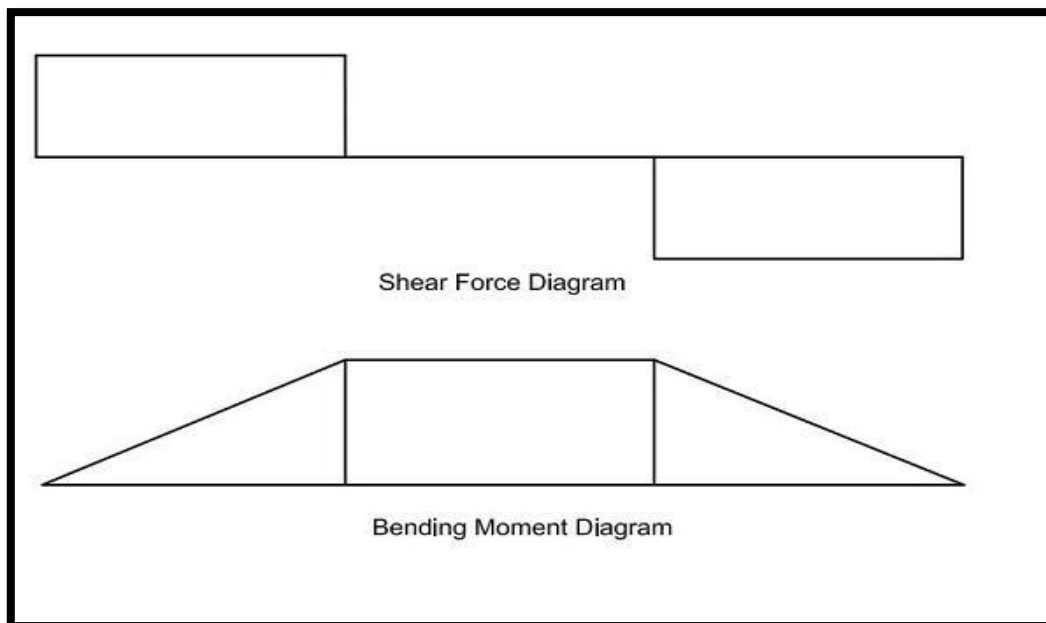


Figure 3-12. Shear force and bending moment diagram for four point static loading

3.3 DESCRIPTION OF SPECIMENS

The experimental program consists of 13 number of simply supported RC T-beams. of same longitudinal reinforcement of two numbers of 20mm ϕ and one number of 10mm ϕ was provided.

3.3.1 BEAM - 1

CONTROL BEAM (CB)

The control beam (CB) not strengthened with GFRP. It is designed to achieve the shear failure under four-point static loading test. It is totally weak in shear i.e., shear deficient beam shown in figure 3-13.

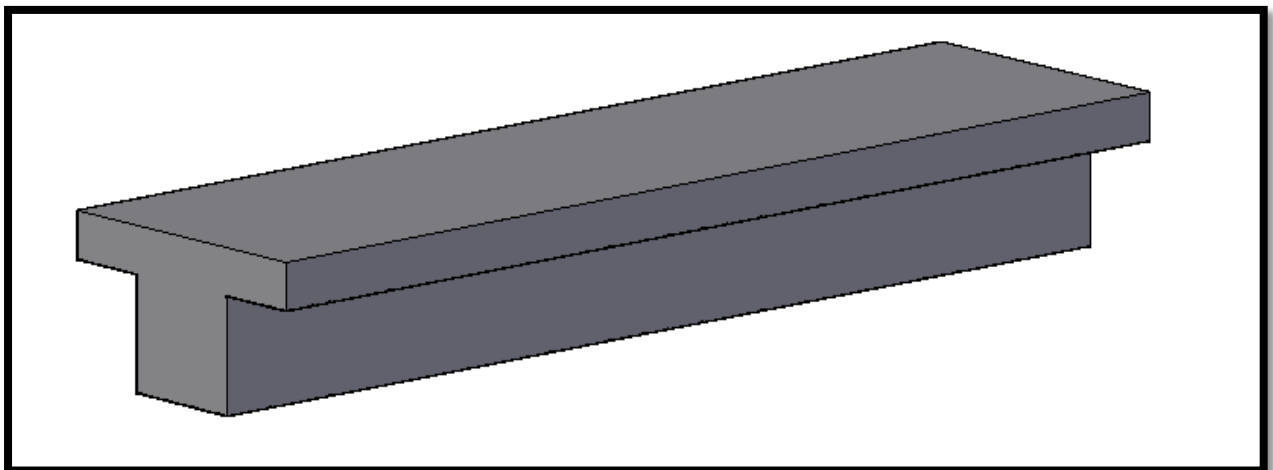


Figure 3-13. Model of T-beam without GFRP – CB

3.3.2 BEAM – 2

STRENGTHENED BEAM 1 (SB1)

The beam (SB1) is modeled with two layers of GFRP having U-wrap on bottom and web portions of the shear span as show in figure 3-14 (0 to $L/3$ and $2L/3$ to L distance from left support). The same four-point static loading is applied at the middle-third locations.

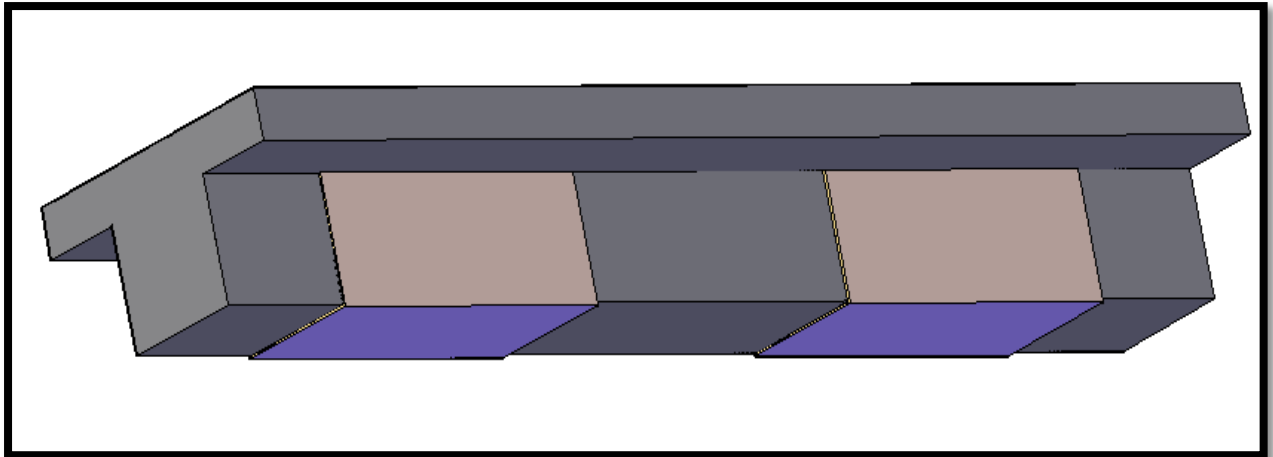


Figure 3-14. Model of T-beam with GFRP – SB1

3.3.3 BEAM – 3

STRENGTHENED BEAM 2 (SB2)

The beam (SB2) was strengthened by applying two layers of GFRP on web portions on shear span region (0 to $L/3$ and $2L/3$ to L distance from left support) only on the sides of the beam as shown in Figure 3-15.

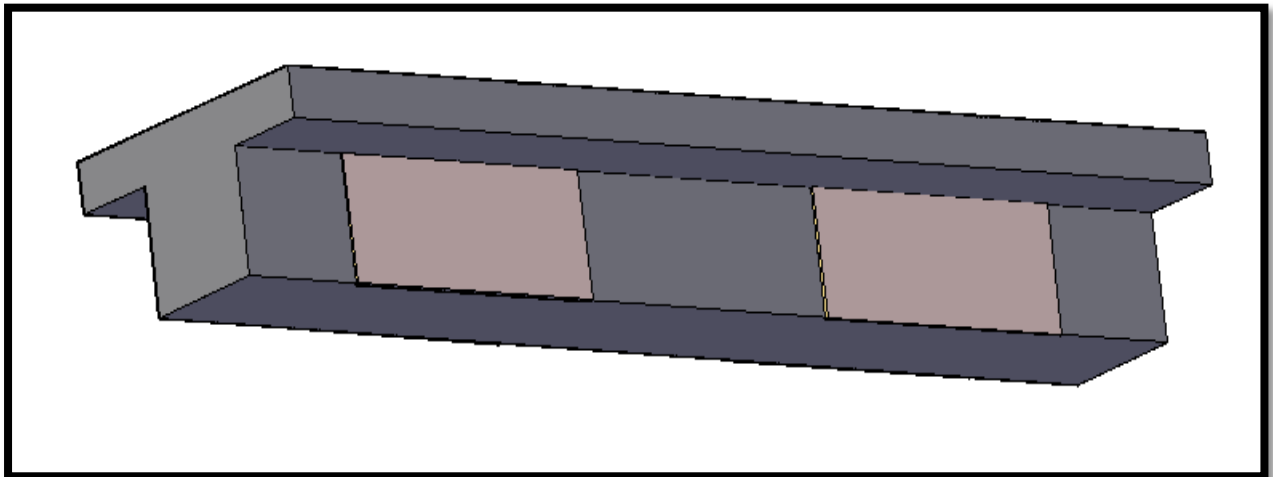


Figure 3-15. Model of T-beam with GFRP – SB2

3.3.4 BEAM – 4

STRENGTHENED BEAM 3 (SB3)

The beam (SB3) was strengthened by applying two layers of GFRP U-strips on web portions and bottom on shear span region (0 to $L/3$ and $2L/3$ to L distance from left support) with three equal strips on both sides of the beam, each strip of size thickness as 50mm and the spacing between the strips is 50mm shown in figure 3-16.

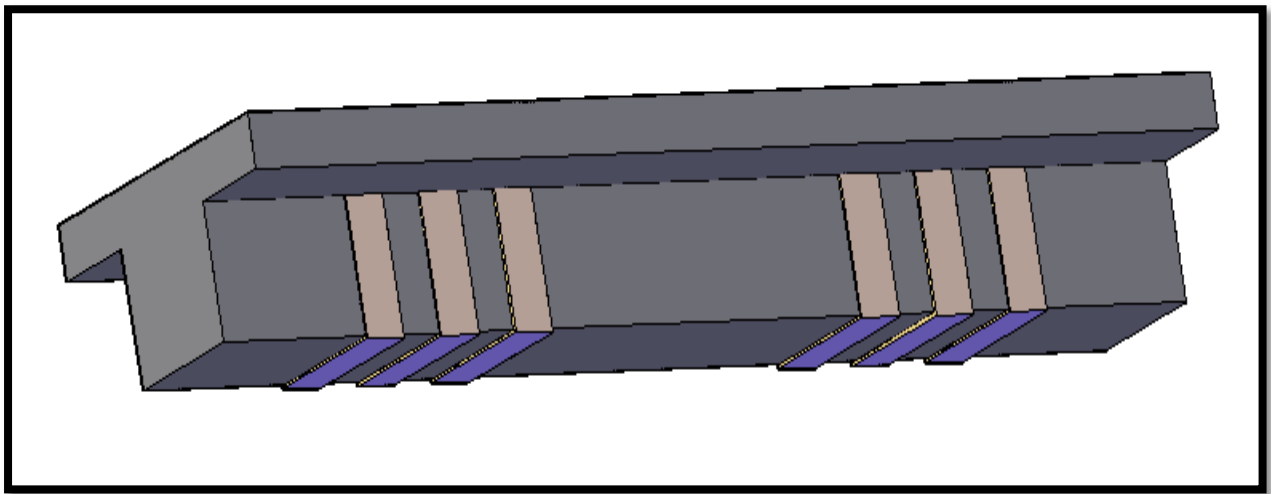


Figure 3-16. Model of T-beam with GFRP – SB3

3.3.5 BEAM – 5

STRENGTHENED BEAM 4 (SB4)

The beam (SB4) was strengthened by applying two layers of GFRP strips only on web portions on shear span region (0 to $L/3$ and $2L/3$ to L distance from left support) with three equal strips on both sides of the beam as shown in figure 3-17.

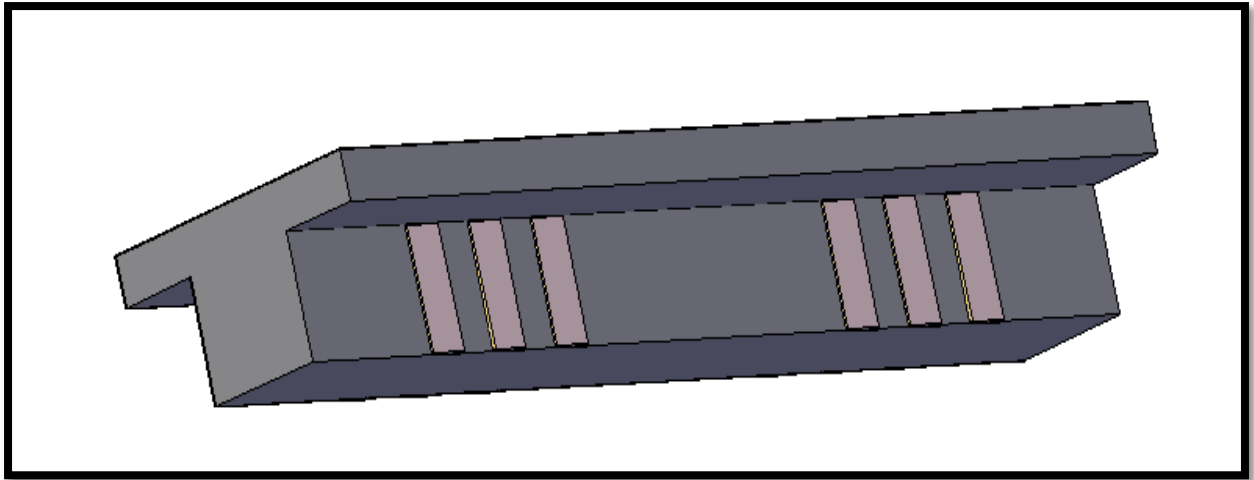


Figure 3-17. Model of T-beam with GFRP – SB4

3.3.6 BEAM – 6

STRENGTHENED BEAM 5 (SB5)

The beam (SB5) was strengthened by applying two layers of GFRP strips only on sides of web portions on shear span region (0 to $L/3$ and $2L/3$ to L distance from left support) with two equal strips on both sides of the beam which is inclined to 45° as shown in figure 3-18, each strip of size thickness as 50mm and the spacing between the strips is 50mm.

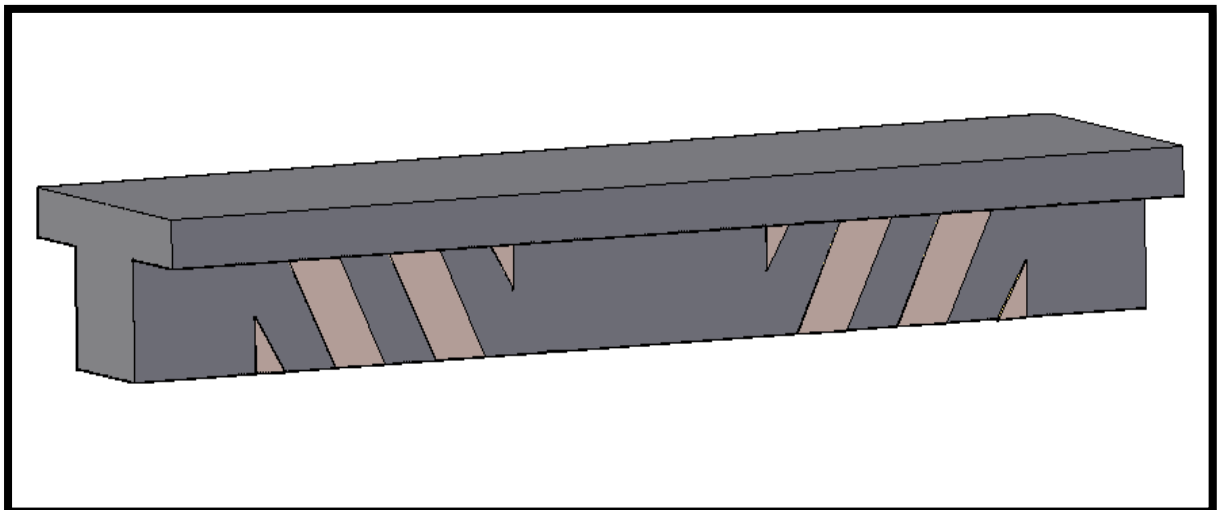


Figure 3-18. Model of T-beam with GFRP – SB5

3.3.7 BEAM – 7

STRENGTHENED BEAM 6 (SB6)

The beam (SB6) was strengthened by applying two layers of GFRP strips only on web portions on shear span region (0 to L/3 and 2L/3 to L distance from left support) with two equal strips on both sides of the beam 'X' shaped orientation is made which is inclined to $+45^{\circ}$ / -45° as shown in figure 3-19, each strip of size thickness as 50mm and the spacing between the strips is 50mm.

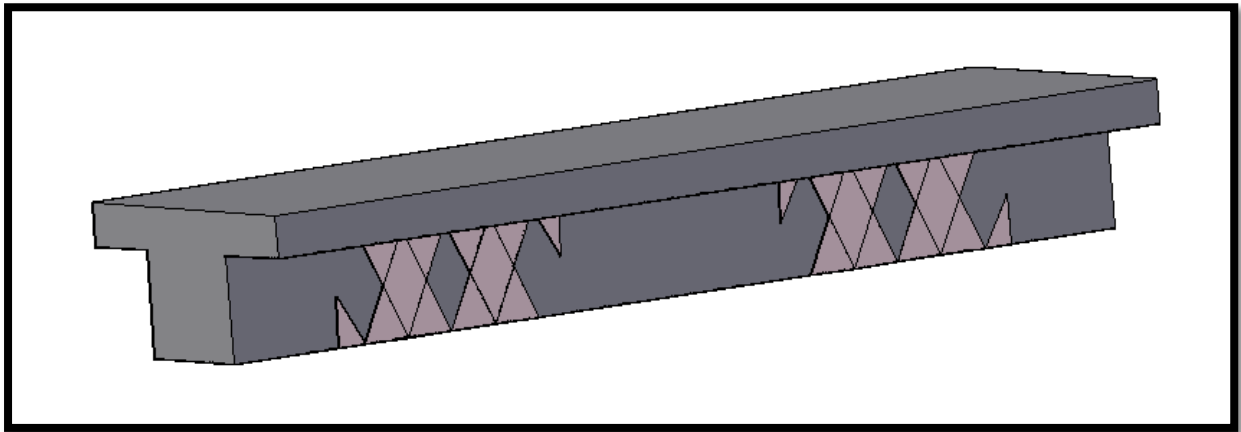


Figure 3-19. Model of T-beam with GFRP – SB6

3.3.8 BEAM – 8

STRENGTHENED BEAM 7 (SB7)

The beam (SB7) was strengthened by applying two layers of GFRP strips only on web portions on shear span region (0 to L/3 and 2L/3 to L distance from left support). The fiber orientation is inclined to $+45^{\circ}$ / -45° to the base of the beam as show in the figure 3-20.

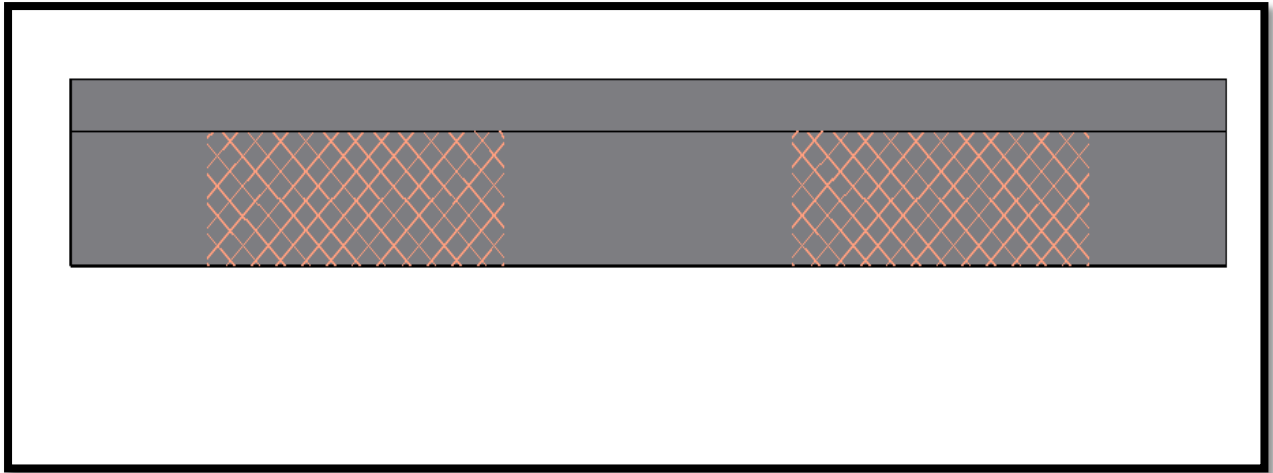


Figure 3-20. Model of T-beam with GFRP – SB7

3.3.9 BEAM – 9

STRENGTHENED BEAM 8 (SB8)

The beam (SB8) is modeled with two layers of GFRP having U-wrap on bottom and web portions on the shear span as show in figure 3-21 (0 to $L/3$ and $2L/3$ to L distance from left support) of the beam. It is found that in most cases debonding happens between the glass-fiber and the concrete. To reduce the debonding effect steel plates are used and tightened with bolts i.e., the anchorage system.

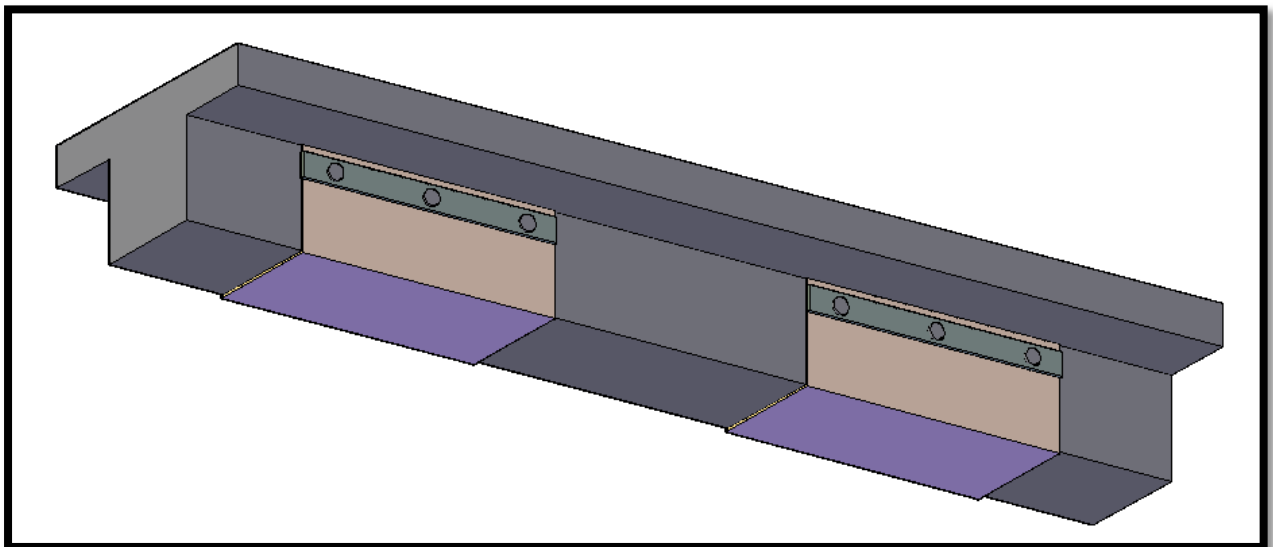


Figure 3-21. Model of T-beam with GFRP – SB8

3.3.10 BEAM – 10

STRENGTHENED BEAM 9 (SB9)

The beam (SB9) is modeled with four layers of GFRP having U-wrap on bottom and web portions on the shear span as show in figure 3-22 (0 to $L/3$ and $2L/3$ to L distance from left support) of the beam. Here, also to reduce the debonding effect steel plates are used and tightened with bolts.

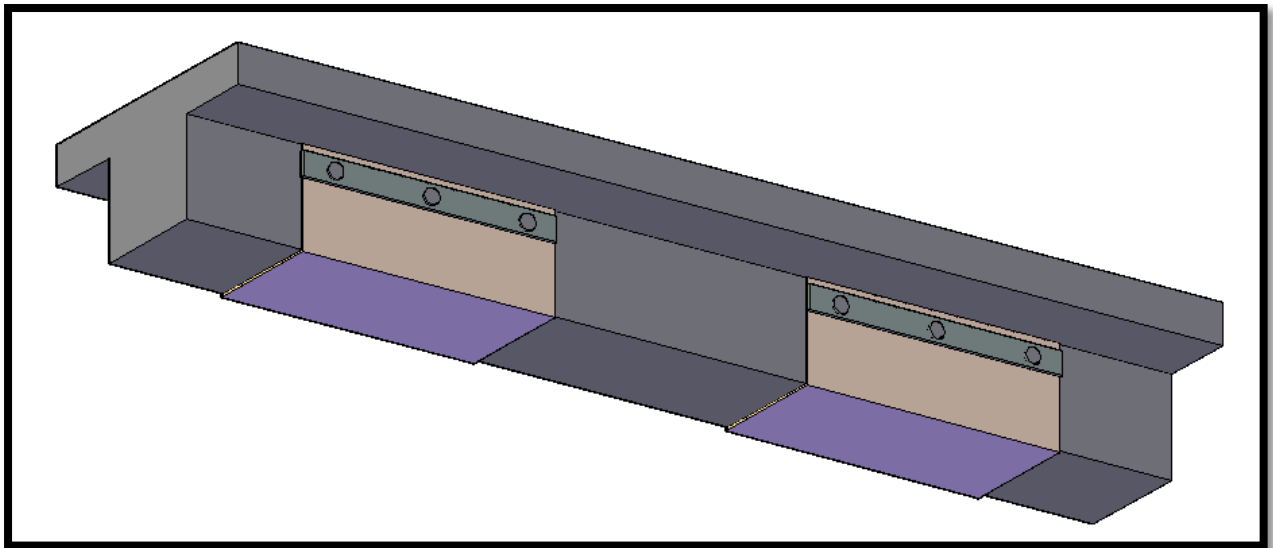


Figure 3-22. Model of T-beam with GFRP – SB9

3.3.11 BEAM – 11

STRENGTHENED BEAM 10 (SB10)

The beam (SB10) is modeled with eight layers of GFRP for the width of 233mm having U-wrap on bottom and web portions on the shear span of the beam as show in figure 3-23. When we wrapping a GFRP for a smaller width (say 233mm) the initial cracks are shifted to RC member where there is no GFRP in the shear region. It is understood that increase in the number of layers are not effective instead the shear zone should be covered with GFRP completely.

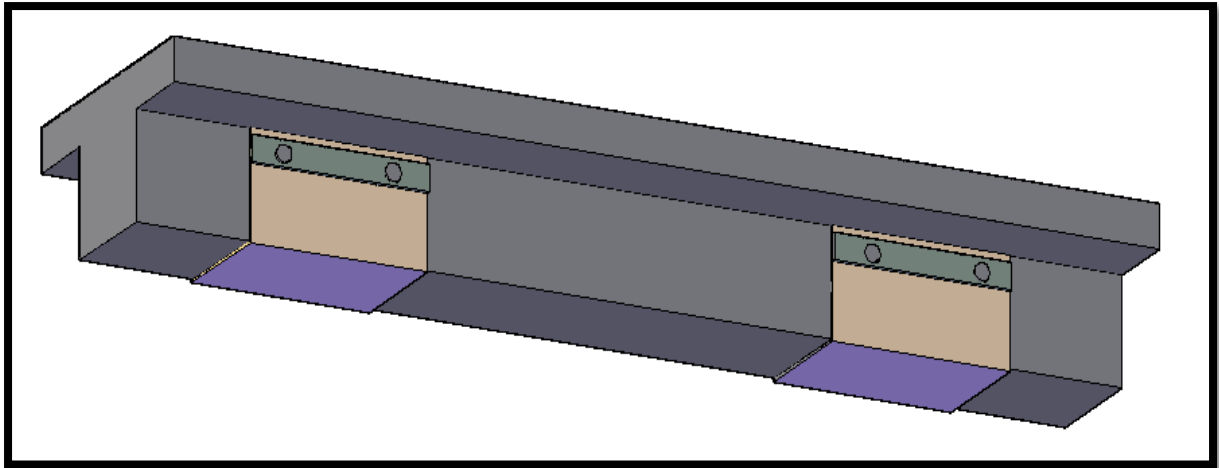


Figure 3-23. Model of T-beam with GFRP – SB10

3.3.12 BEAM – 12

STRENGTHENED BEAM 11 (SB11)

The beam (SB11) was strengthened by applying four layers of GFRP having U-wrap on bottom and web portions on the shear span (0 to $L/3$ and $2L/3$ to L distance from left support) with web opening in the shear zone of the RC beam as shown in figure 3-24. The same four point loading is applied at the middle-third locations. GFRP is used to increase the shear capacity of the beam.

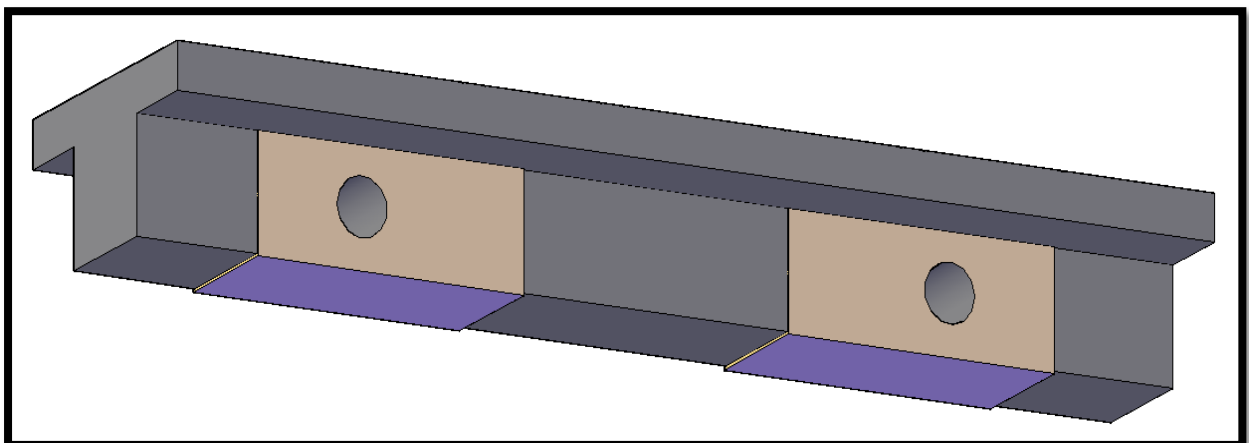


Figure 3-24. Model of T-beam with GFRP – SB11

3.3.13 BEAM – 13

STRENGTHENED BEAM 12 (SB12)

The beam (SB12) was strengthened by applying four layers of GFRP having U-wrap on bottom and web portions on the shear span (0 to $L/3$ and $2L/3$ to L distance from left support) with web opening in the shear zone of the RC beam as shown in figure 3-25. It is found that previous case debonding happens between the glass-fiber and the concrete. To reduce the debonding effect steel plates are used and tightened with bolts. The same four point loading is applied at the middle-third locations.

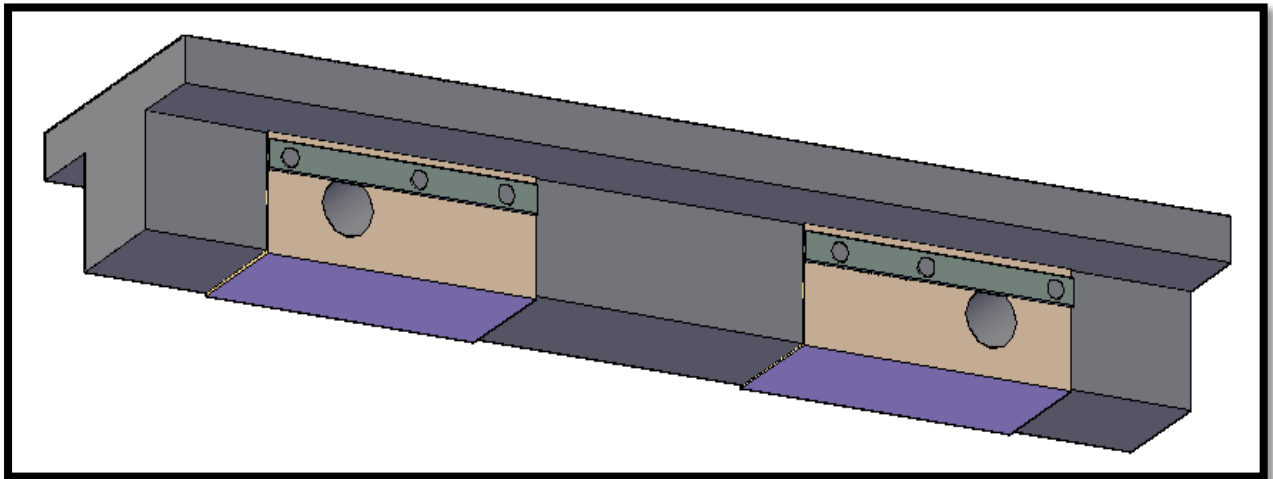


Figure 3-25. Model of T-beam with GFRP – SB12

3.4 SUMMARY

Thirteen beams were tested in this experimental investigation. One control beams was tested, seven beams were strengthened with different orientations of GFRP, three beams were strengthened with epoxy bonded GFRP with anchorage system to avoid debonding and other two beams were strengthened with GFRP which has a hole in the shear region and with an anchorage system. The detail descriptions of above mentioned beams are presented in Table 3.8.

Table 3.8 Beam test parameters and material properties

Beam ID	f_c (MPa)	Tension Reinforcement	Yield Stress, f_y (MPa)	Material Type	Sheet Thickness (mm)	Strengthening system with GFRP sheets
CB	22.21	2 ϕ 20mm, 1 ϕ 10mm	470, 529	--	--	Control Beam (No sheets)
SB1	24.88	2 ϕ 20mm, 1 ϕ 10mm	470, 529	GFRP	1	Two layers bonded to the bottom and sides of shear span of beam (U-shape)
SB2	24.00	2 ϕ 20mm, 1 ϕ 10mm	470, 529	GFRP	1	Two layers continuous bonded only in the sides of shear span of beam
SB3	23.32	2 ϕ 20mm, 1 ϕ 10mm	470, 529	GFRP	1	Two layers strip bonded to the bottom and sides of shear span of beam (U-shape strip)
SB4	23.13	2 ϕ 20mm, 1 ϕ 10mm	470, 529	GFRP	1	Two layers strip bonded only in the sides of shear span of beam
SB5	24.12	2 ϕ 20mm, 1 ϕ 10mm	470, 529	GFRP	1	Two layers bonded in inclined strip (+45°) angle only in the sides of shear span of beam

SB6	23.68	2 ϕ 20mm, 1 ϕ 10mm	470, 529	GFRP	1	Two layers bonded 'X' shape orientation strip (+45°/-45°) angle only in the sides of shear span of beam
SB7	24.10	2 ϕ 20mm, 1 ϕ 10mm	470, 529	GFRP	1	Two layers fully continuous bonded (+45°) angle only in the sides of shear span of beam
SB8	24.06	2 ϕ 20mm, 1 ϕ 10mm	470, 529	GFRP	1	Two layers bonded to the bottom and sides with steel bolt-plate (SBP) arrangement i.e., Anchoring System only in shear span of the beam (U-shape)
SB9	23.08	2 ϕ 20mm, 1 ϕ 10mm	470, 529	GFRP	2.5	Four layers bonded to the bottom and sides with steel bolt-plate (SBP) arrangement i.e., Anchoring System only in shear span of the beam (U-shape)
SB10	23.47	2 ϕ 20mm, 1 ϕ 10mm	470, 529	GFRP	4.5	Eight layers bonded to the bottom and sides with steel bolt-plate (SBP) arrangement i.e., Anchoring System only in shear span upto 233mm distance from the support of the beam (U-shape)
SB11	23.68	2 ϕ 20mm, 1 ϕ 10mm	470, 529	GFRP	2.5	Four layers bonded to the bottom and sides of shear span excluding the hole part of beam

SB12	23.92	2 ϕ 20mm, 1 ϕ 10mm	470, 529	GFRP	2.5	Four layers bonded to the bottom and sides of shear span excluding the hole part with steel bolt-plate (SBP) arrangement i.e., Anchoring system of beam.
-------------	-------	---------------------------------------	-------------	------	-----	----------------------------------------------------------------------------------------------------------------------------------------------------------

CHAPTER - 4

TEST RESULTS &

DISCUSSIONS



CHAPTER - 4

TEST RESULTS AND DISCUSSIONS

4.1 INTRODUCTION

In this chapter, the results obtained from the testing of thirteen number RC T-Beams for the experimental program are interpreted. Their behaviours throughout the test are described with respect to initial crack load and ultimate load carrying capacity, deflection, crack pattern and modes of failure.

All the beams except the control beam (CB) are strengthened with various patterns of GFRP sheets. All of the specimens were cast without stirrups. The beam designated as SB1 was strengthened with two layers of bi-directional GFRP sheets having U-wrap on shear spans (0 to $L/3$ and $2L/3$ to L distance from left support) of the beam. The beam SB2 was strengthened with two layers of bi-directional GFRP sheets having only on sides of web on shear span of the beam. The beam SB3 was strengthened with two layers of bi-directional GFRP strips in the form of U-wrap on shear span with three equal strips on both sides of the beam, each strip having width 50mm and the spacing between the strips being 50mm of the beam. The beam SB4 was strengthened with two layers of bi-directional GFRP strips only on sides of web on shear span of the beam. The beam SB5 was strengthened with two layers of GFRP strips inclined at 45° (each strip of width 50mm and the spacing is 50mm) on the sides of the web on the shear span of the beam. The beam SB6 was strengthened with two layers of GFRP strips inclined at $+45^\circ$ fiber orientations in one direction and $+135^\circ$ fiber orientations in another direction making an “X-shape” (each strip is width 50mm and the spacing is 50 mm) on the sides of web on the shear span of the beam. The beam SB7 was strengthened with two layers of GFRP continuous wrap inclined at $+45^\circ$ fiber orientation in one direction and $+135^\circ$ fiber orientations in another direction to the base of the beam on the sides of web on shear span of the beam. The beam SB8 was strengthened with two layers of bi-directional GFRP sheets having U-wrap on shear span (0 to $L/3$ and $2L/3$ to L distance from left support) of the beam. The beam SB9 was strengthened with four layers of bi-directional GFRP sheets having U-wrap on shear span of the beam anchored with steel bolt-plate technique. The beam SB10 was strengthened with eight layers of bi-directional GFRP sheets for a length of 233mm having U-wrap on shear span of the beam anchored with steel bolt-plate technique. The beam SB11 was strengthened with four layers of bi-directional GFRP sheets having U-wrap on

shear span (0 to $L/3$ and $2L/3$ to L distance from left support) excluding the web openings of the beam. The beam SB12 was strengthened with four layers of bi-directional GFRP sheets having U-wrap on shear span (0 to $L/3$ and $2L/3$ to L distance from left support) excluding the web openings of the beam.

4.1.1 Crack Behaviour and Failure Modes

The crack behaviour and failure modes of the thirteen number of beams tested in the experimental program are described below.

4.1.1.1 Control Beam (CB)

The control beam (CB) was cast with a reinforcement of two numbers of 20 mm bar and one number of 10 mm bar on tension face. The stirrups were not provided in the beam to make it shear deficient. The beam was tested by applying the point loads gradually. Figure 4-1 (a) shows the experimental test setup of control beam under four point loading. The first hair crack was visible in the shear span at a load of 70 kN as shown in figure 4-1 (b). This crack appeared at the mid-height zone of the web of the beam. As the load increased beyond the first crack load, many inclined cracks were also developed and the first visible crack started widening and propagated as illustrated in figure 4-1 (c). With further increase in load, the beam finally failed in shear at a load of 162 kN exhibiting a wider diagonal shear crack as shown in figure 4-1 (d). The first shear crack became the critical crack for the ultimate failure of the control beam.



(a) Experimental Setup of the CB under four-point loading



(b) Hair line crack started at 70kN in shear region



(c) Crack Pattern at L/3 distance (Near Left Support)



(d) Crack Pattern at ultimate failure of specimen CB

Figure 4-1. (a) Experimental Setup of the CB under four-point loading, (b) Hair line crack started at 70kN in shear region, (c) Crack Pattern at L/3 distance (Near Left Support), (d) Crack Pattern at ultimate failure of specimen CB

4.1.1.2 STRENGTHENED BEAM (SB)

4.1.1.2.1 Strengthened Beam 1 (SB1)

The beam SB1 was strengthened with two layers of bi-directional GFRP sheets having U-wrap on shear spans (0 to $L/3$ and $2L/3$ to L distance from left support). The test setup of the beam is shown in figure 4-2 (a). The initial crack in concrete as appeared in case of control beam could not be traced out because the shear zones were fully wrapped with GFRP sheets. The failure was initiated by the debonding of GFRP sheets (with a layer of concrete adhered to them) over the main shear crack in the same location as observed in beam SB1. The crack patterns became visible after debonding of GFRP sheets as shown in Figure 4-2 (b). As the load was enhanced, the debonding failure was followed by a shear failure at an ultimate load of 230 kN as shown in Figure 4-2 (c). The strengthening of beam SB1 with GFRP U-wraps resulted in a 29.56% increase in shear capacity over the control beam.



(a) Experimental Setup of beam SB1



(b) Initiation of debonding of GFRP sheet



(c) Complete debonding followed by shear failure

Figure 4-2. (a) Experimental Setup of beam SB1, (b) Initiation of debonding of GFRP sheet,

(c) Complete debonding followed by shear failure

4.1.1.2.2 Strengthened Beam 2 (SB2)

The beam SB2 was strengthened with two layers of bi-directional GFRP sheets having only on sides of web on shear span (0 to $L/3$ and $2L/3$ to L distance from left support). The test setup of the beam is shown in figure 4-3 (a). The initial crack in concrete as appeared in SB2 could not be observed because the shear zones were fully wrapped with GFRP sheets. The failure mode was initiated by the debonding of GFRP sheets with concrete cover of beam SB1 as shown in figure 4-3 (b). The crack patterns became visible after debonding of GFRP sheets. The debonding failure of GFRP sheet was followed by shear failure and the beam finally failed at load of 200 kN as shown in figure 4-3 (c). There is no noticeable increase in shear capacity compared to beam SB1. However, there is a 19% increase in shear capacity over the control beam.



(a) Experimental Setup of beam SB2



(b) Initiation of debonding of GFRP sheet



(c) Shear failure of beam -Debonding of GFRP sheet

Figure 4-3. (a) Experimental Setup of beam SB2, (b) Initiation of debonding of GFRP sheet,

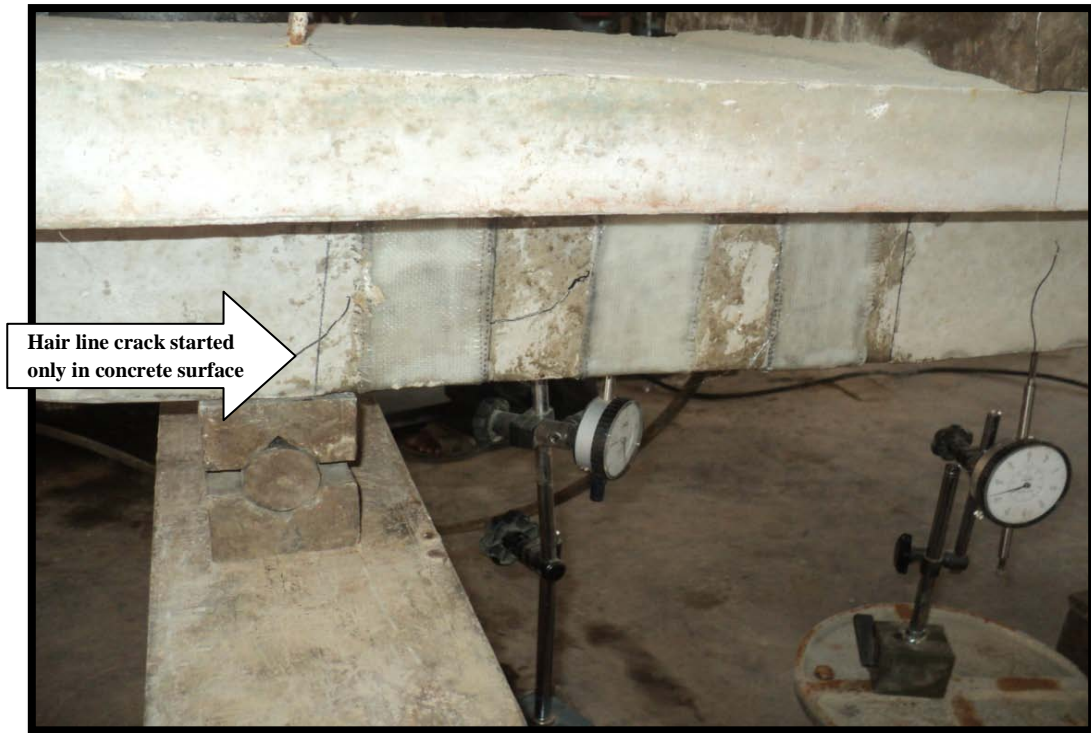
(c) Shear failure of beam - Debonding of GFRP sheet

4.1.1.2.3 Strengthened Beam 3 (SB3)

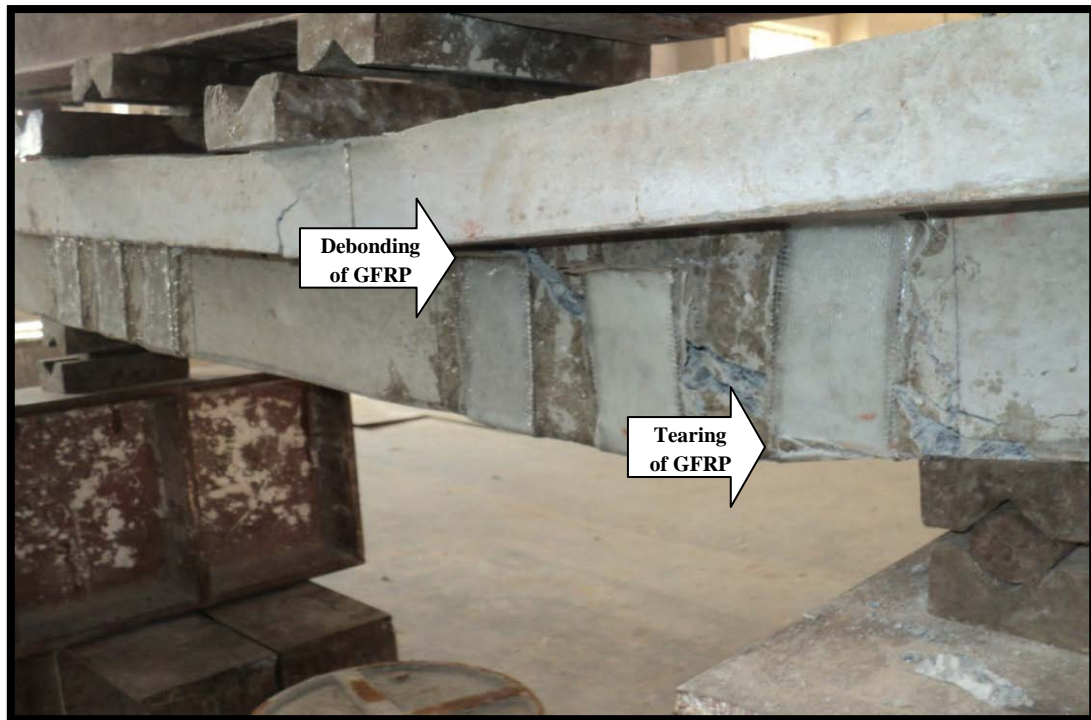
The beam SB3 was strengthened with two layers of bi-directional GFRP strips in the form of U-wrap on shear span (0 to $L/3$ and $2L/3$ to L distance from left support) with three equal strips on both sides of the beam, each strip of width 50mm and the spacing between the strips is 50mm. The test setup of the beam is shown in figure 4-4 (a). The initial diagonal shear crack started at a load of 100 kN only on the concrete surface and failed by first tearing the GFRP sheet, then debonding occur in which the FRP sheet was separated. The failure occurred due to debonding of GFRP over the main diagonal shear crack, in the area between the centre of shear crack and its upper end as shown in figure 4-4 (b). The load carrying capacity of beam SB3 with GFRP strips is relatively close to that of beam SB1 with continuous sheets. Sudden failure of beam SB3 occurred at an ultimate load of 215 kN as shown in figure 4-4 (c). The strengthening of beam SB3 with GFRP U-wrap strips on the beam resulted in a 24.65% increase in the shear capacity over the control beam.



(a) Experimental Setup of beam SB3



(b) Hair Line Crack Started at load of 100 kN on concrete surface



(c) Completely tearing & debonding of GFRP sheet followed by shear failure

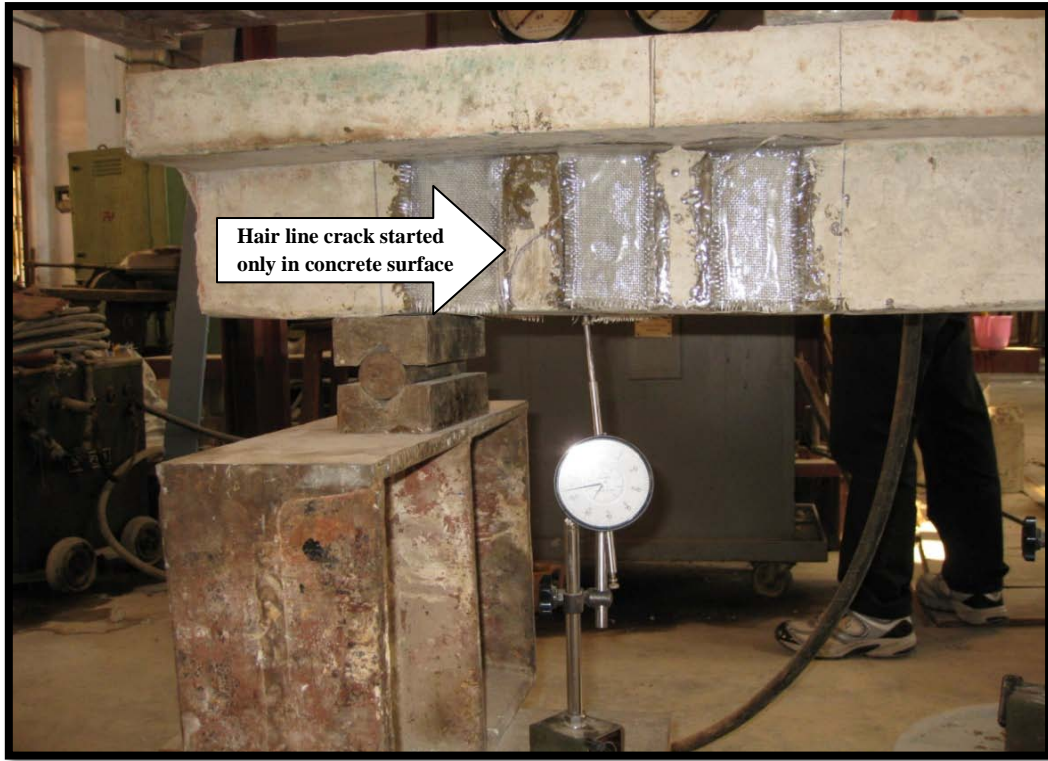
Figure 4-4. (a) Experimental Setup of beam SB3, (b) Hair Line Crack Started at load of 100 kN on concrete surface, (c) Completely tearing & debonding of GFRP sheet followed by shear failure

4.1.1.2.4 Strengthened Beam 4 (SB4)

The beam SB4 was strengthened with two layers of bi-directional GFRP strips only on sides of web on shear span of the beam (0 to $L/3$ and $2L/3$ to L distance from left support). The test setup of the beam is shown in figure 4-5 (a). The initial diagonal shear crack was formed at a load of 90 kN only in the concrete surface and propagated as the load increased in a similar manner as in CB and SB3 as shown in figure 4-5 (b). Brittle failure occurred at a load of 172 kN by debonding of GFRP strips followed by shear failure as shown in figure 4-5 (c). The location of debonding area was different from beam SB3 which was below the main shear crack between its centre and its lower end. Strengthening of beam SB4 with GFRP strips on the beam sides resulted in a 5.81% increase in the shear capacity.



(a) Experimental Setup of beam SB4



(b) Hair Line Crack Started at load of 90 kN on concrete surface



(c) Debonding of GFRP sheet followed by shear failure

Figure 4-5. (a) Experimental Setup of beam SB4, (b) Hair Line Crack Started at load of 90 kN on concrete surface, (c) Debonding of GFRP sheet followed by shear failure

4.1.1.2.5 Strengthened Beam 5 (SB5)

The beam SB5 was strengthened with two layers of GFRP strips inclined at 45° (each strip of width 50mm and the spacing is 50mm) on the sides of web on shear span (0 to $L/3$ and $2L/3$ to L distance from left support) of the beam. The test setup of the beam is shown in figure 4-6 (a). The initial diagonal shear crack was formed at a load of 116 kN on the concrete surface and failed by tearing the GFRP sheet as shown in figure 4-6 (b). The brittle failure occurred at an ultimate load of 220 kN by tearing of GFRP strips followed by shear failure as shown in figure 4-6 (c). The location of tearing area was in between the centre and upper end of the main shear crack. The strengthening of beam SB5 with GFRP inclined strips on the beam sides resulted in a 26.36% increase in the shear capacity over the control beam.



(a) Experimental Setup of beam SB5



(b) Initiation of tearing of GFRP sheet Started at load of 80 kN



(c) Tearing of GFRP sheet followed by shear failure

Figure 4-6. (a) Experimental Setup of beam SB5, (b) Initiation of tearing of GFRP sheet Started at load of 80 kN, (c) Tearing of GFRP sheet followed by shear failure

4.1.1.2.6 Strengthened Beam 6 (SB6)

The beam SB6 was strengthened with two layers of GFRP strips inclined at $+45^\circ$ fiber orientations in one direction and $+135^\circ$ fiber orientations in another direction i.e., “X-shape” (each strip of width 50mm and the spacing is 50mm) on the sides of web on shear span (0 to $L/3$ and $2L/3$ to L distance from left support) of the beam. The test setup of the beam is shown in figure 4-7 (a). The initial diagonal shear crack was formed at a load of 108 kN on the concrete surface and the crack propagated as the load increased in a similar manner of CB. The brittle shear failure was followed at an ultimate load of 228 kN due to the debonding of GFRP sheets as shown in figure 4-7 (b). The load carrying capacity of beam SB6 with GFRP strips was relatively close to that of beam SB5. The location of debonding area was in between the centre and upper end of the main shear crack. The strengthening of beam SB6 with GFRP inclined strips on the beam sides resulted in a 28.94% increase in the shear capacity over the control beam.



(a) Experimental Setup of beam SB6



(b) Debonding of GFRP sheet followed by shear failure

Figure 4-7. (a) Experimental Setup of beam SB6, (b) Debonding of GFRP sheet followed by shear failure

4.1.1.2.7 Strengthened Beam 7 (SB7)

The beam SB7 was strengthened with two layers of GFRP continuous wrap inclined at $+45^\circ$ fiber orientation in one direction and $+135^\circ$ fiber orientations with respect to the longitudinal direction of the beam on the sides of web on shear span (0 to $L/3$ and $2L/3$ to L distance from left support) of the beam. The test setup of the beam is shown in figure 4-8 (a). The initial crack on the concrete surface as appeared in SB7 could not be noticeable because the shear zones were fully wrapped with GFRP sheets. The failure mode was initiated by the debonding of GFRP sheets and the brittle shear failure was followed at an ultimate load of 230 kN as shown in figure 4-8 (b). The load carrying capacity of beam SB7 was almost close to that of the beam SB6 & SB5. Strengthening of beam SB7 with GFRP inclined continuous wrap on the sides of the beam resulted in a 30.17% increase in the shear capacity over the control beam.



(a) Experimental Setup of beam SB7



(b) Debonding of GFRP sheet followed by shear failure

Figure 4-8. (a) Experimental Setup of beam SB7, (b) Debonding of GFRP sheet followed by shear failure

4.1.1.2.8 Strengthened Beam 8 (SB8)

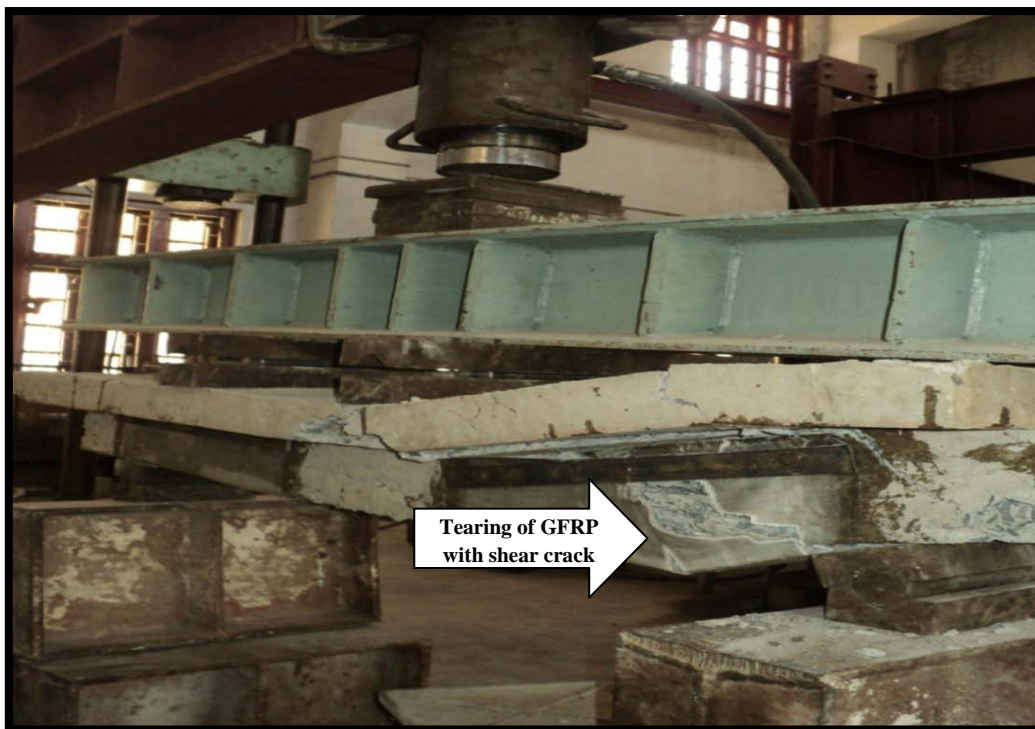
The beam SB8 was strengthened with two layers of bi-directional GFRP sheets having U-wrap on shear spans (0 to $L/3$ and $2L/3$ to L distance from left support) of the beam. The free ends of the U-wrap were anchored using steel bolt-plate arrangement. The test setup of the beam is shown in figure 4-9 (a). The failures of the previous strengthened beams were mainly due to debonding of GFRP sheets. In this experiment, the effect of anchorage system on the debonding of GFRP sheet from concrete was studied. The initial crack in concrete as appeared in control beam could not be traced out because the shear zones were fully wrapped with GFRP sheets. The failure was initiated by tearing of GFRP sheets over the main shear crack in the same location observed in beam CB as shown in figure 4-9 (b). As the load was enhanced, the failure was followed by shear failure at an ultimate load of 252 kN as shown in figure 4-9 (c). The strengthening of beam SB8 with GFRP U-wraps with anchorage system resulted in a 35.71% increase in shear capacity over the control beam.



(a) Experimental Setup of beam SB8



(b) Magnified view of Tearing of GFRP



(c) Failure pattern of SB8

Figure 4-9. (a) Experimental Setup of beam SB8, (b) Magnified view of Tearing of GFRP, (c) Failure pattern of SB8

4.1.1.2.9 STRENGTHENED Beam 9 (SB9)

The beam SB9 was strengthened with four layers of bi-directional GFRP sheets having U-wrap on shear spans (0 to $L/3$ and $2L/3$ to L distance from left support) of the beam and anchored with steel bolt-plate arrangement. The test setup of the beam is shown in figure 4-10 (a). Here, the initial crack in concrete as appeared in control beam could not be traced out because the shear zones were fully wrapped with GFRP sheets. The failure was initiated by tearing of GFRP sheets over the main shear crack as shown in figure 4-10 (b). As the load was enhanced, the failure was followed by shear failure at an ultimate load of 268 kN as shown in figure 4-10 (c). There was a marginal increase in shear strength compared to the beam SB8. The strengthening of beam SB9 with 4 layers of GFRP U-wrap with anchorage system resulted in a 39.55% increase in shear capacity over the control beam.



(a) Experimental Setup of beam SB9



(b) Prevention of debonding of GFRP sheet due to Anchoring System



(c) Magnified view of Tearing of GFRP followed by shear failure

Figure 4-10. (a) Experimental Setup of beam SB9, (b) Prevention of debonding of GFRP sheet due to Anchoring System, (c) Magnified view of Tearing of GFRP followed by shear failure

4.1.1.2.10 Strengthened Beam 10 (SB10)

The beam SB10 was strengthened with eight layers of bi-directional GFRP sheets for a length of 233mm having U-wrap on shear span (0 to $L/3$ and $2L/3$ to L distance from left support) of the beam and anchored with steel bolt-plate arrangement. The test setup of the beam is shown in figure 4-11 (a). It is observed that there is no failure in the shear span zone where strengthening was made. The crack shifted to the un-strengthened part of the shear span as shown in figure 4-11(b). The crushing of concrete near the support and the loading point was observed as shown in figure 4-11(c). The beam finally failed at an ultimate load of 272 kN as shown in figure 4-11(d). There was no significant increase in shear capacity compared to beam SB8 & SB9. However, there was an 40.44% increase in shear capacity compared to the control beam.



(a) Experimental Setup of beam SB10



(b) Crack shifted to the un-strengthened part of the shear span



(c) Crushing of concrete near the support and the loading point



(d) Failure pattern of SB10

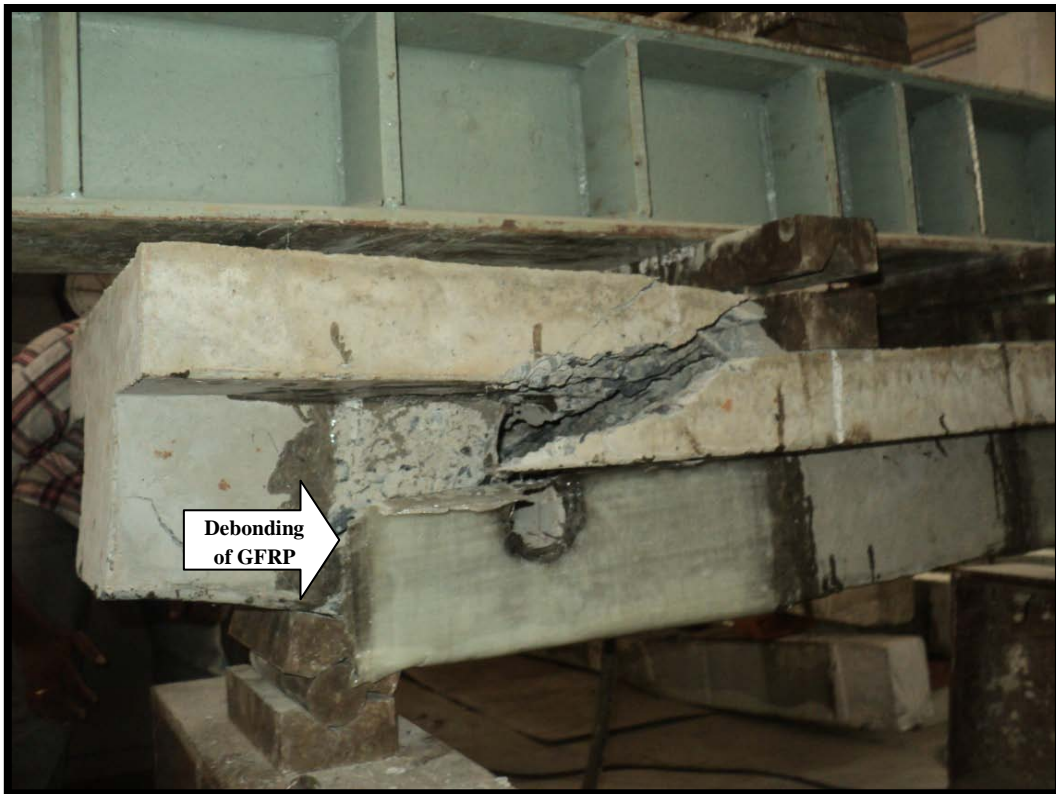
Figure 4-11. (a) Experimental Setup of SB10, (b) Crack shifted to the un-strengthened part of the shear span, (c) Crushing of concrete near the support and the loading point, (d) Failure pattern of SB10

4.1.1.2.11 Strengthened Beam 11 (SB11)

The beam with web openings SB11 was strengthened with four layers of bi-directional GFRP sheets having U-wrap on shear span (0 to $L/3$ and $2L/3$ to L distance from left support). The test setup of the beam is shown in figure 4-12 (a). The initial crack in concrete as appeared in case of control beam could not be traced out because the shear zones were fully wrapped with GFRP sheets. In this beam, failure was initiated by debonding of GFRP sheets over the main shear crack as shown in figure 4-12 (b). The debonding failure was followed by a beam-type shear failure at an ultimate load of 186 kN shown in figure 4-12 (c).



(a) Experimental Setup of beam SB1



(b) Debonding of GFRP sheet



(c) Failure Pattern of SB11 (Beam-type shear failure)

Figure 4-12. (a) Experimental Setup of beam SB11, (b) Debonding of GFRP sheet, (c) Failure Pattern of SB11 (Beam-type shear failure)

4.1.1.2.12 Strengthened Beam 12 (SB12)

The beam with web openings SB12 was strengthened with four layers of bi-directional GFRP sheets having U-wrap on shear span (0 to $L/3$ and $2L/3$ to L distance from left support). The free ends of the U-wrap were anchored using steel bolt-plate arrangement. The test setup of the beam is shown in figure 4-13 (a). The failure of the previous beam was mainly due to debonding of GFRP sheets. The effect of anchorage system on the debonding of GFRP sheet from concrete was studied. The initial crack in concrete as appeared in control beam could not be traced out because the shear zones were fully wrapped with GFRP sheets. The failure was initiated by tearing of GFRP sheets over the main shear crack as shown in figure 4-13 (b). A beam-type shear failure was observed at an ultimate load of 202 kN as shown in figure 4-13 (c). The shear strength of the beam SB12 with GFRP U-wraps with anchorage system was higher than the beam without end anchorage.



(a) Experimental Setup of beam SB12



(b) Tearing of GFRP sheet followed by Beam-type shear failure



(c) Crack Pattern of SB12

Figure 4-13. (a) Experimental Setup of beam SB12, (b) Tearing of GFRP sheet followed by Beam-type shear failure, (c) Crack Pattern of SB12

4.1.1 Load-deflection history

The mid-span deflection of the control and strengthened beams were measured at different load steps and the deflections under the point loads were also recorded. The load-deflection histories are illustrated in figures-4.14 to 4.26. It was observed that the deflection under the point load was less than that at the centre. These figures below show that the deflection curve was initially straight showing the linear relationship between the load and deflection and became non-linear with further increase in load.

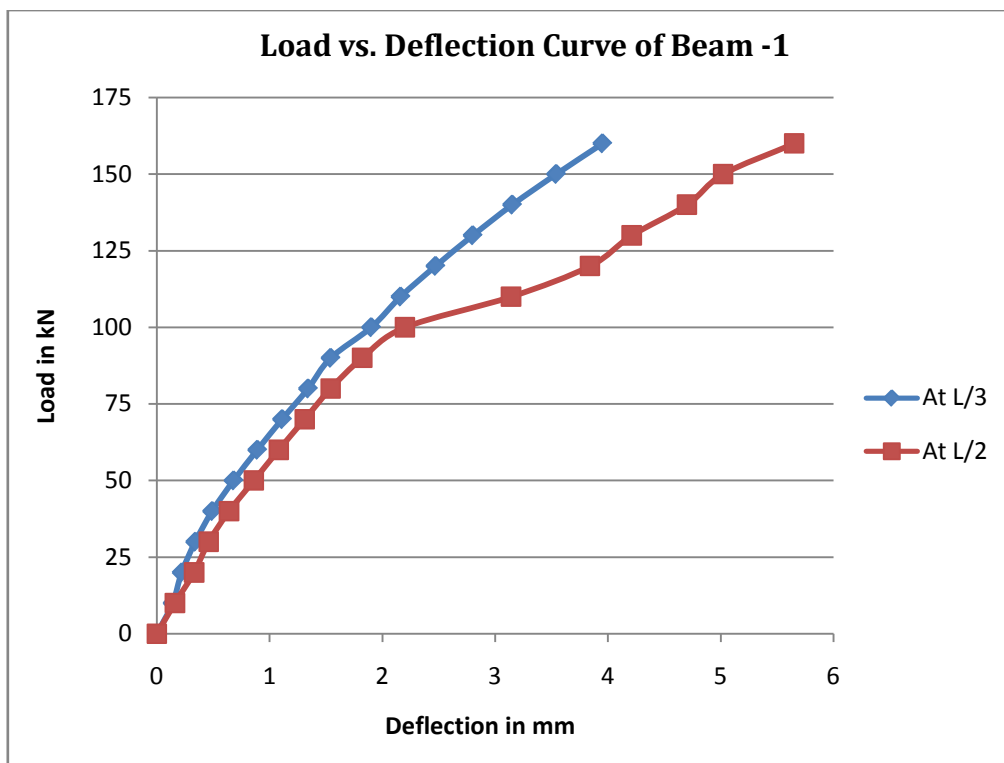


Figure 4-14. Load vs. Deflection Curve for CB

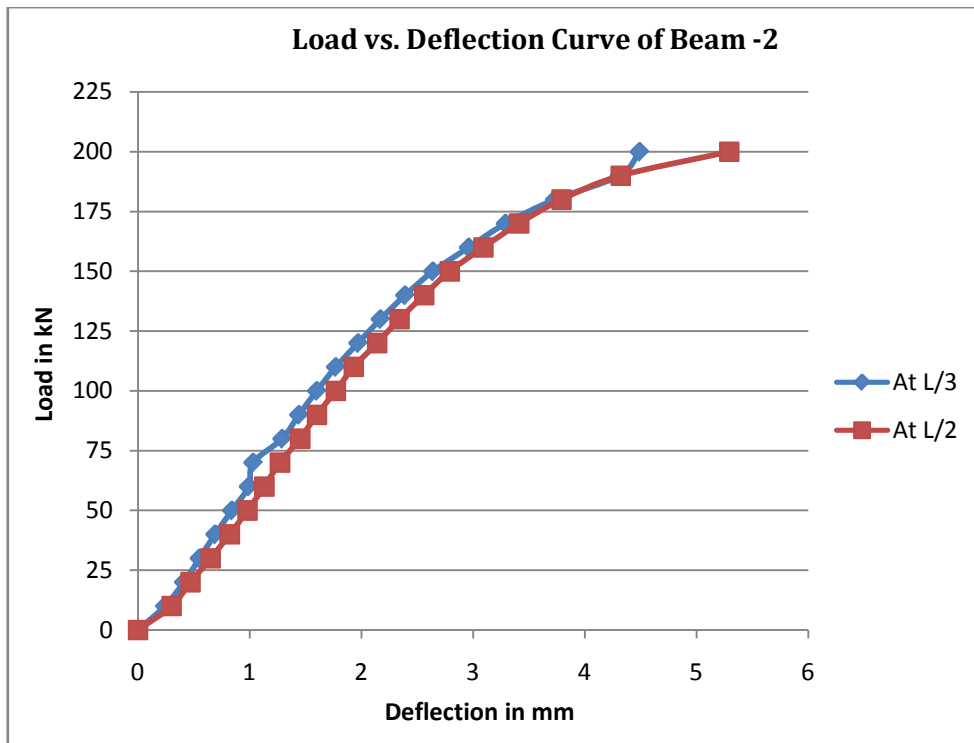


Figure 4-15. Load vs. Deflection Curve for SB1

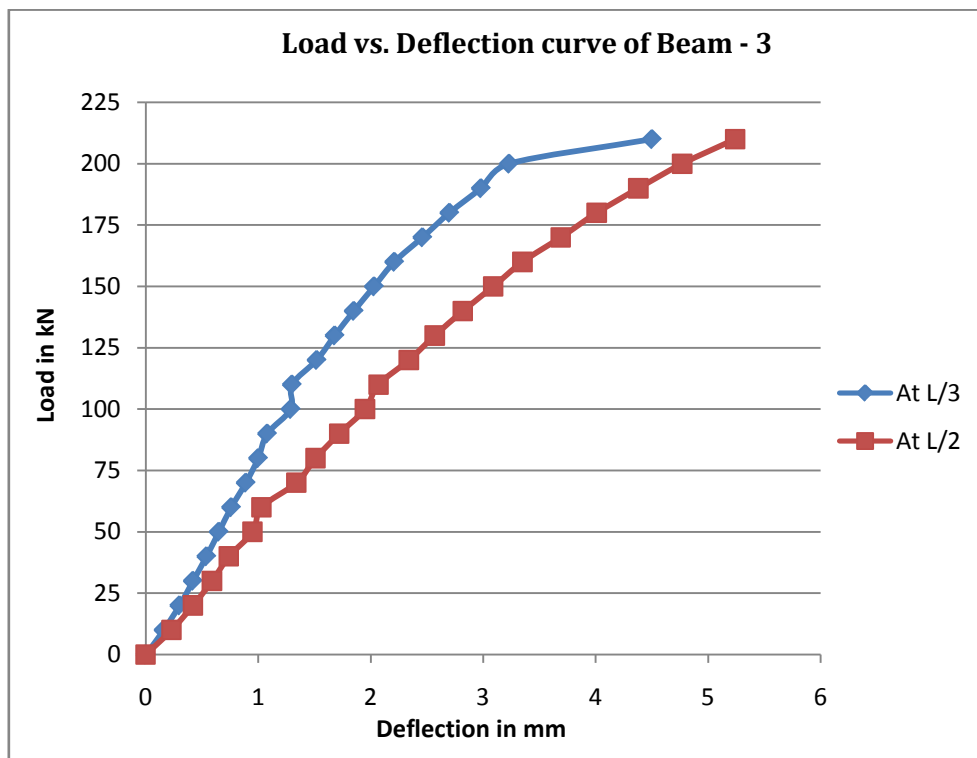


Figure 4-16. Load vs. Deflection Curve for SB2

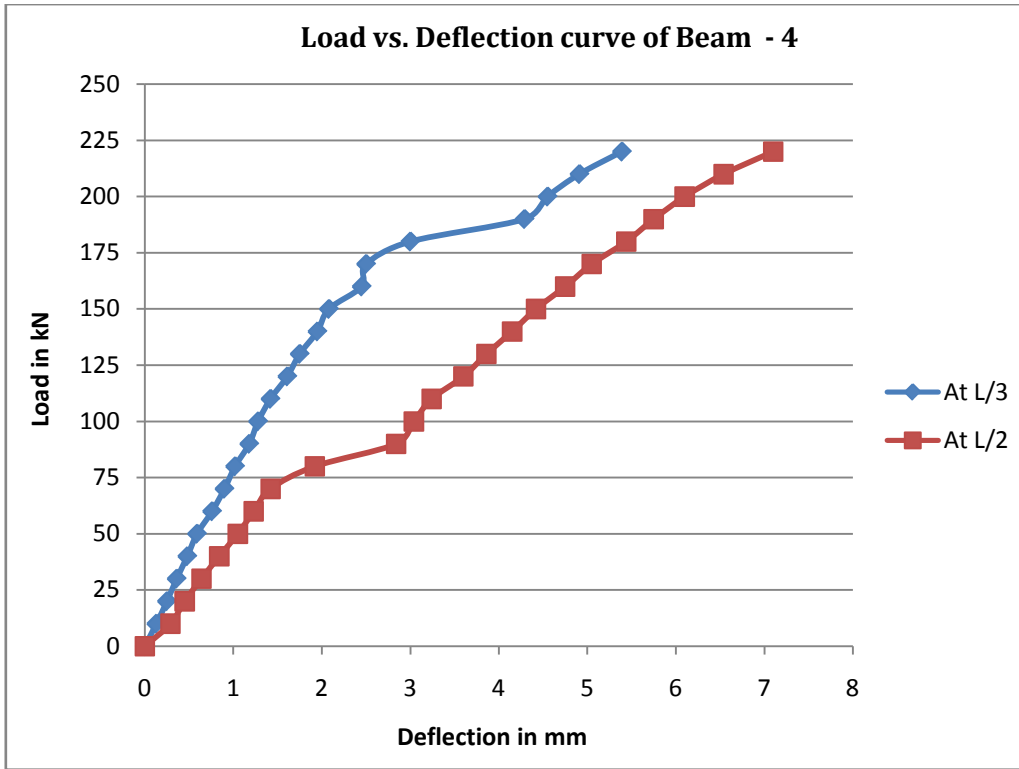


Figure 4-17. Load vs. Deflection Curve for SB3

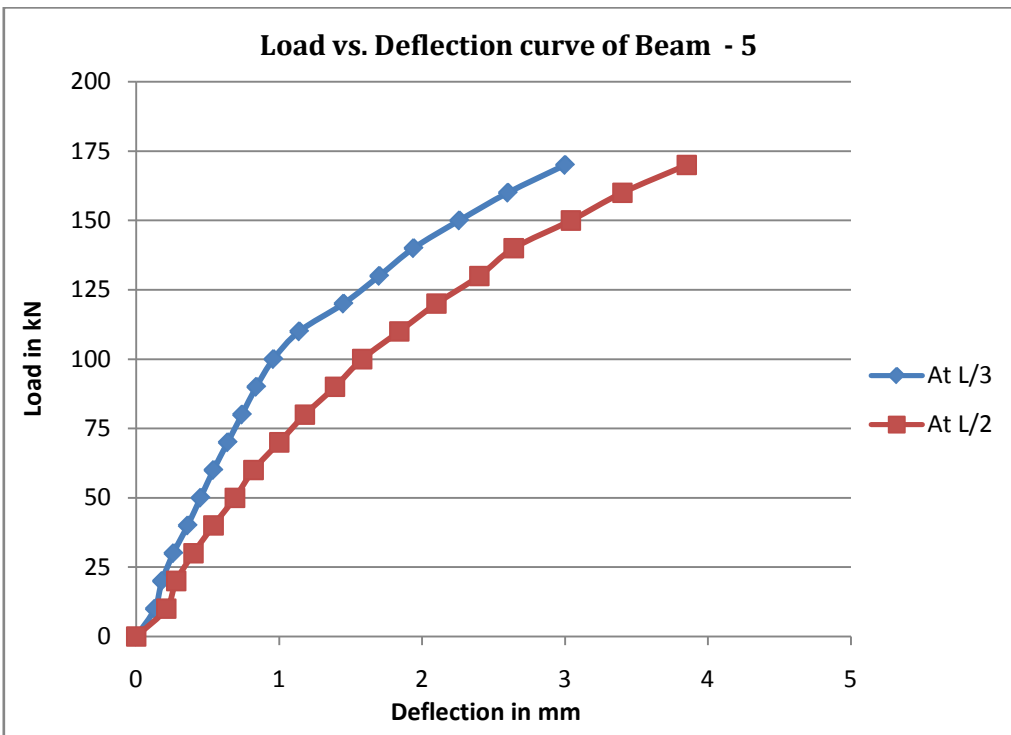


Figure 4-18. Load vs. Deflection Curve for SB4

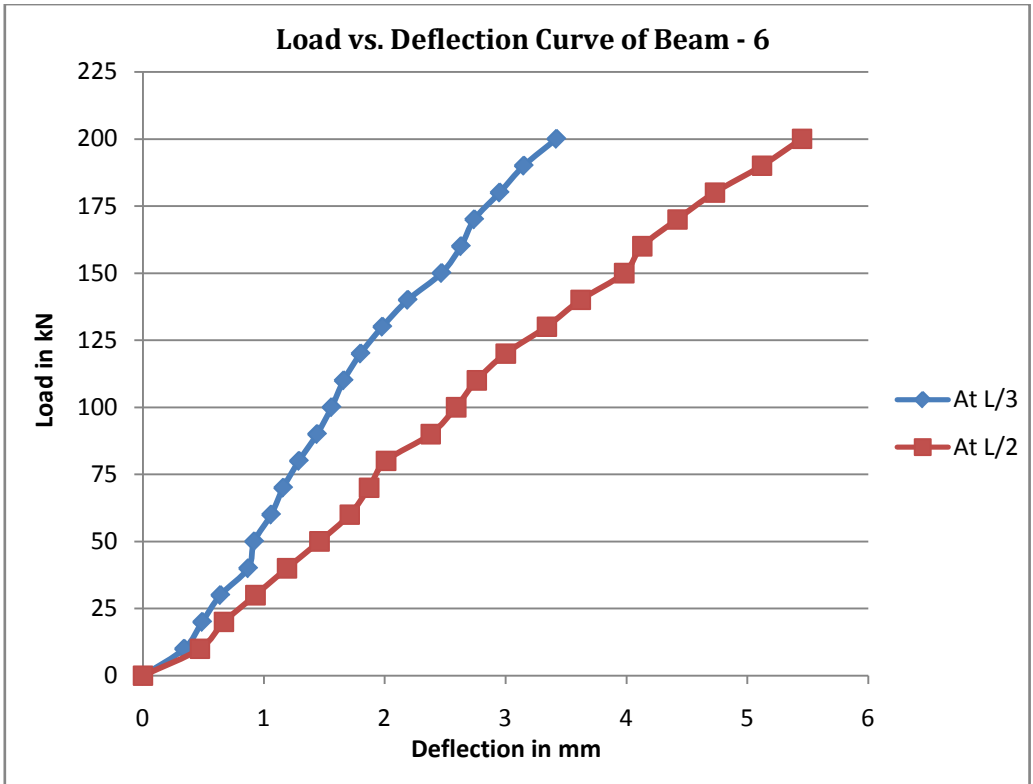


Figure 4-19. Load vs. Deflection Curve for SB5

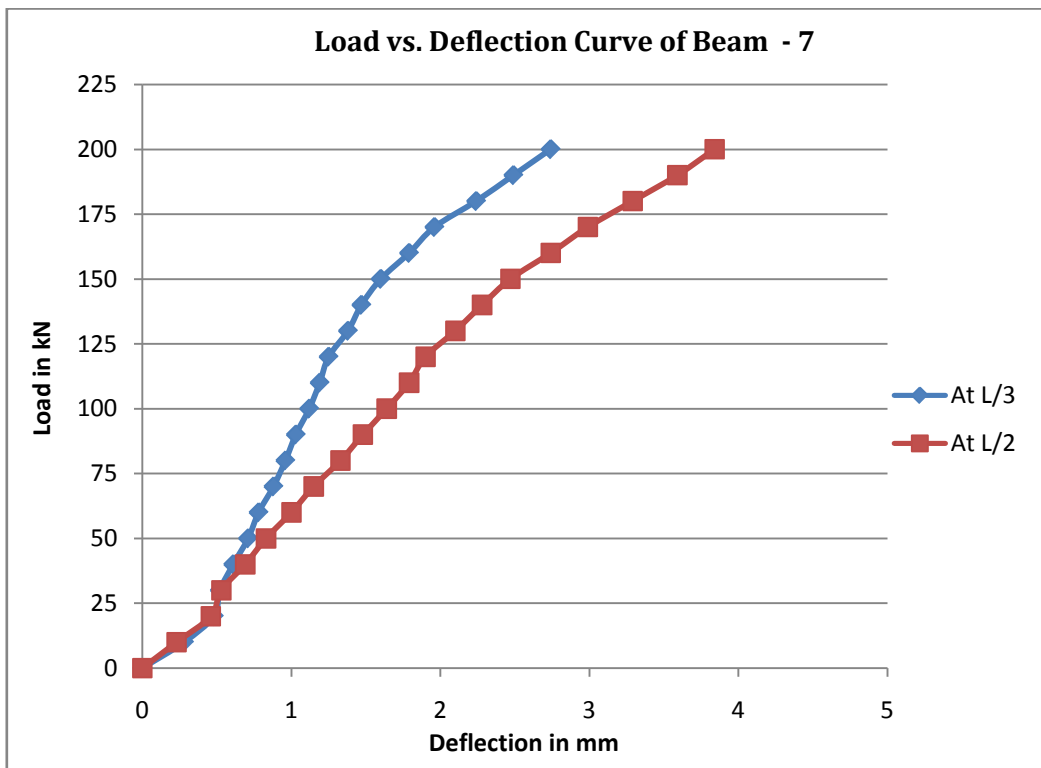


Figure 4-20. Load vs. Deflection Curve for SB6

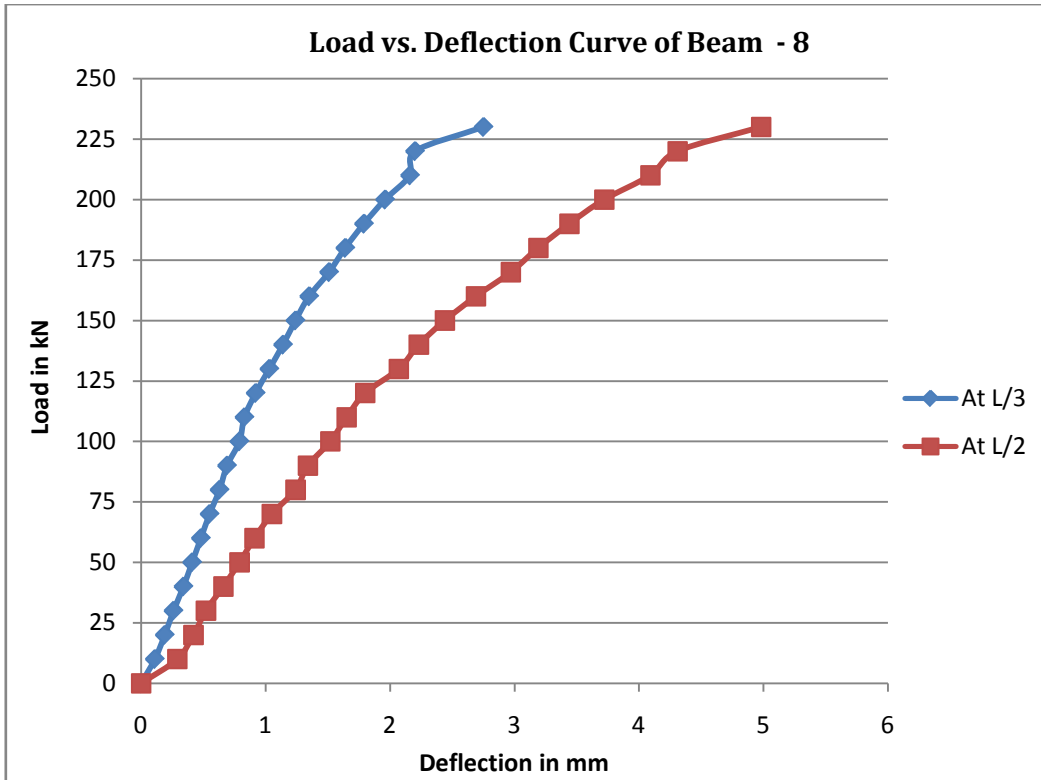


Figure 4-21. Load vs. Deflection Curve for SB7

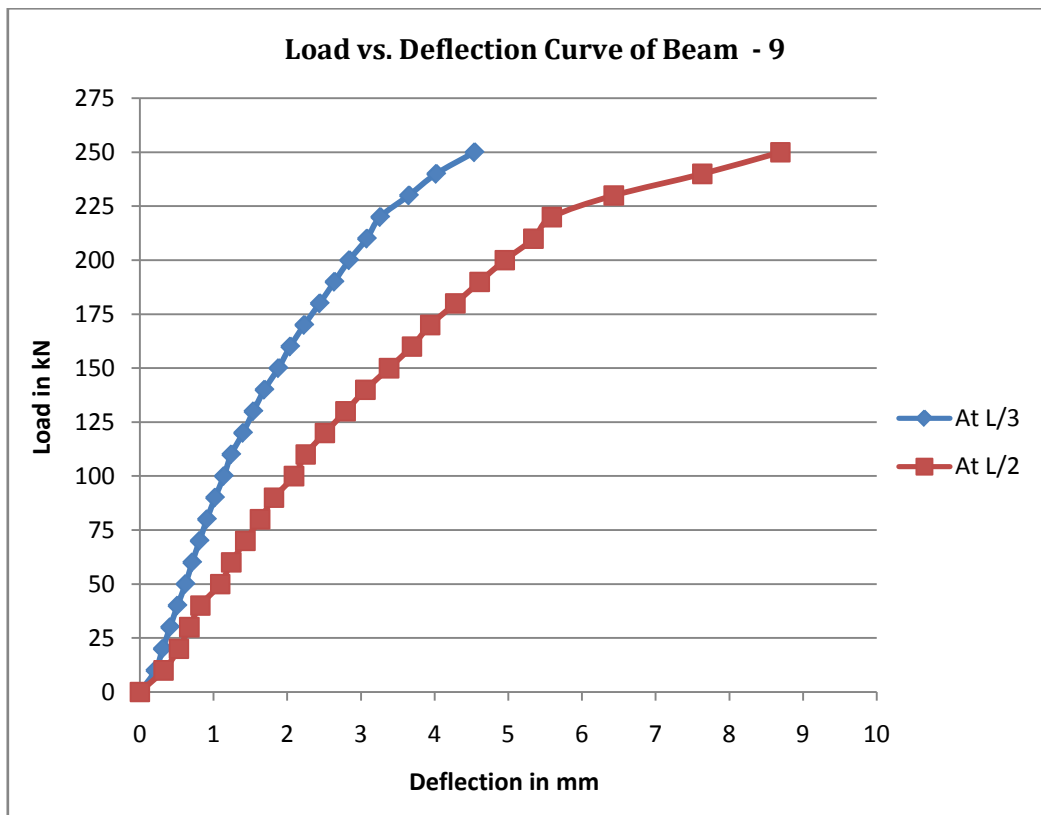


Figure 4-22. Load vs. Deflection Curve for SB8

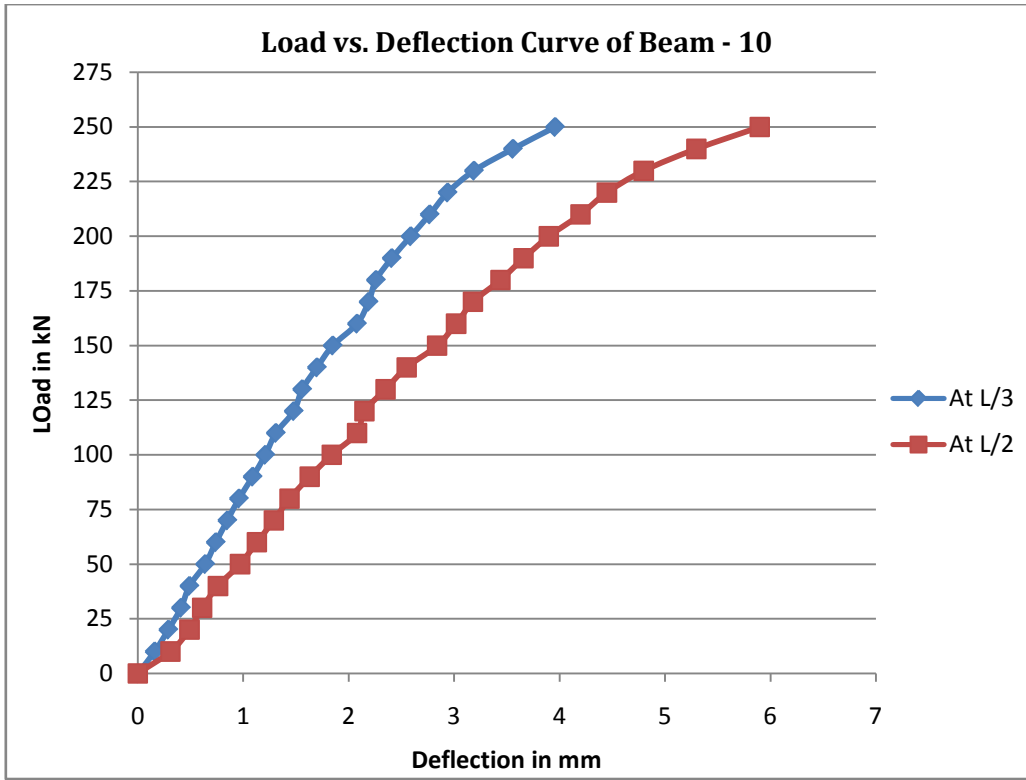


Figure 4-23. Load vs. Deflection Curve for SB9

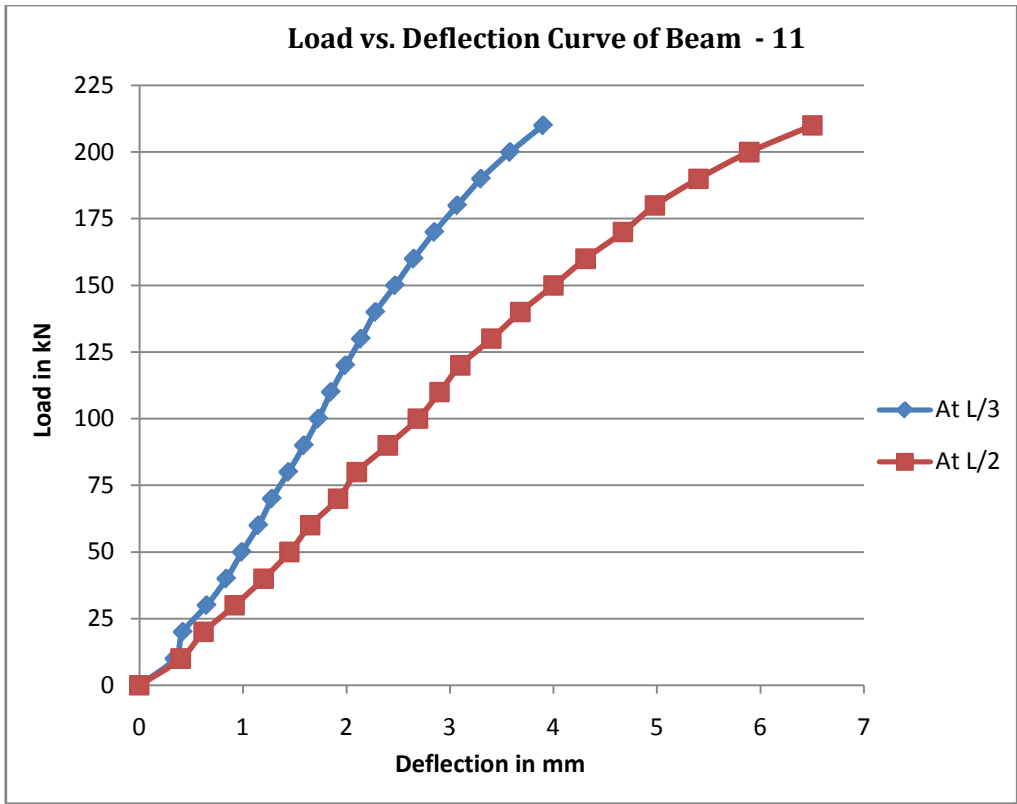


Figure 4-24. Load vs. Deflection Curve for SB10

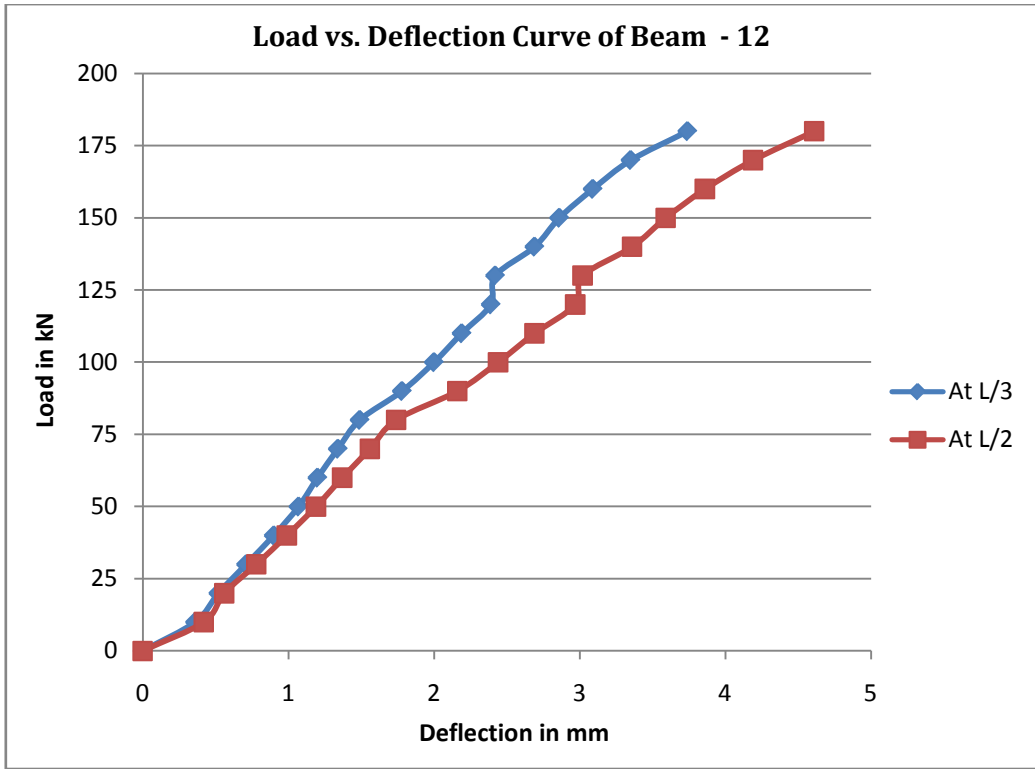


Figure 4-25. Load vs. Deflection Curve for SB11

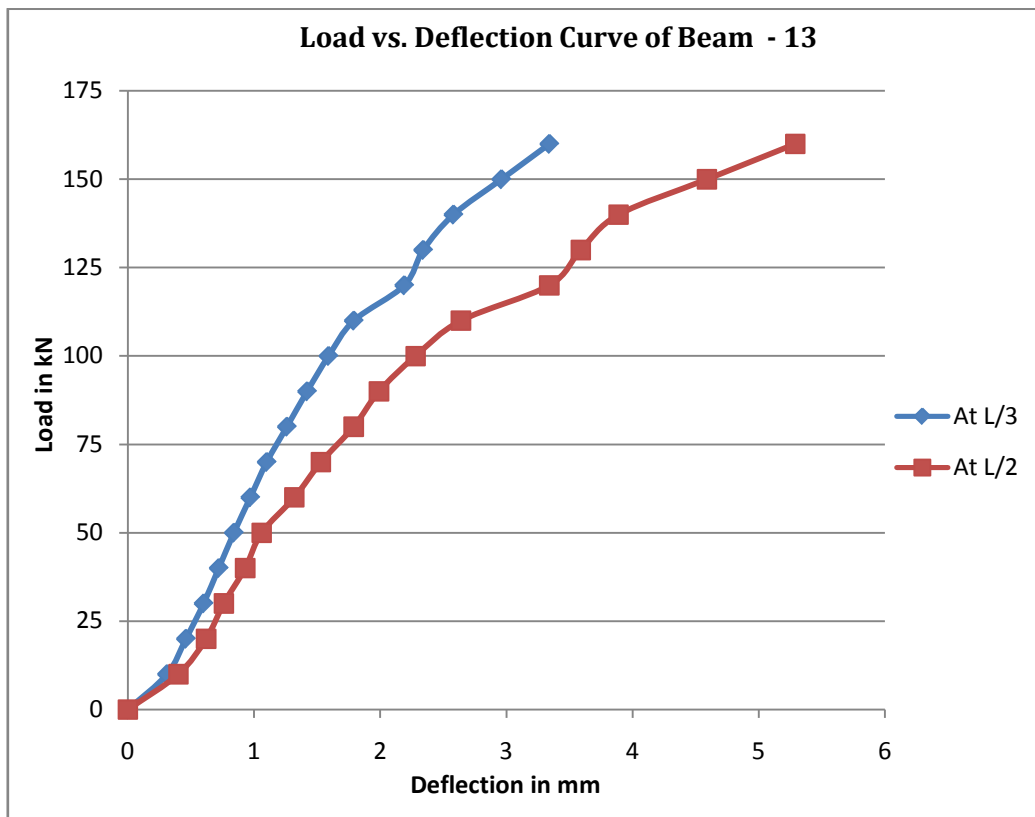


Figure 4-26. Load vs. Deflection Curve for SB12

The deflection profile for the control beam CB and beams SB1 (strengthened with continuous U-wrap) and SB3 (strengthened with strip U-wrap) are presented in figure 4-27. From the figure 4-27, it is observed that SB1 performs well compared to CB and SB3. The reduction in mid-span deflection of the beam SB1 compared to CB and SB3 are 45.30% and 34.95% respectively under the applied load of 160 kN.

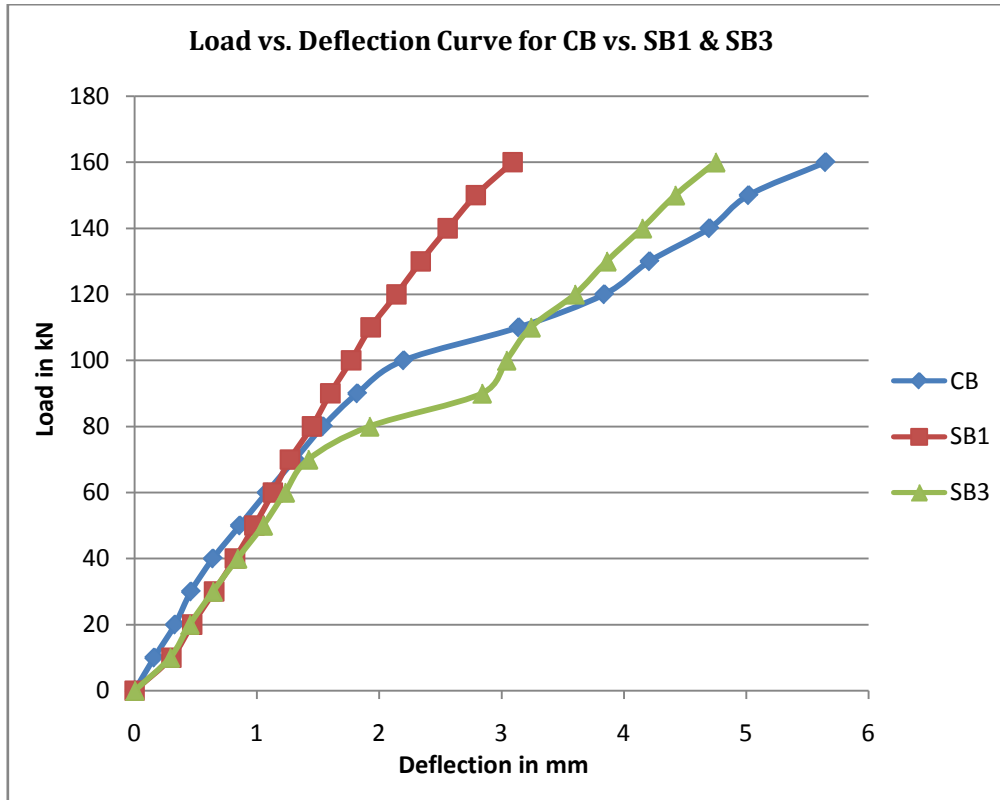


Figure 4-27. Loads vs. Deflection Curve for CB vs. SB1 and SB3

The deflection profile for the control beam CB and beams SB2 (strengthened with continuous side wrap) and SB4 (strengthened with strip side wrap) are shown in figure 4-28. From the figure 4-28, it is observed that beams SB4 and SB2 perform well compared to the control beam. The behaviour of beams SB4 and SB2 are nearly similar; however, the performance of the former is better. The percentage decrease in mid-span deflection of SB2 and SB4 compared to CB are 40.70 and 39.82 respectively under the same loading condition.

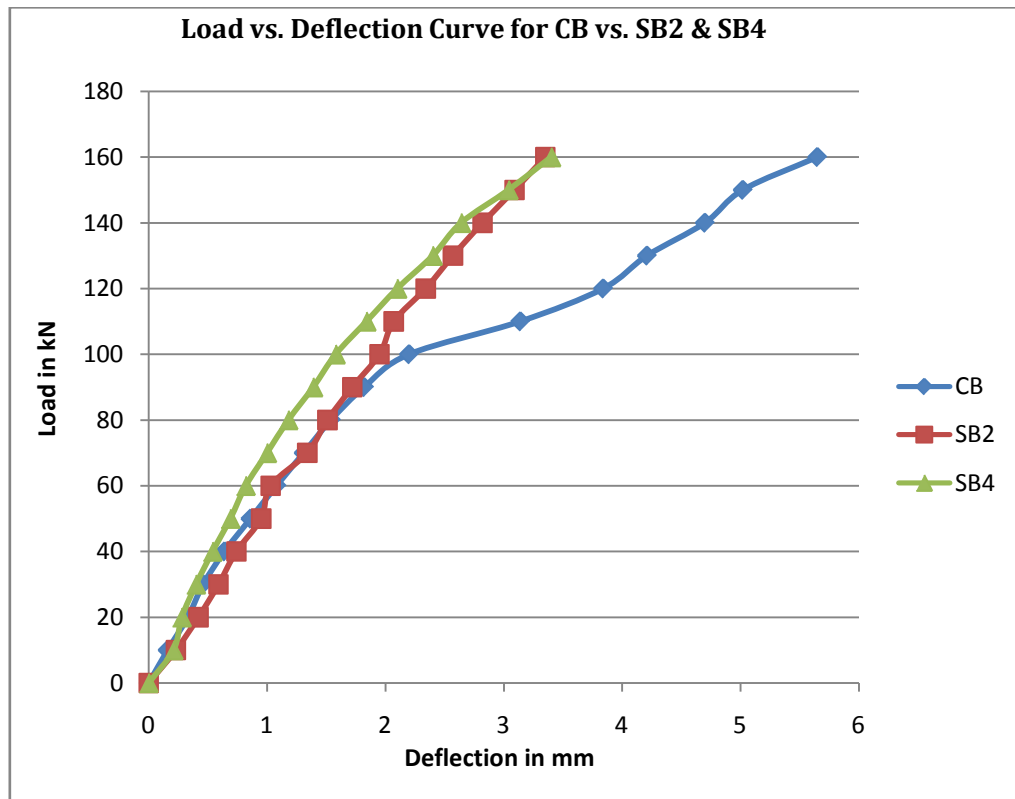


Figure 4-28. Load vs. Deflection Curve for CB vs. SB2 and SB4

The deflection profile for the control beam CB and beams SB5 (strengthened with inclined (45°) side strips), SB6 (strengthened with X-shape side strips) and SB7 (strengthened with continuous side wrap with one of the fiber directions oriented at 45°) are shown in figure 4-29. From the figure 4-29, it is observed that all the strengthened beams perform better than the control beam. The behaviour of the beams SB6 and SB7 are similar and better than the SB5. The percentage decrease in mid-span deflection of SB7, SB6 and SB5 compared to CB are reported to be 52.38, 51.50 and 26.90 respectively under the same loading condition.

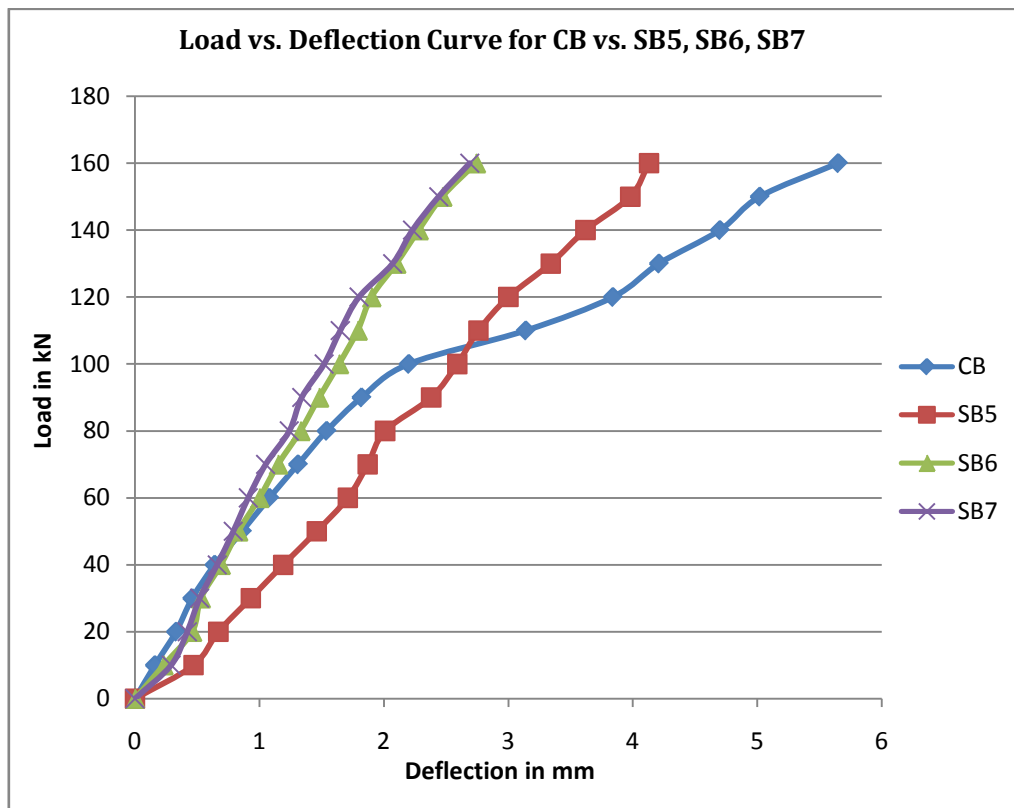


Figure 4-29. Load vs. Deflection Curve for CB vs. SB5, SB6 and SB7

The deflection profile for the control beam CB and beams SB8 (strengthened with two layers continuous U-wrap with end anchorage) and SB9 (strengthened with four layers continuous U-wrap with end anchorage) are shown in figure 4-30. From the figure 4-30, it is observed that the performance of the beam is improved by increasing the number of layers. The percentage decrease in mid-span deflection of SB8 and SB9 compared to CB are 34.69 and 46.54 respectively under the same loading condition.

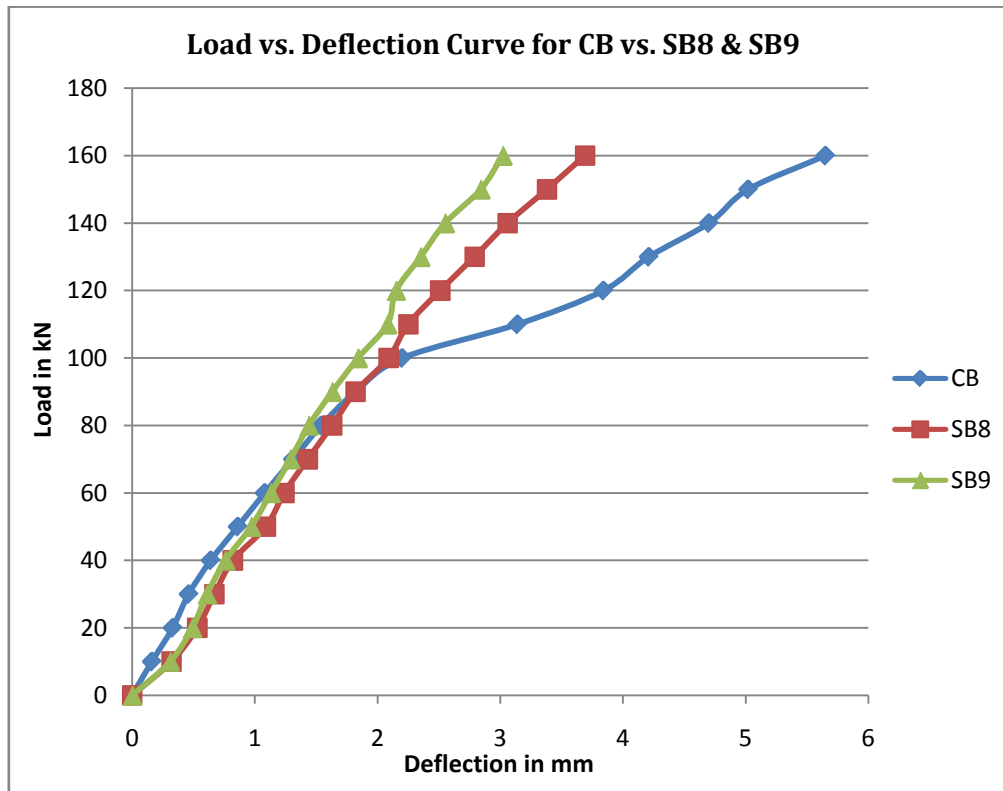


Figure 4-30. Load vs. Deflection Curve for CB vs. SB8 and SB9

The deflection profile for the beam SB9 (strengthened with 4 layers continuous U-wrap with end anchorage on full shear span) and SB10 (strengthened with 8 layers continuous U-wrap with end anchorage on shear span over a length of 233mm from support) are shown in figure 4-31. The beam SB9 with less number of GFRP layers performs better compared to SB10 because of full wrapping of shear span. The mid-span deflection of SB9 is 29.93% less than the corresponding value of SB10.

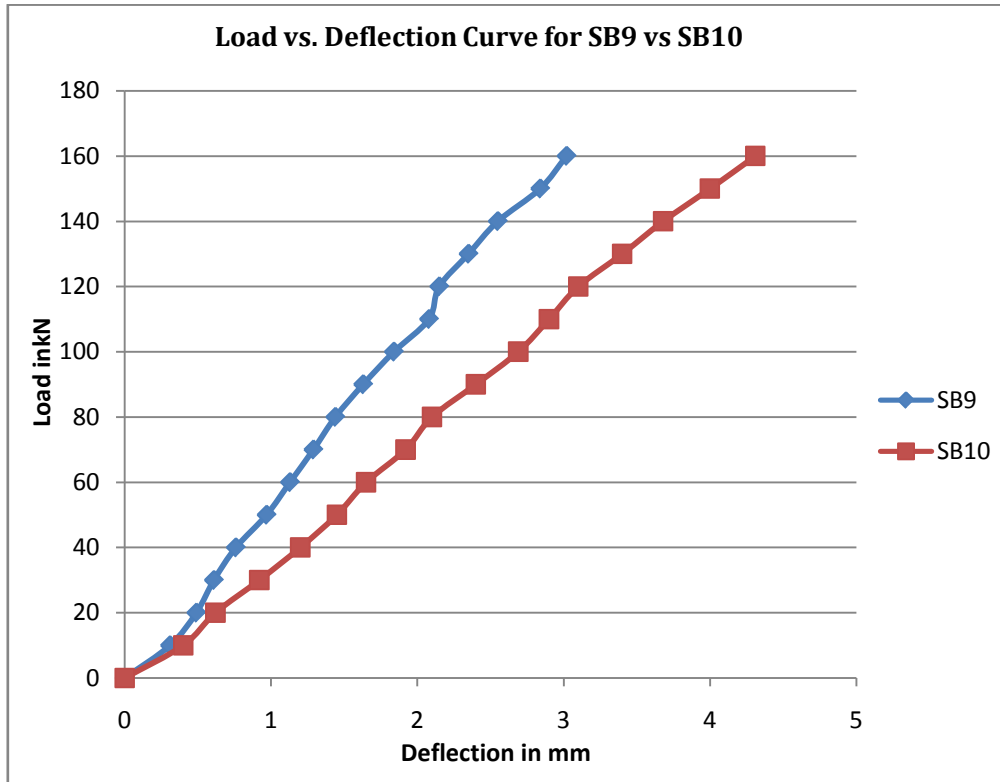


Figure 4-31. Load vs. Deflection Curve for SB9 vs. SB10

The deflection profile for the beam with web openings, SB11 (strengthened with 4 layers continuous U-wrap without end anchorage) and SB12 (strengthened with 4 layers continuous U-wrap with end anchorage) are shown in figure 4-32. From the figure 4-32, it is observed that SB12 performs well compared to SB11 because of end anchorage of GFRP sheet which prevents the debonding failure. The mid-span deflection of SB12 is 27.03% less compared to SB11.

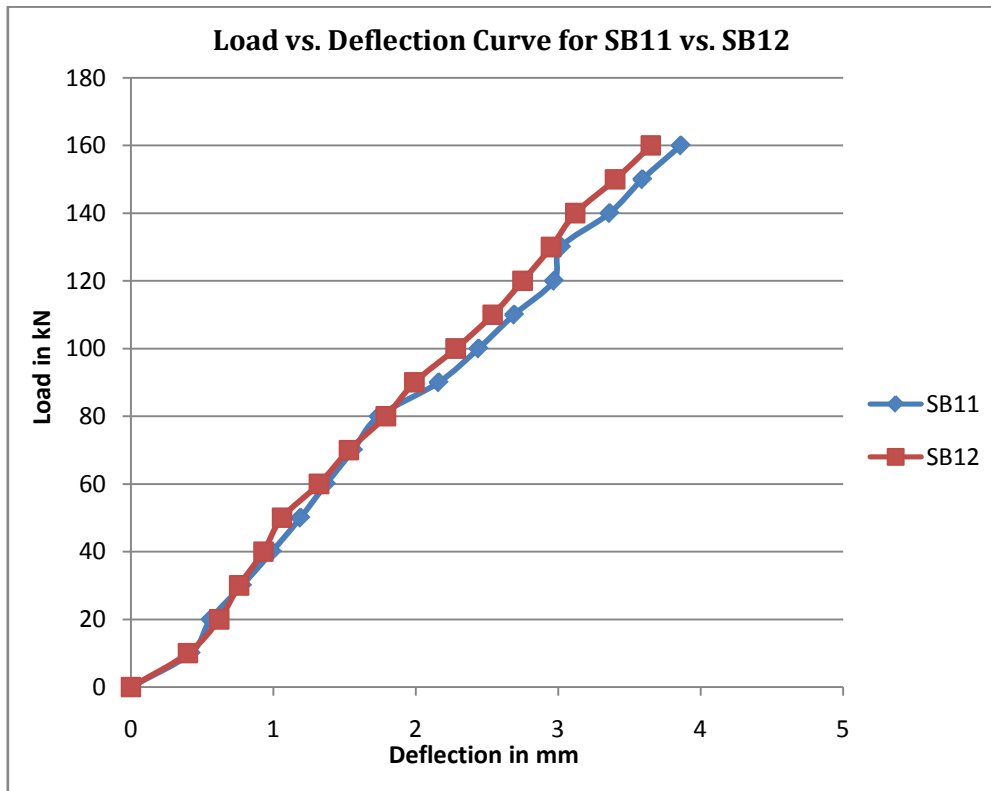


Figure 4-32. Load vs. Deflection Curve for SB11 vs. SB12

4.2 LOAD AT INITIAL CRACK

The crack patterns of the beams were observed with the progress of the load. The load at initial crack of the beams was recorded and presented in figure 4-33. It is observed that the initial cracks in the strengthened RC beams are developed at a higher load than the control beam. From figure 4-33, the load at first crack of SB5 is 39.65% higher than the control beam and is the highest among the strengthened beams.

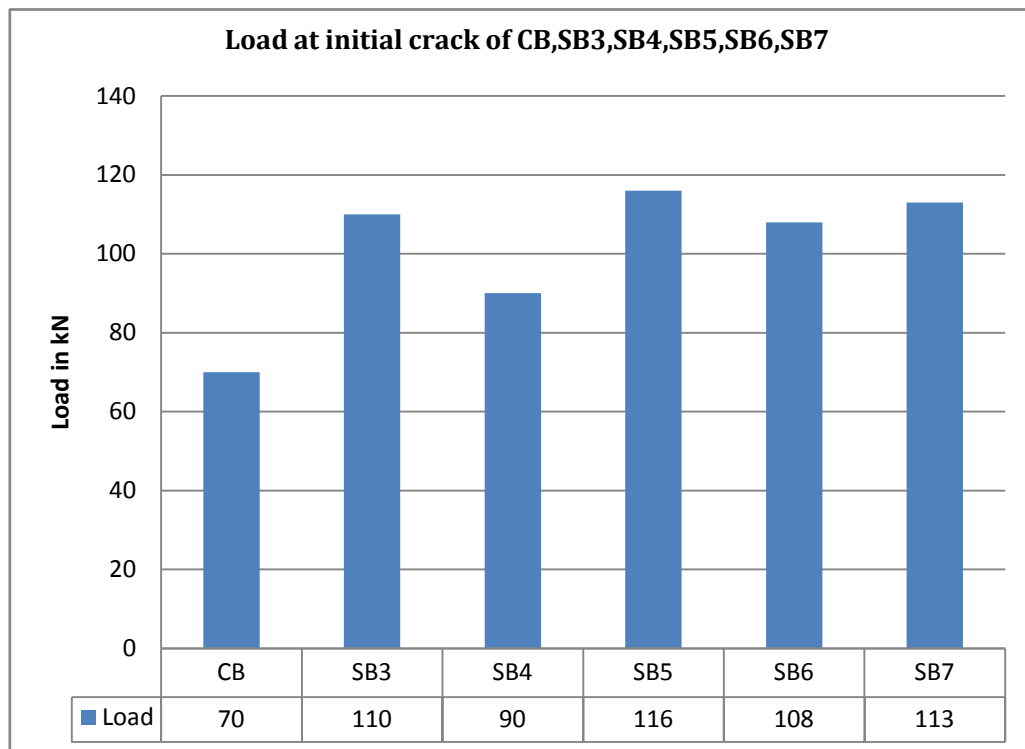


Figure 4-33. Load at initial crack of Beams CB, SB3, SB4, SB5, SB6, and SB7

4.3 ULTIMATE LOAD CARRYING CAPACITY

The ultimate load carrying capacity of the control beam CB and beams SB1 (strengthened with continuous U-wrap) and SB3 (strengthened with strip U-wrap) are presented in figure 4-34. From figure 4-34, the ultimate load carrying capacity of SB1 is 29.56% higher than the control beam and is 6.52% higher than the beam SB3.

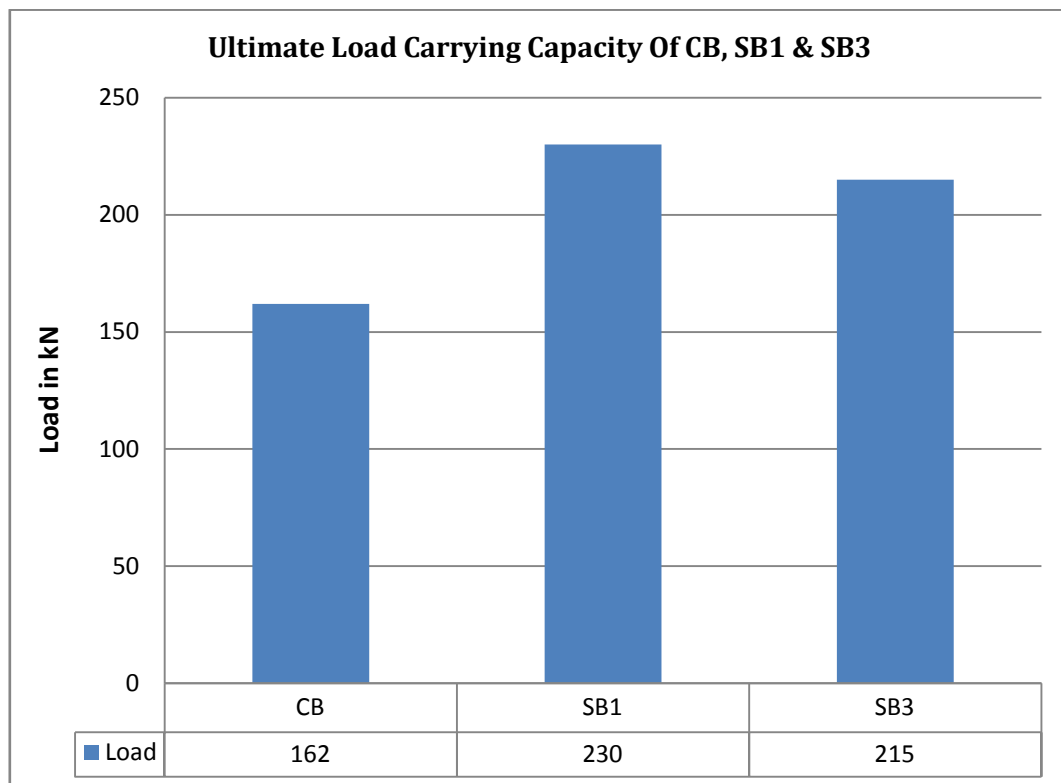


Figure 4-34. Ultimate load carrying capacity of beams CB, SB1 and SB3

The ultimate load carrying capacity of the control beam CB and beams SB2 (strengthened with continuous side wrap) and SB4 (strengthened with strip side wrap) are presented in figure 4-35. From figure 4-35, the ultimate load carrying capacity of SB2 is 19% higher than the control beam and is 14.0% higher than the beam SB4.

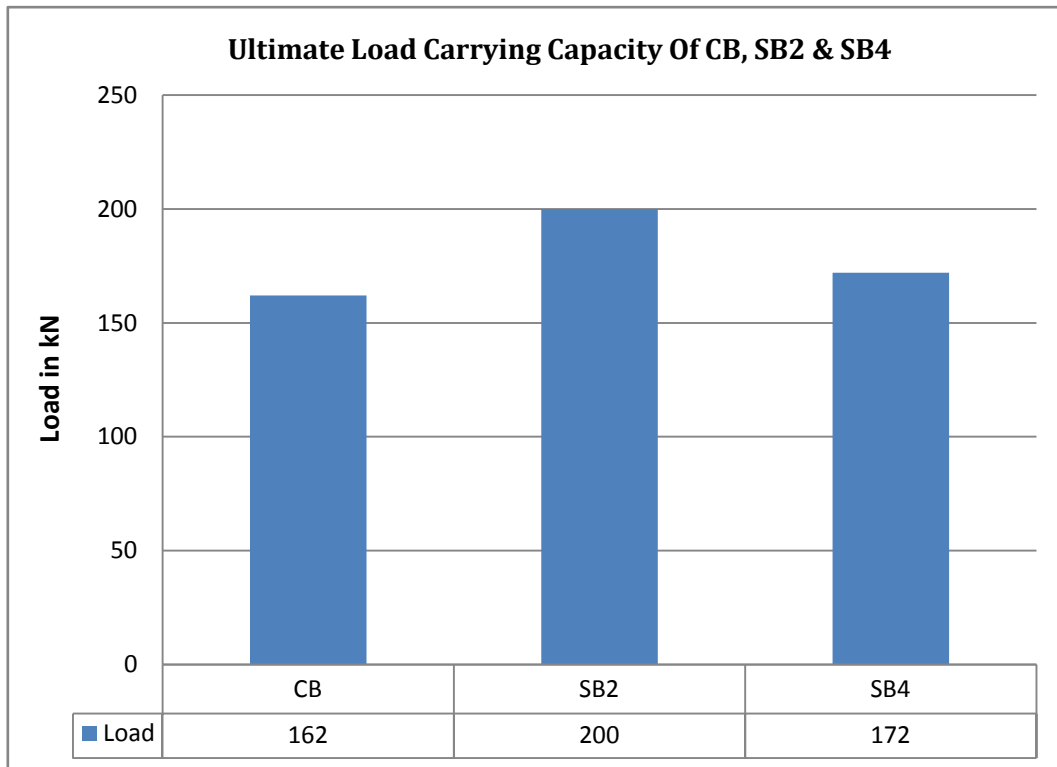


Figure 4-35. Ultimate load carrying capacity of beams CB, SB2 and SB4

The ultimate load carrying capacity of the control beam CB and beams SB5 (strengthened with inclined (45°) side strips), SB6 (strengthened with X-shape side strips) and SB7 (strengthened with continuous side wrap with one of the fiber directions oriented at 45°) are shown in figure 4-36. The ultimate load carrying capacity of SB7 is the highest among the beams presented in figure 4-36 and is 30.17%, 5.17% and 1.72% higher than the control beam, SB5 and SB6, respectively.

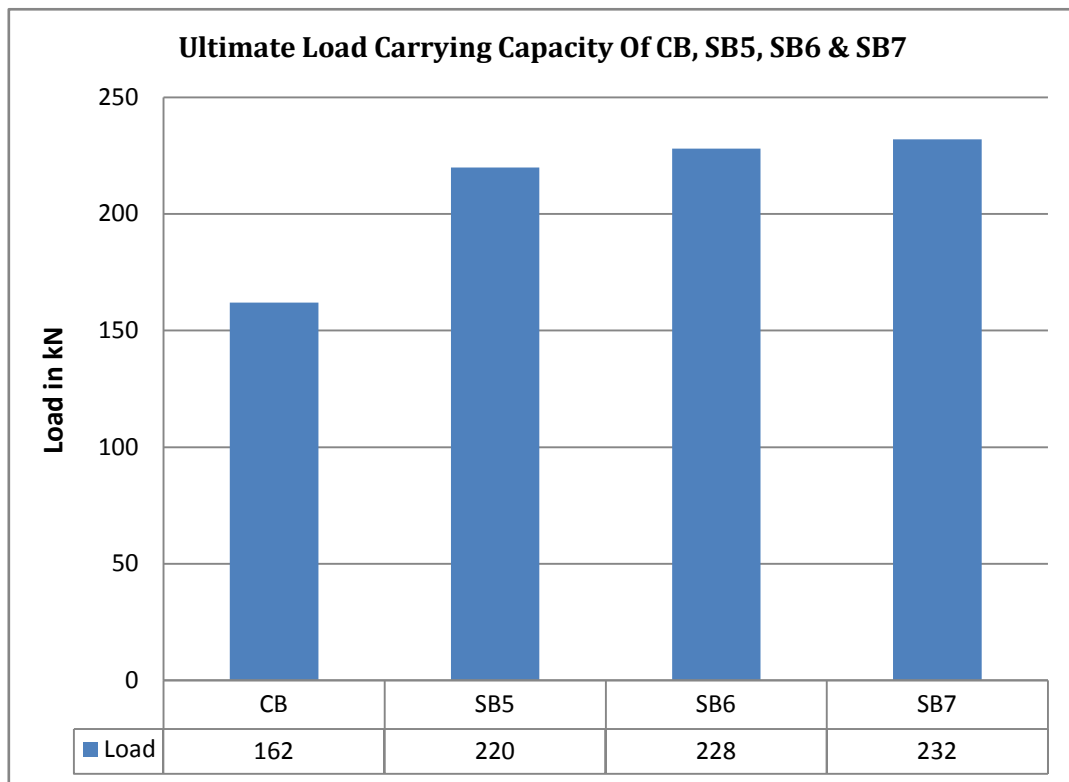


Figure 4-36. Ultimate load carrying capacity of beams CB, SB5, SB6 and SB7

The ultimate load carrying capacity of the control beam CB and beams SB8 (strengthened with two layers continuous U-wrap with end anchorage) and SB9 (strengthened with four layers continuous U-wrap with end anchorage) are shown in figure 4-37. The ultimate load carrying capacity of SB9 is the highest among the beams presented in figure 4-37 and is 39.55% and 5.97% higher than the control beam and SB8, respectively.

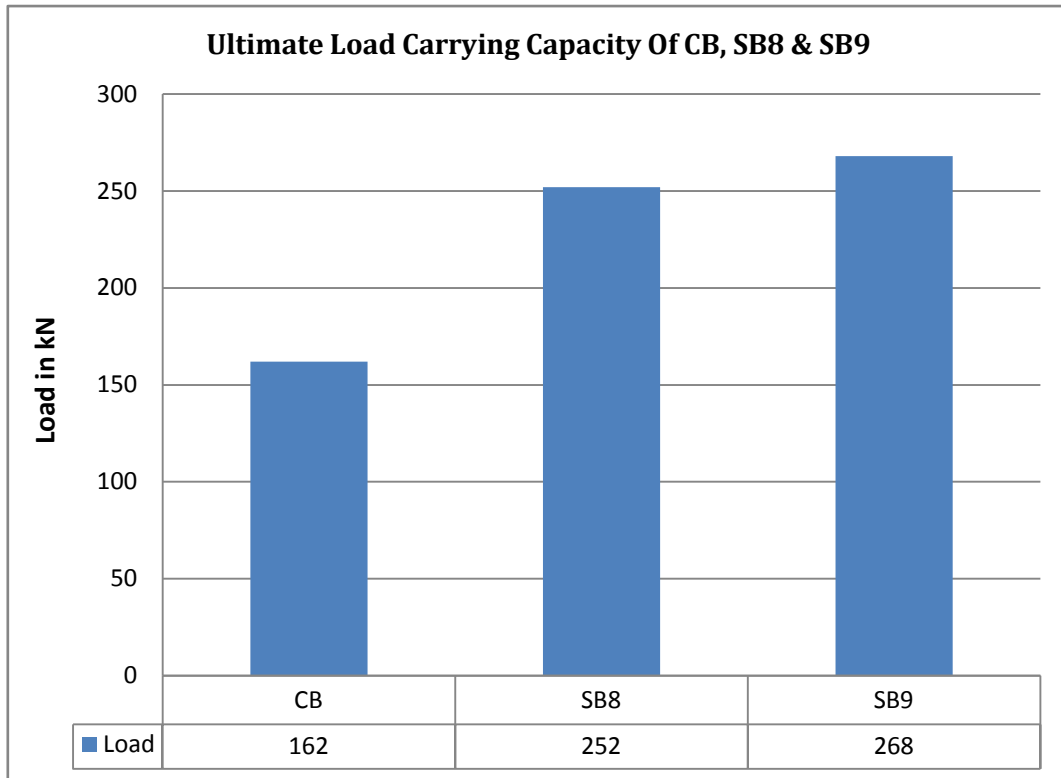


Figure 4-37. Ultimate load carrying capacity of beams CB, SB8 and SB9

The ultimate load carrying capacity for the beam SB9 (strengthened with 4 layers continuous U-wrap with end anchorage on full shear span) and SB10 (strengthened with 8 layers continuous U-wrap with end anchorage on shear span over a length of 233mm from support) are shown in figure 4-38. The ultimate load carrying capacity of SB9 is higher than the beam SB9.

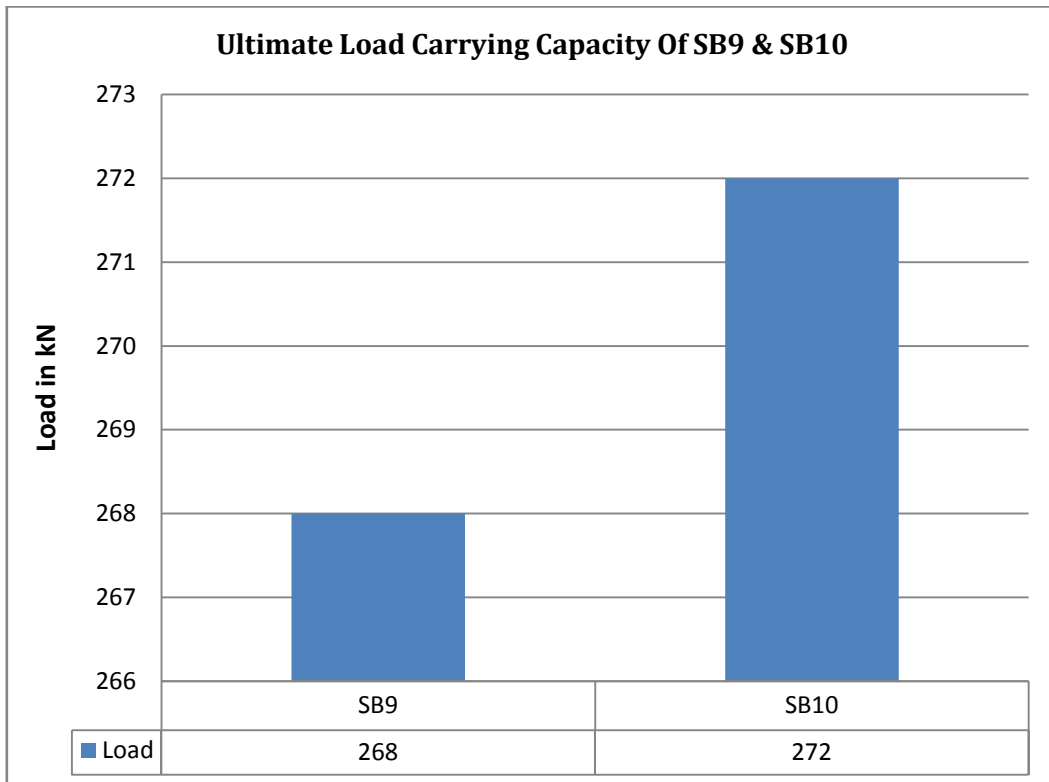


Figure 4-38. Ultimate load carrying capacity of beams SB9 and SB10

The ultimate load carrying capacity for the beam with web openings, SB11 (strengthened with four layers continuous U-wrap without end anchorage) and SB12 (strengthened with 4 layers continuous U-wrap with end anchorage) are shown in figure 4-39. The ultimate load carrying capacity of SB12 is 8.60% higher than the beam SB11 as observed in figure 4-39.

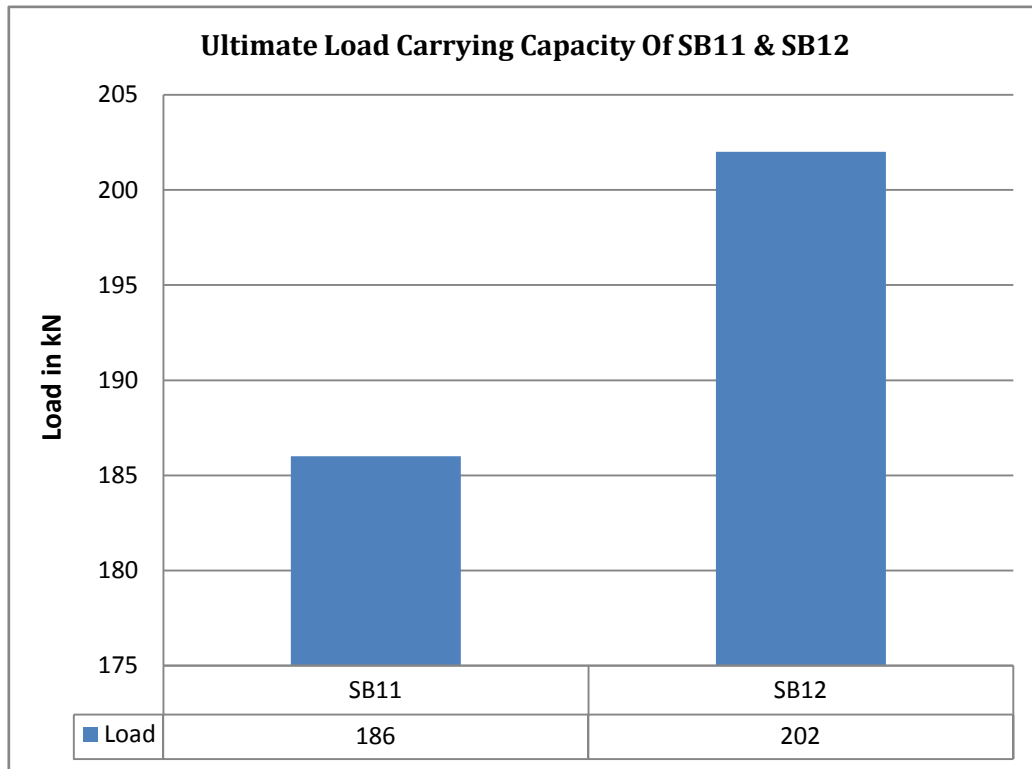


Figure 4-39. Ultimate load carrying capacity of beams SB11 and SB12

It was noted that of all the beams, the strengthened beams had the higher load carrying capacity compared to the controlled beam.

It is observed from above figures that, the ultimate load carrying capacity of all strengthened beams is higher than the control beam. With the introduction of end anchorage system, the ultimate shear carrying capacity of the beam is increased significantly. The improvement in shear capacity is also observed in case of beam with web opening by using the end anchorage.

The ultimate load carrying capacities of all the beams along with the nature of failure are summarized in Table 4.1. The ratio of ultimate load carrying capacity of strengthened beam to control beam are computed and presented in Table 4.1. It is observed from the table that the ratio is highest for beam SB10 among all the beams tested in this experimental program.

Table 4.1 Ultimate load and nature of failure for various beams

Beam Designation	Nature of Failure	P_u (kN)	$\lambda = \frac{P_u(\text{Strengthened Beam})}{P_u(\text{Control Beam})}$
CB	Shear failure	162	-
SB1	Debonding of GFRP with concrete crushing + Shear failure	230	1.42
SB2	Debonding of GFRP with concrete cover + Shear failure	200	1.23
SB3	Tearing and Debonding of GFRP without concrete cover + Shear failure	215	1.32
SB4	Debonding failure + Shear failure	172	1.06
SB5	Tearing of GFRP + Shear failure	220	1.35
SB6	Debonding failure + Shear failure	228	1.40
SB7	Debonding failure + Shear failure	232	1.43
SB8	Tearing of GFRP + Shear failure	252	1.55
SB9	Tearing of GFRP + Shear failure	268	1.65
SB10	Shear crack shifted to the non-strengthened zone of shear span	272	1.67
SB11	Debonding of GFRP + Beam-type shear failure	186	1.14
SB12	Tearing of GFRP + Beam-type shear failure	202	1.24

CHAPTER - 5

THEORETICAL STUDY



CHAPTER - 5

THEORETICAL STUDY

5.1 GENERAL

The design approach for computing the shear capacity of RC T-beams strengthened with externally bonded GFRP sheets is presented in this chapter. The design approach is expressed in American Concrete Institute (ACI) design code format. The main factors affecting the additional strength that may be achieved by the externally bonded GFRP reinforcement have been considered. The experimental model described two possible failure mechanisms of GFRP reinforcement such as GFRP debonding and GFRP rupture. The shear strength of Reinforced Concrete (RC) T-beams are theoretically computed for varying degree of FRP strengthening.

5.2 FACTORS AFFECTING THE SHEAR CONTRIBUTION OF FRP

Based upon the results of the experimental study, the contribution of externally bonded FRP to the shear capacity is influenced by the following parameters:

- Amount and distribution of FRP reinforcement
- Fiber orientation
- Wrapping schemes (U-wrap, or fiber attached on the two web sides of the beam)
- Presence of FRP end anchor
- Concrete surface preparation and surface roughness

5.3 SHEAR STRENGTH OF RC BEAMS STRENGTHENED WITH FRP REINFORCEMENT USING ACI CODE GUIDELINES

5.3.1 Design of Material Properties

The material properties reported by the manufacturers, such as the ultimate tensile strength, typically do not consider long-term exposure to environmental conditions and should be considered as initial properties. Because long-term exposure to various types of environments can reduce the tensile properties and creep-rupture and fatigue endurance of FRP laminates,

the material properties used in design equations should be reduced based on the environmental exposure condition.

Eq.s (1) through (3) gives the tensile properties that should be used in all design equations. The design ultimate tensile strength should be determined using the environmental reduction factor given in the ACI 440.2R-02 document for the appropriate fiber type and exposure condition:

$$\text{Design ultimate tensile strength} = f_{fu} = C_E f_{fu}^* \quad (1)$$

where,

f_{fu} = design ultimate tensile strength of FRP,(MPa)

C_E = environmental reduction factor

f_{fu}^* = ultimate tensile strength of the FRP materials as reported by the manufacturer,(MPa)

Similarly, the design rupture strain should also be reduced for environmental-exposure conditions:

$$\text{Design rupture strain} = \varepsilon_{fu} = C_E \varepsilon_{fu}^* \quad (2)$$

where,

ε_{fu} = design rupture strain of FRP reinforcement,(mm/mm)

ε_{fu}^* = ultimate rupture strain of the FRP reinforcement,(mm/mm)

Because FRP materials are linearly elastic until failure, the design modulus of elasticity can then be determined from Hook's law. The expression for the modulus of elasticity, given in Eq. (3), recognizes that the modulus is typically unaffected by environmental conditions. The modulus given in this equation will be the same as the initial value reported by the manufacturer.

$$E_f = \frac{f_{fu}}{\varepsilon_{fu}} \quad (3)$$

The material used for this present work is glass fiber and epoxy resin, and the exposure condition is internal exposure. For present calculation the environmental reduction factor (C_E) is used as 0.75.

5.3.2 Nominal Shear Strength

The nominal shear strength of an RC beam may be computed by basic design equation presented in ACI 318-95 and given as in Eq. (4)

$$V_n = V_c + V_s \quad (4)$$

In this equation the nominal shear strength is the sum of the shear strength of the concrete (which for a cracked section is attributable to aggregate interlock, dowel action of the longitudinal reinforcement, and the diagonal tensile strength of the uncracked portion of the concrete) and the strength of the steel shear reinforcement.

In the case of beams strengthened with externally bonded FRP sheets, the nominal shear strength may be computed by the addition of a third term to account for the contribution of FRP sheet to the shear strength. This is expressed in Eq. (5)

$$V_n = V_c + V_s + V_f \quad (5)$$

5.3.3 Design Shear Strength

The design shear strength is calculated by multiplying the nominal shear strength by a strength reduction factor, ϕ . It is suggested that the reduction factor of $\phi = 0.85$ given in code ACI 318-95 be maintained for the concrete and the steel terms.

The basic design equation for the shear capacity of a concrete member is;

$$V_u \leq \phi V_n \quad (6)$$

where,

V_u is the total shear force applied at a given section due to the factored loads.

The nominal shear strength of an FRP-strengthened concrete member can be determined by adding the contribution of the FRP reinforcing to the contributions from the reinforcing steel (stirrups, ties, or spirals) and the concrete Eq. (7). An additional reduction factor ψ_f is applied to the contribution of the FRP system.

$$\phi V_n = \phi (V_c + V_s + \psi_f V_f) \quad (7)$$

It is suggested that an additional reduction factor ψ_f be applied to the shear contribution of the FRP reinforcement. For bond-critical shear reinforcement, an additional reduction factor of 0.85 (Completely wrapped members) is recommended. For contact-critical shear reinforcement, an additional reduction factor of 0.95 (Three-sided U-wraps or bonded face piles) is recommended in code ACI 440.2R-02.

5.3.4 FRP system contribution to shear strength

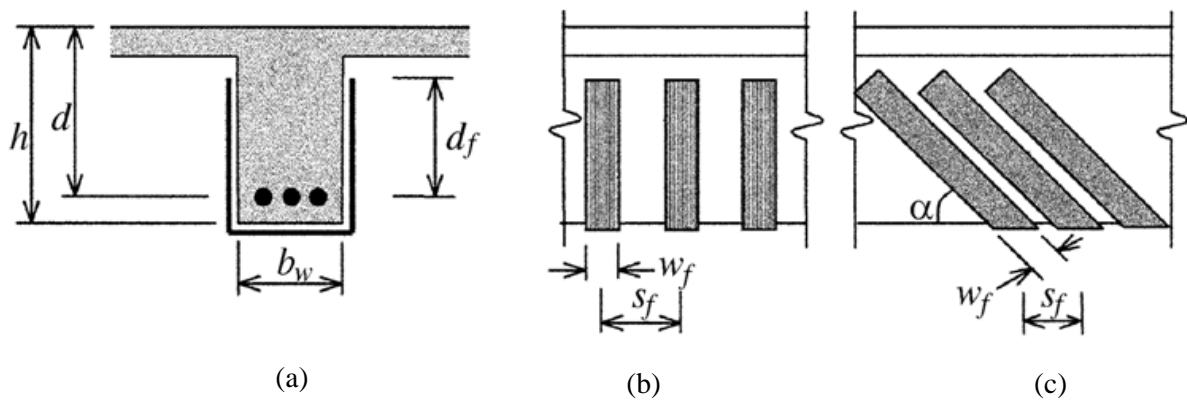


Figure - 5.1. Illustration of the dimensional variables used in shear-strengthening calculations for repair, retrofit, or strengthening using FRP laminates.

(a) Cross-section, (b) Vertical FRP strips, (c) Inclined FRP strips.

Figure – 5.1 illustrates the dimensional variables used in shear-strengthening calculations for FRP laminates. The contribution of the FRP system to shear strength of a member is based on the fiber orientation and an assumed crack pattern [Khalifa et al. 1998]. The shear strength provided by the FRP reinforcement can be determined by calculating the force resulting from the tensile stress in the FRP across the assumed crack. The shear contribution of the FRP shear reinforcement is then given by Eq. (8).

$$V_f = \frac{A_{fv} f_{fe} (\sin\alpha + \cos\alpha) d_f}{S_f} \quad (8)$$

where,

In Eq. (8), A_{fv} is the area of one strip of transverse FRP reinforcement covering two sides of the beam. This area may be expressed as follows:

$$A_{fv} = 2 t_f w_f \quad (9)$$

The area of GFRP shear reinforcement A_{fv} is the total thickness of the sheet (usually $2t_f$ for sheets on both sides of the beam) times the width of the GFRP sheet w_f in the longitudinal direction. The dimensions used to define the area of GFRP are shown in Figure 1. The spacing between the strips, s_f , is defined as the distance from the centerline of one strip to the centerline of an adjacent strip. For multilayered beam it is n times the area of GFRP shear reinforcement A_{fv} where, n is the number of layers. For the continuous vertical FRP reinforcement, the spacing of the strip, s_f , and the width of the strip, w_f , are equal. The angle α is angle between principal fiber orientation and longitudinal axis of the beam.

The other variable in Eq. (8), the tensile stress in the FRP shear reinforcement at ultimate stage, f_{fe} is directly proportional to the level of strain that is developed in the FRP shear reinforcement at ultimate as expressed in Eq. (10).

$$f_{fe} = \varepsilon_{fe} E_f \quad (10)$$

5.3.5 Effective strain in FRP laminates

The effective strain is the maximum strain that can be achieved in the FRP system at the ultimate load stage and is governed by the failure mode of the FRP system and the strengthened reinforced concrete member. All possible failure modes should be considered and the effective strain should be used which is the representative of the critical failure mode. The following subsections give guidance on determining this effective strain for different configurations of FRP laminates used for shear strengthening of reinforced concrete members.

Completely wrapped members:

For reinforced concrete beams completely wrapped by the FRP system, loss of aggregate interlock of the concrete has been observed to occur at fiber strains less than the ultimate fiber strain. To preclude this mode of failure, the maximum strain used for design should be limited to 0.4% for applications that can be completely wrapped with the FRP system as given in Eq. (11).

$$\varepsilon_{fe} = 0.004 \leq 0.75 \varepsilon_{fu} \quad (\text{for completely wrapping around the members cross section}) \quad (11)$$

This strain limitation is based on testing [Priestley et al. 1996] and experience. Higher strains should not be used for FRP shear-strengthening applications.

Bonded U-wraps or bonded face plies:

FRP systems that do not enclose the entire section (two- and three-sided wraps) have been observed to delaminate from the concrete before the loss of aggregate interlock of the section. For this reason, bond stresses should be analyzed to determine the usefulness of these systems and the effective strain level that can be achieved [Triantafillou 1998a]. The effective strain is calculated using a bond-reduction coefficient k_v applicable to shear.

$$\varepsilon_{fe} = k_v \varepsilon_{fu} \leq 0.004 \quad (\text{for bonded U-wraps or bonding to two sides}) \quad (12)$$

where,

k_v = bond-reduction coefficient for shear.

5.3.6 Reduction coefficient based on Rupture failure mode

There is no particular guideline indicated for GFRP. The model proposed by Khalifa et al. (1998) is used to find out the reduction coefficient for rupture failure mode. The reduction coefficient presented as a function of $\rho_f E_f$ is shown in Equation (11) for $\rho_f E_f \leq 0.7$ GPa:

$$R = 0.5622 (\rho_f E_f)^2 - 1.218 (\rho_f E_f) + 0.778 \quad (11)$$

where,

ρ_f is the GFRP shear reinforcement ratio = $(2t_f/b_w) (w_f/s_f)$

E_f is the tensile modulus of elasticity of GFRP.

5.3.7 Reduction coefficient based on Debonding failure mode

The reduction coefficient based on debonding failure mode, is given in ACI 440.2R-02 design approach. k_v is used as bond reduction coefficient.

The bond-reduction coefficient is a function of the concrete strength, the type of wrapping scheme used, and the stiffness of the laminate. The bond-reduction coefficient can be computed from Eq. (13) through (16) [Khalifa et al. 1998].

$$k_v = \frac{k_1 k_2 L_e}{11,900 \varepsilon_{fu}} \leq 0.75 \quad (13)$$

The active bond length L_e is the length over which the majority of the bond stress is maintained.

This length is given by Eq. (14).

$$L_e = \frac{23,300}{(n t_f E_f)^{0.58}} \quad (14)$$

The bond-reduction coefficient also relies on two modification factors, k_1 and k_2 , that account for the concrete strength and the type of wrapping scheme used, respectively. Expressions for these modification factors are given in Eq. (15) and (16).

$$k_1 = \left(\frac{f'_c}{27} \right)^{2/3} \quad (15)$$

$$k_2 = \begin{cases} \frac{d_f - L_e}{d_f} & \text{for } U - \text{wraps} \\ \frac{d_f - 2L_e}{d_f} & \text{for two sides bonded} \end{cases} \quad (16)$$

where,

f'_c is the concrete strength in MPa and

E_f is the tensile modulus of elasticity of GFRP in MPa.

5.4 Theoretical Calculations

The shear strength of the control beam and two strengthened beams (one failed by debonding while other failed by rupture) are theoretically computed and presented below.

Control Beam (CB):

The shear contribution of the concrete and steel are given below.

$$V_c = \frac{\sqrt{f_c'}}{6} b_w d = \frac{\sqrt{17.76} \times 150 \times 140}{6 \times 1000} = 14.75 \text{ kN}$$

$$V_s = \frac{A_s f_y d}{s} = 0 \text{ (for no shear reinforcement in the beam)}$$

$$V_n = V_c + V_s = 14.75 + 0 = 14.75 \text{ kN}$$

$$\phi V_n = 0.85 (14.75) = 12.53 \text{ kN}$$

Strengthened Beam 1 (SB1):

The shear contribution of the concrete and steel are given below.

$$V_c = \frac{\sqrt{f_c'}}{6} b_w d = \frac{\sqrt{19.9} \times 150 \times 140}{6 \times 1000} = 15.61 \text{ kN}$$

$$V_s = \frac{A_s f_y d}{s} = 0 \text{ (for no shear reinforcement in the beam)}$$

Shear contribution of the FRP:

Reduction coefficient for failure controlled by debonding

For continuous U-wrap with two layers,

$$\rho_f = \frac{2 t_f}{b_w} \left(\frac{w_f}{s_f} \right)$$

For continuous vertical oriented ($\beta = 90^\circ$) GFRP, $w_f / s_f = 1$

$$\rho_f = \frac{2(1)}{150} = 0.0133$$

$$E_f = 6.829 \text{ GPa}$$

$$\rho_f E_f = 0.0133 \times 6.829 = 0.091 \text{ GPa}$$

$$A_f = 2 \times t_f \times w_f = 2 \times 1 \times 1000 = 2000 \text{ mm}^2$$

$$R = \frac{0.0042 (f_c')^{\frac{2}{3}} w_{fe}}{t_f E_f^{0.58} \epsilon_{fu} d_f} = \frac{0.0042 (19.9)^{\frac{2}{3}} \times 90}{6.829^{0.58} \times 0.0189 \times 140} = 0.343$$

$$R = \frac{\epsilon_{fe}}{\epsilon_{fu}}$$

Design ultimate strength (f_{fu})

$$f_{fu} = C_E f_{fu}^*$$

C_E = Environmental reduction factor = 0.75 (for exterior condition , Glass and epoxy)

$$f_{fu} = 0.75 \times 172.79 = 129.59 \text{ MPa}$$

$$\epsilon_{fu}^* = \frac{f_{fu}^*}{E_f} = \frac{172.79}{6.829} = 0.0253$$

$$\epsilon_{fu} = C_E \times \epsilon_{fu}^* = 0.75 \times 0.0253 = 0.0189$$

$$\epsilon_{fe} = R \times \epsilon_{fu} = 0.343 \times 0.0189 = 0.006$$

$$\epsilon_{fe} \leq 0.004 \text{ (As per ACI 440.2R)}$$

$$\text{So used } \epsilon_{fe} = 0.004$$

$$f_{fe} = \epsilon_{fe} \times E_f = 0.004 \times 6.829 = 27.31 \text{ MPa}$$

$$V_f = \frac{A_{fv} f_{fe} (\sin \alpha + \cos \alpha) d_f}{S_f} = \frac{2000 \times 27.31 \times 140}{1000} = 7.646 \text{ kN}$$

$$\phi V_n = 0.85 (15.61 + 0) + 0.7(7.646) = 13.26 + 5.35 = 18.61 \text{ kN}$$

Strengthened Beam 3 (SB3):

The shear contribution of the concrete and steel are computed below.

$$V_c = \frac{\sqrt{f_c'}}{6} b_w d = \frac{\sqrt{18.656} \times 150 \times 140}{6 \times 1000} = 15.117 \text{ kN}$$

$$V_s = \frac{A_s f_y d}{s} = 0 \text{ (for no shear reinforcement in the beam)}$$

Shear contribution of the FRP:

Reduction coefficient for failure controlled by rupture

For U-strips with two layers,

$$\rho_f = \frac{2 t_f \left(\frac{w_f}{s_f} \right)}{b_w}$$

For continuous vertical oriented ($\beta = 90^\circ$) GFRP, $w_f / s_f = 1$

$$\rho_f = \frac{2(1)}{150} = 0.0133$$

$$E_f = 6.829 \text{ GPa}$$

$$\rho_f E_f = 0.0133 \times 6.829 = 0.091 \text{ GPa}$$

$$A_f = 2 \times t_f \times w_f = 2 \times 1 \times 1000 = 2000 \text{ mm}^2$$

$$R = \frac{0.0042 (f_c')^{\frac{2}{3}} w_{fe}}{t_f E_f^{0.58} \epsilon_{fu} d_f} = \frac{0.0042 (18.656)^{\frac{2}{3}} \times 90}{6.829^{0.58} \times 0.0189 \times 140} = 0.328$$

$$R = \frac{\epsilon_{fe}}{\epsilon_{fu}}$$

Design ultimate strength (f_{fu})

$$f_{fu} = C_E f_{fu}^*$$

C_E = Environmental reduction factor = 0.75 (for exterior condition, Glass and epoxy)

$$f_{fu} = 0.75 \times 172.79 = 129.59 \text{ MPa}$$

$$\epsilon_{fu}^* = \frac{f_{fu}^*}{E_f} = \frac{172.79}{6.829} = 0.0253$$

$$\epsilon_{fu} = C_E \times \epsilon_{fu}^* = 0.75 \times 0.0253 = 0.0189$$

$$\epsilon_{fe} = R \times \epsilon_{fu} = 0.328 \times 0.0189 = 0.006$$

$$\epsilon_{fe} \leq 0.004 \text{ (As per ACI 440.2R)}$$

$$\text{So used } \epsilon_{fe} = 0.004$$

$$f_{fe} = \epsilon_{fe} \times E_f = 0.004 \times 6.829 = 27.31 \text{ MPa}$$

$$V_f = \frac{A_{fv} f_{fe} (\sin\alpha + \cos\alpha) d_f}{S_f} = \frac{2000 \times 27.31 \times 140}{1000} = 7.646 \text{ kN}$$

$$\phi V_n = 0.85 (15.11+0) + 0.7(7.646) = 12.843 + 5.35 = 18.19 \text{ kN}$$

The design shear strength of the remaining beams can be computed in similar way. The nominal and design strength of all the strengthened and control beams are tabulated in Table 5.1 along with the experimental results.

5.5 Comparison of Experimental Results with ACI prediction

The shear strength of the beams strengthened with GFRP sheets obtained from the experimental study is compared to the design shear strength predicted by the ACI code (ACI 440.2R-02) guidelines. Different nomenclatures used in Table 5.1 are explained below for clarity.

$V_{n,test}$ = Total nominal shear strength by test,

$V_{c,test}$ = nominal shear strength provided by concrete obtained from test,

$V_{s,test}$ = nominal shear strength provided by steel shear reinforcement obtained from test,

$V_{f,test}$ = nominal shear strength provided by shear reinforcement obtained from test,

$V_{n,theor}$ = nominal shear strength calculated theoretically using ACI guidelines,

$V_{c,theor}$ = nominal shear strength provided by concrete theoretically,

$V_{s,theor}$ = nominal shear strength provided by steel shear reinforcement theoretically,

$V_{f,theor}$ = nominal shear strength provided by GFRP shear reinforcement theoretically.

Table 5.1 Comparisons of experimental and ACI predicted shear strength results

Specimen	Experimental Results						Theoretical results predicted by ACI 440.2R-02 Design approach			
	Load at failure	$V_{n,test}$ (kN)	$V_{c,test}$ (kN)	$V_{s,test}$ (kN)	$V_{f,test}$ (kN)	$(V_{f,test}/V_{n,test})*100$ (%)	$V_{f,theor}$ (kN)	$V_{c,theor}$ (kN)	$V_{s,theor}$ (kN)	$\phi V_{n,theor}$ (kN)
CB	162	81	81	0	-	-	-	14.75	0	12.53
SB1	230	115	81	0	34	29.56	7.646	15.61	0	18.62
SB2	200	100	81	0	19	19	7.646	15.33	0	18.38
SB3	215	107.5	81	0	26.5	24.65	7.646	15.11	0	18.19
SB4	172	86	81	0	5	5.81	7.646	15.05	0	18.14
SB5	220	110	81	0	29	26.36	10.814	15.37	0	20.63
SB6	228	114	81	0	33	28.94	10.814	15.23	0	20.51
SB7	232	116	81	0	35	30.17	10.814	15.37	0	20.63
SB8	252	126	81	0	45	35.71	7.646	15.35	0	18.39
SB9	268	134	81	0	53	39.55	21.805	15.04	0	28.04
SB10	272	136	81	0	55	40.44	36.95	15.16	0	38.75

It is observed from the Table 5.1 that the ACI prediction give satisfactory and conservative results when compared to that of experimental results for the all strengthened beams except the beam SB4 where vertical GFRP side sheets are used for strengthening.

Table 5.2 Comparison of shear contribution of GFRP sheet from experimental and ACI Guidelines

Specimen Designation	Experimental Results	Results as per ACI Guideline	
	$V_{f,test}$ (kN)	$V_{f,theor}$ (kN)	$V_{f,test}/V_{f,theor}$
SB1	34	7.646	4.45
SB2	19	7.646	2.48
SB3	26.5	7.646	3.465
SB4	5	7.646	0.65
SB5	29	10.814	2.68
SB6	33	10.814	3.05
SB7	35	10.814	3.23
SB8	45	7.646	5.88
SB9	53	21.805	2.43
SB10	55	36.95	1.48

It is found from the Table 5.2 that the ratio of $V_{f,test}$ to $V_{f,theor}$ is the highest for the beam SB8 strengthened with continuous FRP U-wrap with end anchorage and lowest for the beam SB4 strengthened with side vertical strips.

CHAPTER - 6

CONCLUSIONS & RECOMMENDATIONS



CHAPTER - 6

CONCLUSIONS AND RECOMMENDATIONS

6.1 CONCLUSIONS

In this experimental investigation the shear behaviour of RC T-beams strengthened by GFRP sheets are studied. The test results illustrated in the present study showed that the external strengthening with GFRP composites can be used to increase the shear capacity of RC T-beams, but the efficiency varies depending on the test variables such as fiber orientations, wrapping schemes, number of layers and anchorage scheme.

Based on the experimental and theoretical results, the following conclusions are drawn:

- Externally bonded GFRP reinforcement can be used to enhance the shear capacity of RC T-beams.
- The test results confirm that the strengthening technique of FRP system can increase the shear capacity of RC T-beams.
- The initial cracks in the strengthened beams are formed at a higher load compared to the ones in the control beam.
- Strengthening of on the webs with GFRP is most vulnerable to debonding with premature failure.
- The beam strengthened with a U-wrap configuration is more effective than the side-wrap configuration.
- Among all the GFRP strip configurations (i.e. vertical strips, strips inclined at 45° and strips inclined at +45° in one direction and +135° in another direction making an “X-shape”), the X-shape is more effective than the others.
- Applying GFRP to the beam with end anchorage is better than strengthening without end anchorage.
- The use of anchorage system eliminates the debonding of the GFRP sheet, and consequently results in a better utilization of the full capacity of the GFRP sheet.
- The test results indicated that the most effective configuration was the U-wrap with end anchorage among all the configurations.
- The load-deflection behaviour was better for beams retrofitted with GFRP inclined strips than the beams retrofitted with GFRP strips on the sides alone.

- A proportional increase in shear capacity with increasing GFRP amount can not be achieved when debonding is not prevented.
- The ultimate load carrying capacity of the strengthen beams were found to be greater than that of the control beams.
- The shear strength of the T-beam strengthened with U-wrap is more than that of the beam without openings.
- The T-beam with web openings strengthened with anchored U-wrap performs better than the beam without anchorage.
- Finally, the use of GFRP sheets as an external reinforcement is recommended to enhance the shear capacity of RC T-Beams with anchorage system.

6.2 RECOMMENDATIONS FOR FUTURE WORK

Based on the finding and conclusions of the current study the following recommendations are made for future research in FRP shear strengthening:

- Study of the bond mechanism between CFRP, AFRP and BFRP and concrete substrate.
- FRP strengthening of RC T-beams with different types of fibers such as carbon, aramid & basalt.
- Strengthening of RC L-beams with FRP composite.
- Strengthening of RC L-section beams with web opening.
- Effects of web openings of different shape and size on the shear behaviour of T & L-beams.
- Effects of shear span to depth ratio on shear strengthening of beams.
- Numerical modeling of RC T & L-beams strengthened with FRP sheets anchored at the end.

CHAPTER - 7

BIBLIOGRAPHY



CHAPTER - 7

BIBLIOGRAPHY

1. ACI 440.2R-02, “Guide for the Design and Construction of Externally Bonded FRP Systems for Strengthening Concrete Structures”, Reported by ACI Committee 440.
2. Al-Amery R., and Al-Mahaidi R. (2006), “Coupled flexural-shear retrofitting of RC Beams using CFRP straps”, *Construction and Building Materials*, 21, 1997-2006.
3. Alex L., Assih J., and Delmas Y. (2001), “Shear Strengthening of RC Beams with externally bonded CFRP sheets”, *Journal of Structural Engineering*, Vol. 127, No. 4, Paper No. 20516.
4. Balamuralikrishnan R., and Jeyasehar C. A. (2009), “Flexural behaviour of RC beams strengthened with Carbon Fiber Reinforced Polymer (CFRP) fabrics”, *The Open Civil Engineering Journal*, 3, 102-109.
5. Bousselham A., and Chaallal O. (2006), “Behavior of Reinforced Concrete T-beams strengthened in shear with carbon fiber-reinforced polymer –An Experimental Study”, *ACI Structural Journal*, Vol. 103, No. 3, pp. 339-347.
6. Bukhari I. A., Vollum R. L., Ahmad S., and Sagaseta J. (2010), “Shear strengthening of reinforced concrete beams with CFRP”, *Magazine of Concrete Research*, 62, No. 1, 65–77.
7. Cao S. Y., Chen J. F., Teng J. G., Hao Z., and Chen J. (2005), “Debonding in RC Beams Shear Strengthened with completely FRP wraps”, *Journal of Composites for Construction*, Vol. 9, No. 5, pp. 417-428.
8. Ceroni F. (2010), “Experimental performances of RC beams strengthened with FRP materials”, *Construction and Building materials*, 24, 1547-1559.
9. Chaallal O., Nollet M. J., and Perraton D. (1998), “Strengthening of reinforced concrete beams with externally bonded fibre-reinforced-plastic plates: design guidelines for shear and flexure”, *Canadian Journal of Civil Engineering*, Vol. 25, No. 4, pp. 692-704.

10. Chajes M. J., Januszka T. F., Mertz D. R., Thomson T. A., and Finch W. W. (1995), "Shear strengthening of Reinforced Concrete beams using externally applied composite fabrics", *ACI Structural Journal*, Vol. 92, Issue No. 3, pp. 295-303.
11. Chen J. F., and Teng J. G. (2003), "Shear capacity of FRP-strengthened RC beams: FRP debonding", *Construction and Building Materials*, 17, 27-41.
12. Chen J. F., and Teng J. G. (2003), "Shear capacity of Fiber-Reinforced Polymer-strengthened Reinforced Concrete Beams: Fiber Reinforced Polymer Rupture", *Journal of Structural Engineering*, Vol. 129, No. 5, ASCE, ISSN 0733-9445, pp. 615-625.
13. Deifalla A., and Ghobarah A. (2010), "Strengthening RC T beams subjected combined torsion and shear using FRP fabrics: Experimental Study", *Journal of Composites for Construction*, ASCE, pp. 301-311.
14. Dias S. J. E., and Barros J. A. O. (2010), "Performance of reinforced concrete T beams strengthened in shear with NSM CFRP laminates", *Engineering Structures*, 32, 373-384.
15. Duthinh D. and Starnes M. (2001), "Strengthening of RC beams with CFRP: Experimental results versus prediction of codes of practice", *Journal of Composites for Construction*, 16,185-195.
16. Esfahani M. R., Kianoush M. R., and Tajari A. R. (2007), "Flexural behaviour of reinforced concrete beams strengthened by CFRP sheets", *Engineering Structures*, 29, 2428–2444.
17. Ghazi J. Al-Sulaimani, Alfarabi Sharif, Istem A. Basunbul, Mohhamed H. Baluch, and Bader N. Ghaleb (1994), "Shear Repair for Reinforced Concrete by Fiberglass Plate Bonding", *ACI Structural Journal*, Vol. 91, Issue No. 4, pp. 458-464.
18. Hadi M. N. S. (2003), "Retrofitting of shear failed reinforced concrete beams", *Composite Structures*, 62, 1-6.
19. Islam M. R., Mansur M. A., and Maalej M. (2005), "Shear strengthening of RC deep beams using externally bonded FRP systems", *Cement & Concrete Composites*, 27, 413–420.

20. Kachlakev D., and McCurry D. D. (2000), “Behavior of full-scale reinforced concrete beams retrofitted for shear and flexure with FRP laminates”, *Composites: Part B*, 31, pp. 445-452.
21. Khalifa A., and Antonio N. (2002), “Rehabilitation of rectangular simply supported RC beams with shear deficiencies using CFRP composites”, *Construction and Building Materials*, Vol. 16, No. 3, pp. 135-146.
22. Khalifa A., Belarbi A., and Antonio N. (2000), “Shear performance of RC members strengthened with externally bonded FRP wraps”, *I2WCEE*.
23. Khalifa A, Gold WJ, Nanni A and Aziz A. (1998), “Contribution of externally bonded FRP to shear capacity of RC flexural members”, *Journal of Composites for Construction*, 2, 195–201.
24. Khalifa A., Lorenzis L. D., and Nanni A. (2000), “FRP composites for shear strengthening of RC beams”, *Proceedings, 3rd International Conference on Advanced Composite Materials in Bridges and Structures*, 15-18 Aug., pp. 137-144.
25. Khalifa A., and Nanni A. (2000), “Improving shear capacity of existing RC T-section beams using CFRP composites”, *Cement & Concrete Composites*, 22, 165-174.
26. Kim G., Sim J., and Oh H. (2008), “Shear strength of strengthened RC beams with FRPs in shear”, *Construction and Building Materials*, 22, pp. 1261–1270.
27. Lee H. K., Cheong S. H., Ha S. K., and Lee C. G. (2011), “Behaviour and performance of RC T-section deep beams externally strengthened in shear with CFRP sheets”, *Composite Structures*, Vol. 93, Issue 2, pp. 911-922.
28. IS: 456-2000, “Plain and Reinforced Concrete - Code of Practice ”, Bureau of Indian Standards.
29. IS: 383-1970, “Specification for Coarse and Fine Aggregates from natural sources for Concrete”, Bureau of Indian Standards.
30. IS: 1786-1985, “Specification for high strength deformed steel bars and wires for concrete reinforcement ”, Bureau of Indian Standards.
31. Maaddawy T. E., and Sherif S. (2009), “FRP composites for shear strengthening of reinforced concrete deep beams with openings”, *Composite Structures*, 89, 60–69.

32. Mansur M. A. (1998), "Effect of openings on the Behaviour and Strength of RC Beams in Shear", *Cement and Concrete Composites*, 20, 477-486.
33. Mansur M. A. (2006), "Design of reinforced concrete beams with web openings", *Proceedings of the 6th Asia-Pacific Structural Engineering and Construction Conference (APSEC 2006)*, Kuala Lumpur, Malaysia, pp.104-120.
34. Martinola G., Meda A., Plizzari G. A., and Rinaldi Z. (2010), "Strengthening and repair of RC beams with fiber reinforced concrete", *Cement & Concrete Composites*, 32, 731–739.
35. Mosallam A. S., and Banerjee S. (2007), "Shear enhancement of reinforced concrete beams strengthened with FRP composite laminates", *Composites: Part B*, 38, pp. 781-793.
36. Nanni A., Di Ludovico M. and Parretti R (2004), "Shear strengthening of a PC bridge girder with NSM CFRP rectangular bars", *Adv Struct Eng* , 7(4), 97-109.
37. Norris T., Saadatmanesh H., and Ehsani M. R. (1997), "Shear and Flexural strengthening of RC beams with carbon fiber sheets", *Journal of Structural Engineering*, Vol. 123, No. 7.
38. Obaidat Y. T., Heyden S., Dahlblom O., Farsakh G. A. and Jawad Y. A. (2011), "Retrofitting of reinforced concrete beams using composite laminates", *Construction and Building Materials*, 25, 591–597.
39. Ozgur A. (2008), "Strengthening of RC T-section beams with low strength concrete using CFRP composites subjected to cyclic load", *Construction and Building Materials* 22, 2355–2368.
40. Pannirselvam N., Nagaradjane V., and Chandramouli K. (2009), "Strength behaviour of fiber reinforced polymer strengthened beam", *ARPJN Journal of Engineering and Applied Sciences*, Vol. 4, NO. 9, ISSN 1819-6608.
41. Priestley, M.; Seible, F.; and Calvi, G.; 1996, *Seismic Design and Retrofit of Bridges*, John Wiley and Sons, New York, N.Y.

42. Rabinovitch O. and Frostig Y. (2003), “Experimental and analytical comparison of RC beams strengthened with CFRP composites”, *Composites: Part B*, 34, 663-677.
43. Saadatmanesh H., and Ehsani M. R. (1992), “RC beams strengthened with GFRP plates: experimental study”, *Journal of Structural Engineering*, Vol. 117, No.11, ISSN 0733-9445/91/0011, Paper No. 26385.
44. Saafan M. A. A. (2006), “Shear strengthening of Reinforced Concrete beams using GFRP wraps”, *Czech Technical University in Prague Acta Polytechnica*, Vol. 46 No. 1, pp. 24–32.
45. Santhakumar R., Chandrasekaran E., and Dhanaraj R. (2004), “Analysis of Retrofitted concrete shear beams using Carbon fiber composites”, *Electronic Journal of Structural Engineering*, 4, 66-74.
46. Shanmugam N. E., and Swaddiwudhipongt S. (1988), “Strength of fiber reinforced concrete deep beams containing openings”, *The International Journal of Cement Composites and Lightweight Concrete*, Volume 10, Number 1.
47. Siddiqui N. A. (2009), “Experimental investigation of RC beams strengthened with externally bonded FRP composites”, *Latin American Journal of Solids and Structures*, 6, 343 – 362.
48. Sheikh S. A., DeRose D., and Mardukhi J. (2002), “Retrofitting of concrete structures for shear and flexure with fiber-reinforced polymers”, *ACI Structural Journal*, Vol. 99, No. 4, pp. 451-459.
49. Sheikh S. A. (2002), “Performance of concrete structures retrofitted with fiber reinforced polymers”, *Engineering Structures*, 24, 869-879.
50. Sundarraja M. C., and Rajamohan S. (2009), “Strengthening of RC beams in shear using GFRP inclined strips – an experimental study”, *Construction and Building Materials*, 23, 856–864.
51. Taljsten B. (2003), “Strengthening concrete beams for shear with CFRP sheets”, *Construction and Building Materials*, 17, 15-26.

52. Tanarslan H. M., and Altin S. (2009), "Behavior of RC T-section beams strengthened with CFRP strips, subjected to cyclic load", *Materials and Structures*, DOI 10.1617/s11527-009-9509-8.
53. Teng J. G., Lam L., and Chen J.F. (2004), "Shear strengthening of RC beams with FRP composites", *Programm Structural. Engineering Material*, 6:173–184.
54. Triantafillou, T. C., 1998a, "Shear strengthening of Reinforced Concrete Beams using Epoxy-Bonded FRP Composites," *ACI Structural Journal*, V. 95, No. 2, Mar.-Apr., pp. 107-115.
55. Varastehpour H., and Hamelin P. (1997), "Strengthening of concrete beams using fiber reinforced plastics", *Materials and Structures*, 30, 160-166.

Publications (Based on the Present Research)

International Conference Papers

- ◆ A. K. Panigrahi, K. C. Biswal and M. R. Barik, “Shear Strengthening of RC T-Beams using externally bonded FRP Systems” RITS International Conference on Advancements in Engineering & Management, RITS ICAEM-2012, 28th & 29th Feb 2012.
- ◆ A. K. Panigrahi, K. C. Biswal and M. R. Barik, “Experimental Analysis on the Shear Behaviour of RC T-Beams Strengthened With GFRP Sheets” 2nd International Conference on Advances in Engineering and Technology (ICAET 2012), E. G. S. Pillay Engineering College, Nagpattinam, In Collaboration with Aichi Institute of Technology, Toyota, Japan.
- ◆ A. K. Panigrahi, K. C. Biswal and M. R. Barik, “Experimental investigation of RC T-Beams strengthened with Externally Bonded FRP composites” SPICON 2012, International Conference on Recent Advances in Engineering, Technology and Management, organized by Sardar Patel College of Engineering, (An autonomous institution affiliated to university of Mumbai), Bhavan’s Campus, Munshi Nagar, J.P.Road, Andheri (West) Mumbai.

International Journal

- ◆ A. K. Panigrahi and K. C. Biswal “Experimental Analysis on the Shear Behaviour of RC T-Beams Strengthened with GFRP Sheets”, ISSN 2249 – 7455 International Journal of Advances in Management, Technology & Engineering Sciences, Vol. 1, Issue 6 (VII), March 2012, pp. 56-60.

National Conference Paper

- ◆ A. K. Panigrahi, K. C. Biswal and M. R. Barik, “Experimental study on behavior of Externally Bonded RC T-beams using GFRP composites” VSS University of Technology, Burla, Odisha, India, Proceedings of RAMM-2012, 25-26 February 2012, Advances in Mechanics and Materials, pp. 123-132.